Appendix A.

Surface-Fault-Rupture Hazard Evaluation

DRAFT
SUPPLEMENTAL
ENVIRONMENTAL
IMPACT STATEMENT

Brightwater
Regional Wastewater
Treatment System

Technical Appendices

King County Brightwater TREATMENT SYSTEM

Appendix A

Surface-Fault-Rupture Hazard Evaluation

April 2005

Prepared for King County by
AMEC Earth & Environmental under subcontract to CH2M Hill

Alternative formats available upon request
by calling 206-684-1280 or 711 (TTY)

King County
Department of Natural Resources and Parks
Wastewater Treatment Division
King Street Center, KSC-NR-0505
201 South Jackson Street
Seattle, WA 98104

Surface-Fault-Rupture Hazard Evaluation
Brightwater Project SR-9 Site
King County Department of
Natural Resources, Washington

April 1, 2005

Prepared for King County by
AMEC Earth & Environmental under
Subcontract to CH2M Hill

4-212-102100

Appendix A
Surface-Fault Rupture Hazard Evaluation

A.1 Introduction

Presented in this appendix are the results of an evaluation of surface-fault-rupture hazards that are based, in part, on trench exposures of the shallow subsurface geology created at the site of the proposed Brightwater Wastewater Treatment Plant. The Brightwater Site is located in southern Snohomish County, Washington, very close to the King County boundary (Figure 1). The adequacy of the Final Environmental Impact Statement (FEIS) issued in the fall of 2003 was challenged in the spring of 2004 on the basis that seismic issues, specifically surface-fault-rupture hazards, were inadequately addressed. The U.S. Geological Survey (USGS) published an open-file report describing aeromagnetic and topographic lineaments as evidence of a possible southeast extension of the Southern Whidbey Island fault (SWIF) from Whidbey Island onto the mainland (Blakely and others, 2004). The ruling of an appeal hearing held in July 2004 directed King County, the Brightwater sponsoring agency, to excavate one or more trenches on the Brightwater Plant site to permit evaluation of Lineament 4 identified in Blakely and others (2004) report.

King County entered into a cooperative agreement with the USGS whereby the USGS would undertake an accelerated research task to locate and excavate three trenches, and evaluate the geology exposed in them with an objective of gathering information regarding the seismic hazard of the SWIF. One of the trenches would be located in the North Mitigation Area of the Brightwater site. Several meetings occurred in August and September 2004 among representatives of the USGS and the Brightwater Design Team. The lead geologist with the USGS, Dr. Brian Sherrod, conducted a supplemental assessment of LiDAR (Light Detection and Ranging) topographic data in the vicinity of the Brightwater site. Members of the Brightwater Design Team conducted geologic reconnaissance of the area between the Burlington Northern Santa Fe (BNSF) railroad tracks and Washington State Route 522. A combined group of USGS and Brightwater Design Team members walked part of the Brightwater Route 9 site in early September and came to consensus on the locations of two trenches: One in the North Mitigation Area and one on a narrow, wooded ridge east of the BNSF tracks where a sliver of King County property is located.

Environmental constraints, particularly restrictions related to excavation in wetland areas, limited the locations where trenching could be considered in the North Mitigation Area. Practical limitations related to steep slopes and heavy tree cover also limited trenching locations. These limitations also affected locations where excavated soil could be stockpiled. Furthermore, the shallow depth to ground water in low-lying areas and the sandy nature of some soil deposits led to concerns regarding stability of trench side slopes, which limited the practical dimensions of any trench excavations.

The remaining sections of this appendix pertain to an overview of earthquake hazards and a discussion of surface-fault-rupture hazards at the Brightwater Route 9 site. Details of the results of the trenching investigation are presented in Appendix A.A to this appendix.

A.2 Overview of Earthquake Hazards

Earthquake hazards can be subdivided into primary, secondary, and tertiary hazards. Primary earthquake hazards originate directly from stresses in the earth's crust, and consist of strong shaking, surface-fault rupture, and tectonic deformation. Secondary hazards are caused by primary hazards. For example, strong shaking can cause earthquake-induced landslides and liquefaction, and surface-fault rupture can displace canals and highways that cross rupture zones. Tertiary hazards are caused by secondary hazards. For example, earthquake-induced landslides can deform buildings that are founded on them, and canals displaced by fault rupture can discharge water, eroding slopes and flooding buildings located downstream from the ruptured canal section.

The Puget Sound region has a tectonic setting where the effects of large-magnitude subduction-zone earthquakes could be felt (Figure 2), and a history of moderate seismicity (Figure 3). Fault traces with evidence of Holocene or latest Pleistocene displacement have been discovered in several areas of the Puget Sound region during the past 10 years (Figure 4). Faults that have been discovered in the Puget Sound region include the Devils Mountain fault, the Utsalady Point fault, the Southern Whidbey Island fault, the Seattle fault, the Tacoma fault, and the Olympia fault. Evaluation of the geology exposed in trenches excavated across traces of some of these faults has shown that glacial and post-glacial deposits are locally deformed and/or displaced. Results for some of the more recent evaluations have been described by Sherrod and others (2004, 2005), Kelsey and others (2004), Booth and others (2004), and Brocher and others (2004).

The engineering design approach to strong shaking hazards caused by earthquakes is based on probabilistic considerations, whereas the design approach to surface-fault-rupture hazards is based on deterministic considerations. Probabilistic assessments define earthquake ground motion in terms of horizontal accelerations that have some probability of being equaled or exceeded during a design time period. Building codes in effect in the United States prior to 2000 were based on a 10% exceedance probability in a 50-year time period. The level of ground shaking corresponding to this 10%-50-year exceedance sometimes is expressed as the 500-year design event. The actual recurrence interval is 475 years for the 10%-50-year exceedance if all earthquakes are considered to be independent events (a Poisson process in statistics terminology). The International Building Code 2003 is based on a 2% exceedance probability in a 50-year time period, or an average recurrence interval of approximately 2,500 years (actually 2,475 years with Poisson statistics).

The definition of an 'active fault' is inherently probabilistic even though it is considered to be deterministic. Active faults are considered to be those which have evidence of displacements during the past 10,000 radiocarbon years before present (^{14}C yr B.P. 1950) or 11,500 calibrated years before present (cal yr B.P. 1950). The geologic name

'Holocene Epoch 'is used for the most recent 10,000 ^{14}C years of earth history (International Commission on Stratigraphy web page: http://www.stratigraphy.org/geowhen/), and faults that have been active during this interval are considered to be Holocene faults. Ordinances for some high-consequence facilities consider faults to be active if they have evidence of displacements during longer intervals of earth history.

Some facilities, particularly linear facilities such as highways and pipelines, cannot avoid crossing active faults. These facilities typically are designed using conventional criteria, and emergency response plans are developed for repair following the unlikely occurrence of a surface-fault displacement that causes damage.

One of the principles of geology is called 'uniformitarianism'. This principle expresses the understanding that earth processes acting today have acted in the same general way throughout earth history, although at varying rates and intensities ('actualism' of Dott and Batton, 1976). The plain English statement of this principle is '*the present is the key to the past'*, meaning, for example, that understanding present stream-flow processes transporting and depositing sand and gravel supports a geologic interpretation of fluvial origin for a sandstone and conglomerate formation having similar characteristics.

The engineering geology corollary to the law of uniformitarianism or actualism is '*the recent past is the key to the near future'*. This corollary means that geologic processes which have been active in the past few thousand years of earth history are expected to remain active for the next few thousand years. The active fault definition described above is based on this corollary.

The State of Washington currently does not define active faults for earthquake hazard reduction. The age of deposits associated with the most recent glaciation ranges from approximately 16,000 to 18,000 calibrated years before present (cal yr B.P. where 'present' is defined as 1950 A.D.), based on Porter and Swanson (1998) and shown on Figure 5A. Porter and Swanson (1998) interpolate radiometric dates from the region and interpret that ice advanced across the Seattle area approximately 17,590 cal yr B.P., reaching a maximum extent approximately 16,950 cal yr B.P., and retreated by about 16,570 cal yr B.P., as shown on Figure 5B. The definition of an active fault being used for the Brightwater Wastewater Treatment Plant site is one that deforms or displaces deposits of or younger than the most recent glaciation. This definition is effectively a Holocene fault definition, but it is tailored to geologic deposits of the Puget Sound region.

A.3 Geologic Setting

A.3.1 Stratigraphy

The stratigraphic framework for the interpretation of trench exposures at the Route 9 site is based on the understanding developed for the geotechnical site characterization by CH2M Hill and Shannon & Wilson (CH2M Hill, 2004a). Radiocarbon age constraints on ice advance and retreat by Porter and Swanson (1998) and glaciofluvial infilling and

scour by Booth (1994) in the Seattle area also provided important aspects of the stratigraphic framework.

Glacial deposits in the vicinity of the Brightwater Route 9 site have a range of ages, but the most recent glaciation is called the Vashon Stade of the Fraser glaciation, which occurred between approximately 18,000 and 16,000 cal yr B.P. (Porter and Swanson, 1998), as shown on Figure 5B. During this glaciation, ice advanced toward the south to a point near Olympia, achieving a thickness greater than 3,000 feet (1,000 meters) in the project area approximately 16,950 cal yr B.P., and then receded rapidly back toward the north during a relatively short period of time. Ice probably covered the site area for slightly more than 1,000 years (Porter and Swanson, 1998), as indicated on Figure 5B. Deposits older than the Vashon Stade of the Fraser glaciation were either overridden by Vashon ice or scoured by advancing ice or subglacial streams. Melt water from receding ice also eroded the Vashon and older deposits and left behind coarse- to fine-grained sediments ranging in character from fluvial to lacustrine.

More detailed descriptions of the stratigraphy of the Brightwater Route 9 site area are included in Appendix A.A. These descriptions are based on the geotechnical site characterization by CH2M Hill, and on interpretation of geotechnical drilling by Aspect Consulting across Lineament 4 and trench exposures created in September 2004.

A.3.2 Tectonics

A tectonic model of the Pacific Northwest (Cascadia) developed by Wells and others (1998) is based on recognition of Neogene deformation, paleomagnetic rotations, and limited geodetic data. (Neogene is a period of earth history from about 23 million years ago to 1.8 million years ago.) Wells and others (1998) interpretation is that a significant amount of the Pacific Northwest is breaking up into large blocks which rotate in response to northward migration of the Cascadia fore arc along the coast of Washington and Oregon. Wells and others (1998) report that seismic hazards are associated with crustal earthquakes caused by relative motions of fore-arc blocks, in addition to the seismic hazards of subduction-zone earthquakes.

Gower and others (1985) inferred the presence of the SWIF on southern Whidbey Island based mainly on northwest-trending steep gravity and magnetic gradients in the vicinity of the contact separating two distinctly different crustal rock types. Johnson and others (1996) used magnetic and gravity anomalies, borehole data, and minor faults exposed in sediments of late Quaternary age to interpret the SWIF to be a regional tectonic feature separating two crustal blocks and contributing to a long history of continental margin rifting, strike-slip faulting, and transpressional deformation in the Puget Lowland area.

Johnson and others (1996) report six lines of evidence supporting their conclusion that the SWIF is capable of generating large-magnitude earthquakes. The lines of evidence are 1) seismic-reflection profiles showing offset and disrupted strata, 2) boreholes adjacent to the SWIF showing offset of the base of Quaternary deposits, 3) fault traces in exposures of Quaternary deposits, 4) late Quaternary folds with dips up to 8°, 5) large-

scale liquefaction features in late Quaternary deposits, and 6) moderate recent seismicity. Focal mechanisms or fault-plane solutions for three earthquakes larger than magnitude 3.5 at depths of 13 to 16 miles (22 to 26 kilometers) show right-lateral strike-slip with reverse slip on northwest-trending planes. Two of the three focal mechanisms showed steep northeast-dipping planes, whereas one focal mechanism showed a relatively low-angle southwest-dipping plane.

Blakely and others (2004) summarize recent studies of geology and geophysics in the Puget Sound region to provide context for their interpretation of aeromagnetic data to indicate a southeast extension of the SWIF onto the mainland to a point southeast of Crystal Lake. Blakely and others (2004) report that north-side-up LiDAR scarps and apparent north-side-up offsets of magnetic layers are consistent with observations of the SWIF on and around Whidbey Island by Johnson and others (1996), who found evidence for three strands of the SWIF in seismic-reflection profiles from Possession Sound, where the northern and southern strands dip steeply northward and exhibit north-side-up displacement, and the central strand dips steeply southward and has its south side up. Johnson and others (1996) interpreted this geometry as an antiformal flower structure, with the central strand rooting into the southern strand. Kelsey and others (2004) interpreted differences in sea-level histories at two marshes on Whidbey Island located on opposite sides of one strand of the SWIF as evidence for 3 to 6 feet (1 to 2 meters) of north-side-up displacement about 3,000 years ago (cal yr B.P. 1950).

Blakely and others (2004) extend the SWIF across areas blanketed by Quaternary deposits. The SWIF traces remained unrecognized until recently because 1) surface-fault rupture has not accompanied historical earthquakes in the region, 2) post-glacial displacement amounts on SWIF traces have been sufficiently small that major Quaternary deposits have not brought into contact with each other and/or topographic features have not been displaced enough to be recognized on conventional topographic maps and aerial photographs, and 3) traditional geologic mapping is based on conventional topographic maps and aerial photographs which are dominated by tree canopy in the densely forested Pacific Northwest. The Seattle fault displays readily apparent topographic features at the modern ground surface from an earthquake 1,100 years ago, and along which sufficient offset has accumulated over time to produce an east-trending alignment of bedrock outcrops (Blakely and others, 2004), but the topographic features are clearly evident only in topographic maps made from high-quality LiDAR data.

Blakely and others (2004) report that approximately north-south crustal shortening in central Puget Sound is inferred in current tectonic models (Wells and others, 1998), and is supported by data from trenches across the Seattle fault (Nelson and others, 2003). Right-lateral reverse slip would be expected on northwest-trending faults in response to north-directed shortening. However, left-lateral reverse slip was interpreted by Johnson and others (2003) from a single trench across the west-northwest-trending Utsalady fault on northern Whidbey Island. Blakely and others (2004) conclude that if left-lateral slip is typical of northern Puget Sound faults, then the SWIF may occupy a transition zone between two strain regimes, and may have reverse slip, with a right-lateral component that increases in a southward direction.

Brocher and others (2004) proposed an alternative, more complicated tectonic framework for the Seattle uplift (SU on Figure 4). This alternative tectonic framework (Figure 6) is called a 'passive roof duplex', and portrays the Seattle fault as north-dipping reverse faults at shallow depth above a south-dipping thrust fault that is the 'floor' of the Seattle uplift at the south edge of the Seattle basin. The surface traces of the Seattle fault would be north-side-up 'shadows' on the edge of a more major south-side-up thrust fault. Members of the Brightwater Design Team discussed this tectonic framework with U.S. Geological Survey geologists, geophysicists, and seismologists as a possible mechanism for the SWIF, in which the southeast part of the Kingston arch (KA on Figure 4) would be analogous to the Seattle uplift. The 'passive roof duplex' cannot be ruled out as a possible mechanism for the SWIF, but the right-lateral reverse-slip fault mechanism is favored at this time, in part because the north edge of the Seattle basin is not known to be fault controlled.

A.4 Southern Whidbey Island Fault Zone

Blakely and others (2004) describe the SWIF as a mostly concealed, northwest-trending tectonic structure extending across southern Whidbey Island toward Vancouver Island. Gower and others (1985) first recognized the SWIF on a regional scale on the basis of gravity and aeromagnetic anomaly maps. Johnson and others (1996) concluded that the SWIF on Whidbey Island consists of three main strands with late Quaternary strike-slip and reverse displacements based on their analysis of seismic-reflection profiles, sea-cliff exposures, and borehole data. Kelsey and others (2004) interpreted differences in relative sea-level histories at two coastal marshes located on opposite sides of a trace of the SWIF as evidence for 3 to 6 feet (1 to 2 meters) of north-side-up displacement during an earthquake of magnitude 6.5 to 7.0 about 3,000 years ago.

The U.S. Geological Survey conducted a high-resolution aeromagnetic survey of the Puget Sound region in 1997 (Blakely and others, 1999). The procedures used by the U.S Geological Survey to process the aeromagnetic data and identify anomalies are described in Blakely and others (1999 and 2004). Alternative subsurface conditions that can produce an anomaly in aeromagnetic data are illustrated on Figure 7. Alignments of anomalies in the aeromagnetic data were interpreted in the context of other geologic and topographic details.

High-precision, aerial topographic surveying was conducted in western King County and the southwest part of Snohomish County in 2002 and 2003. The procedure used to collect the data was light detection and ranging (LiDAR) from an airplane. King County commissioned the survey that covers the Brightwater site (http://www.metrokc.gov/gis/sdc/raster/elevation/). The Puget Sound LiDAR Consortium is the clearinghouse for other LiDAR data in western Washington (http://duff.geology.washington.edu/data/raster/lidar/). The collected data are processed to remove tree cover and produce a bare-earth digital elevation model. The USGS geologists examined the King County LiDAR data in the region of Cottage Lake and Crystal Lake because of the strength of the aeromagnetic anomalies that appeared to be aligned with southeast projections of SWIF from localities

on Whidbey Island and off-shore geophysical survey results (Johnson and others, 1996). LiDAR swath boundary elevation mismatches are noticeable at some places in the King County data. LiDAR data processing artifacts are described in Blakely and others (2004) and were discussed in informal meetings among USGS scientists and Brightwater Design Team members.

The following sections of this appendix pertain to aeromagnetic and LiDAR lineaments in the vicinity of the Brightwater Route 9 site.

A.4.1 Aeromagnetic and LiDAR Lineaments

Residual aeromagnetic anomalies from Blakely and others (2004) are shown on Figure 8. They used an automated procedure to define aligned magnetic contacts (white dots on Figure 8) and interpreted some of them as aeromagnetic lineaments (black dashed lines on Figure 8). The LiDAR data in the vicinity of the Cottage Lake lineament are shown as a hillshade map on Figure 9 combined with the aeromagnetic anomaly map. LiDAR scarps and lineaments discussed in Blakely and others (2004) are shown as numbered black solid, dashed, and dotted lines. LiDAR Lineament 4 on Figure 9 projects across the North Mitigation Area of the Brightwater Route 9 site, and is the one that was the subject of the Appeal Hearing ruling.

A magnetic contact on Figure 8 crosses the south tip of the site, but was not shown as a feature on Figure 9 or discussed in Blakely and others (2004). Members of the Brightwater Design Team discussed this magnetic contact with U.S. Geological Survey geologists, geophysicists, and seismologists, and learned that they intend to identify the magnetic contact as a magnetic anomaly in the next version of the SWIF report. This lineament is being called Lineament X. It is shown on Sherrod and others (2005) and is described below.

A.4.2 Lineament 4

Blakely and others (2004) describe Lineament 4 as being about 1.8 miles (3 kilometers) long and following the lower Bear Creek drainage (gray dashed line on Figure 10). They note that the southeastern part of Lineament 4 is aligned along a deep ravine, a low ridge or scarp, and two additional scarps, which they identify as Lineament 8. They further note that Lineament 4 nearly coincides with an aeromagnetic anomaly that is located approximately 1 mile (1.5 kilometers) southwest of the Cottage Lake aeromagnetic lineament.

A seismic refraction evaluation was performed in the North Mitigation Area in April 2004 (AMEC, 2004). The interpretation of the seismic refraction data conducted in April 2004 focused on the greatest depth that could be achieved from the data. The results of the April 2004 evaluation were inconclusive because seismic velocity contrasts interpreted in some short survey lines were not represented in a longer survey line across the same location. Borings drilled along the centerline of a proposed trench provided valuable subsurface information which served as a basis for reinterpreting the seismic

refraction data with a focus on the shallow subsurface. The results of the seismic refraction reinterpretation are presented in Appendix A.B. An anomalous shallow high velocity feature is located in a position that could be correlated with the projection of Lineament 4 near where it is shown on Figure 10.

Two trenches were excavated across Lineament 4 at the Brightwater Route 9 site in September 2004 (Figure 11). A detailed discussion of these trenches is presented in Appendix A.A. Trench 2a in the North Mitigation Area exposed glacial outwash deposits, post-glacial wetland deposits, and modern fill sediments. Trench 2b east of the StockPot Soups building exposed glacial till and lacustrine deposits that are compact, indicating that they have been overridden by ice. Hence, the deposits exposed in Trench 2b are older than recessional deposits of the Vashon Stade of the Fraser glaciation. Deformation features were observed in both trenches, but the deformation in each trench has completely different character. Exposures in Trench 2b do not yield useful information for paleoseismology interpretations of Lineament 4, other than deformation is younger than deposits that were overridden by Vashon Stade ice but older than the Vashon ice that compressed tectonically deformed sediments.

Two ages of deformation features exist in Trench 2a and consist of a monoclinal to antiformal fold in Vashon recessional outwash sediments, two unconformities, small-scale faulting, and injected sand zones and dikes. The monoclinal to antiformal fold is interpreted to have a tectonic origin because of the fold geometry and stratigraphic relationships described in Appendix A.A. The amplitude of the monoclinal to antiformal fold is at least 3 feet (1 meter), and could be greater than 6 feet (2 meters) because the upper part of the fold has been truncated by erosion. A buttress unconformity separates the folded outwash deposits from gently dipping outwash deposits, indicating that the deformation event occurred during recession of Vashon Stade ice. Therefore, it is estimated to have occurred approximately 16,000 cal yr B.P. (1950). Sherrod and others (2005) state that this deformation could have occurred between 16,400 and about 12,000 cal yr B.P.

At the location of Trench 2a, wetland conditions existed after the glacial recession was complete. A dark, organic-rich wetland soil formed on the former ground surface. Two small-scale faults were observed in the folded outwash deposits, and liquefied sand was injected into the wetland soil deposit. The basal contact of the wetland soil deposit appeared to have been warped in the vicinity of some of the sand injection features. The wetland soil deposit was buried by modern fill soil. The USGS obtained radiometric ages of approximately 2,730 cal yr B.P. from charcoal samples in the wetland soil deposit (Sherrod and others, 2005) supporting a mid- to late Holocene age. Therefore, the small-scale faulting and sand injection is interpreted to be late Holocene, no more than about 3,000 years old. Possible coincidence with other dated earthquakes is unknown, but earthquakes occurred approximately 1,100 years ago on the Seattle fault (Johnson and others, 1999) and 3,000 years ago on the SWIF (Kelsey and others, 2004).

Sedimentary beds on opposite sides of the small-scale faults in Trench 2a show that a small amount of reverse separation occurred on the faults. The beds have different

thickness on opposite sides of the faults, showing that lateral separation also occurred. The small-scale faults were observed on the northwest side of Trench 2a, but could not be found on the southeast side. Warping of the base of the wetland soil deposits is less than approximately 1 foot (0.3 meters).

The southwest side of the monoclinal to antiformal fold is clearly marked by a buttress unconformity. The northeast side of the fold is not clearly evident, but may be located within 40 to 50 feet (12 to 15 meters) of the southwest side of the fold. The small-scale faults are located within the monoclinal fold, but liquefied sand injection features are exposed over a distance of approximately 100 feet (30 meters) in Trench 2a.

A.4.3 Lineament X

A magnetic contact is shown on Figure 8 as an alignment of white dots on the projecting through the southern end of the site. A detail of this area is shown on Figure 12. A detail of the LiDAR and aeromagnetic anomaly map shown on Figure 9 is presented on Figure 13, and the hillshade LiDAR map of the site is shown on Figure 14. An electronic file of the positions of the white dots representing magnetic contacts in Figures 8 and 12 was provided to the Brightwater Design Team by the USGS. These points were projected into Washington State Plane North Zone coordinates and plotted on a King County LiDAR hillshade map, as shown on Figure 15.

Northwest-trending linear features are visible in the LiDAR data (Figures 14 and 15). A prominent gully is visible to the west of the Brightwater site and aligned with one branch of a gully located southeast of the south end of the site. The aligned white magnetic contact dots crossing the south end of the Brightwater site (Figures 8, 12, and 15) are approximately parallel to the topographic alignment of the prominent gully.

Two dashed white lines are shown on Figure 15, one representing Lineament 4 and the other representing Lineament X. The location of Lineament X was guided by the prominent northwest-trending gully. Lineament X is located approximately parallel to the white magnetic contact dots where the dots cross the south part of the Brightwater site. Lineament X projects across the white dots about 1,000 feet (300 meters) south of the south end of the site.

Features located along Lineament X appear to be similar to features along Lineament 4. As can be seen on Figure 15, a section of white magnetic contact dots east of the Brightwater site is approximately parallel to a section of white dots that cross the south part of the site. The USGS located Lineament 4 on the basis of a ravine, low ridge, and scarps that were aligned in proximity to a magnetic contact. Where Lineament 4 crosses the Brightwater site, it is approximately 400 to 500 feet (120 to 150 meters) southwest of the aligned white magnetic contact dots (Figure 15). Similarly, where Lineament X crosses the Brightwater site, it also is approximately 400 to 500 feet (120 to 150 meters) southwest of the white dots (Figure 15). The magnetic contacts represented by aligned white dots on Figure 15 cross Lineament 4 and Lineament X east and south of the Brightwater site, respectively.

The LiDAR topography in the vicinity of Lineament X (Figure 15) was examined for evidence of low scarps. No scarps were found that appear to be aligned with the trend of Lineament X, but, as shown on Figure 15, LiDAR swath boundaries with elevation mismatches are clearly evident in the vicinity of Lineament X. Blakely and others (2004) state that they excluded from consideration lineaments that might have been LiDAR data processing artifacts. Sherrod and others (2005) include Lineament X as a LiDAR lineament without LiDAR scarps. The apparent absence of scarps in the LiDAR data aligned with Lineament X does not necessarily indicate that Lineament X can be dismissed from consideration as an active fault. However, the apparent absence of LiDAR scarps supports an interpretation that any fault that might somehow be associated with Lineament X is not significantly more prominent than the zone of deformation now known to be associated with Lineament 4 at the Brightwater site. Therefore, it appears to be reasonable at this time to assume that Lineament X is comparable to Lineament 4 for the surface-fault-rupture hazard evaluation.

A.4.5 Brightwater Route 9 Plant Site

Traces of the SWIF described by Blakely and others (2004) and Sherrod and others (2005) consistently are associated with aeromagnetic anomalies and scarps or lineaments in LiDAR data. Aeromagnetic and LiDAR conditions at the Brightwater Route 9 site, including the area between Lineament 4 and Lineament X, are shown on Figures 12, 13, 14, and 15. The aeromagnetic anomaly maps (Figures 12 and 13) appear to show generally uniform magnetic conditions (at the resolution of the aeromagnetic data) on the site between the two lineaments. It seems reasonable to conclude that another magnetic contact similar in scale to those associated with Lineament 4 and Lineament X is unlikely to exist between them. A ground magnetic survey conducted by the USGS in the vicinity of Trench 2a (Sherrod and others, 2005) revealed a northwest-trending anomaly (cyan dots labeled GA on Figure 15) located approximately 50 feet (15 meters) southwest of the end of Trench 2a. Anomaly GA is approximately 245 feet (75 meters) long, and appears to end within the area of the ground magnetic survey.

A geotechnical boring drilled on the Brightwater Route 9 site (Boring PB-12, CH2M Hill, 2004a) shows soil deformation at depths greater than approximately 200 feet (60 meters). The deformation appeared in hard and very dense soils. Sand fill in apparent fractures was very dense and fractures had been tightly rehealed, suggesting that the disturbed soil had been compressed by the weight of ice during the Vashon or older glacial advance. Boring PB-12 is located approximately 730 feet (220 meters) northeast of the projection of Lineament X shown on Figure 15, and approximately 180 feet (55 meters) northeast of the line of white magnetic contact dots on Figure 15.

LiDAR topography of the site and surrounding area is shown on Figures 14 and 15. Swath-boundary elevation mismatch errors exist in the LiDAR data, as indicated by Blakely and others (2004). An example of the swath-boundary mismatch is identified on Figure 15. Ground disturbance related to grading and urban development could have modified or obliterated low scarps. Consequently, the absence of LiDAR scarps in the

vicinity of the Brightwater site cannot be used as evidence that active faults do not exist between Lineament 4 and Lineament X. However, it is reasonable to conclude that a fault with a greater degree of activity than that associated with the Lineament 4 deformation would have produced scarps visible in the LiDAR data, even with the swath-boundary errors. The absence of aeromagnetic anomalies and LiDAR scarps that project through the Brightwater site between Lineament 4 and Lineament X suggest that active fault traces may be unlikely between the two lineaments.

Soil disturbance observed in samples below a depth of 200 feet (60 meters) in Boring PB-12 can be explained by glacial processes and earthquake-related processes. At its maximum extent, ice in the Puget Lobe of the most recent glaciation was more than 3,000 feet (1,000 meters) thick (Porter and Swanson, 1998). The load of moving glaciers can exceed the strength of unconsolidated and uncemented sediment deposits, causing them to shear and deform (Flint, 1971). Earthquake-related processes include liquefaction and landsliding induced by strong ground shaking, in addition to tectonic fault displacement. Ground shaking strong enough to cause liquefaction in susceptible sediments at the Brightwater site could have been generated by earthquakes on faults other than the SWIF. Such earthquakes could have deformed sediments without representing a surface-fault rupture hazard at the site. Liquefaction- or landslide-induced sediment deformation in samples at depth of 200 feet (60 meters) or more in Boring PB-12 would have occurred at a time before glacial, fluvial, lacustrine, and marine sediments buried the former landscape.

A.5 Fault Rupture Hazard Evaluation

Based on the discussion presented above and in Appendix A.A, it appears that Lineament 4 meets the definition of an active fault and presents a surface-fault-rupture hazard at the Brightwater Route 9 site along a trend shown on Figure 15. Geologic evidence of two, and possibly three, surface-deforming earthquakes was interpreted from Trench 2a. The oldest earthquake occurred during recession of the Vashon Stade of the Fraser glaciation, and the youngest earthquake occurred after deposition of a wetland organic soil. The character of vertical deformation of the oldest earthquake was 3.3 to 6.5 ft (1 to 2 m), possibly more, of north-side-up folding over a zone 40 to 50 ft (12 to 15 m) wide, possibly wider. The geologic evidence of vertical deformation caused by the youngest earthquake appeared to be small-scale (<< 1 m) faulting in recessional Vashon deposits and liquefaction-induced warping of the wetland soil.

Geologic arguments by Johnson and others (1996) suggest that the SWIF has a right-lateral strike-slip component, and geologic evidence of lateral separation was observed in Trench 2a. Therefore, right-lateral displacement could have occurred across the zone of folding associated with Lineament 4, but evidence to support the amount and sense of lateral deformation was not observed. If the vertical and lateral components were approximately equal, then as much as 4.7 to 9.2 ft (1.4 to 2.8 m) of total deformation may have occurred during the older surface-deforming earthquake, whereas much less deformation occurred during the younger surface-deforming earthquake. The actual amount of total displacement that might occur in a future earthquake on Lineament 4 of

the SWIF would depend on whether it were similar to the oldest event interpreted in Trench 2a, or to the youngest event, and on the amount of lateral displacement.

Lineament X may be a feature that meets the definition of an active fault. Lineament X is postulated to exist along a trend shown on Figure 15 on the basis of aligned topographic features that are subparallel to a northwest-trending magnetic contact. Lineament X and Lineament 4 each are located approximately the same distance southwest of northwest-trending magnetic contacts, as shown on Figure 15. It appears reasonable to speculate that, if it is a feature that meets the definition of an active fault, Lineament X is reasonably likely to have characteristics that are somewhat similar to those of Lineament 4 exposed in Trench 2a. Therefore, at this time, it may be prudent to assume that Lineament X presents a surface-fault rupture hazard at the Brightwater Route 9 site along a trend shown on Figure 15 with characteristics similar to those of Lineament 4.

The terrain on the Brightwater Route 9 site between Lineament 4 on the north and Lineament X on the south appears to be free of features that suggest another lineament of similar scale with similar characteristics might be present. The aeromagnetic anomaly maps (Figures 12 and 13) and LiDAR topography (Figures 14 and 15) support this speculation. Soil disturbance observed in samples below a depth of 200 feet (60 meters) in Boring PB-12 could have been caused by several different processes, only one of which is tectonic faulting. If the soil disturbance below a depth of 200 feet (60 meters) in Boring PB-12 were not caused by faulting, or if the most recent movement were older than the age of the Vashon Stade of the Fraser glaciation, then the definition of an active fault would not be met and the soil disturbance in Boring PB-12 would not represent a surface-fault rupture hazard at the Brightwater Route 9 site. Alternatively, in the absence of conclusive evidence demonstrating that active faults do not exist between Lineament 4 and Lineament X, it may be prudent to assume that surface-fault rupture hazards might exist between the two lineaments. It appears reasonably conservative to assume that any features meeting the definition of an active fault that are located on the Brightwater site between the two lineaments would be smaller in scale than Lineament 4 and have smaller amounts of displacement than those associated with past earthquakes on Lineament 4 as interpreted from the geology exposed in Trench 2a.

A.6 References

AMEC, 2004, Report, Seismic Refraction Evaluation, Brightwater Final EIS, Snohomish County, Washington: unpublished consultant's report to King County Wastewater Treatment Division, dated April 27, 2004, 32 p.

Blakely, R.J., Sherrod, B.L., Wells, R.E., Weaver, C.S., McCormack, D.H., Troost, K.G., and Haugerud, R.A., 2004, The Cottage Lake aeromagnetic lineament: A possible onshore extension of the Southern Whidbey Island Fault, Washington: U.S. Geological Survey Open-File Report 2004-1204, 60 p.

Blakely, R.J., Wells, R.E., and Weaver, C.S., 1999, Puget Sound aeromagnetic maps and data: U.S. Geological Survey Open-File Report 99–514, http://geopubs.wr.usgs.gov/openfile/of99-514.

Booth, D.B., Glaciofluvial infilling and scour of the Puget Lowland, Washington, during ice-sheet glaciation: Geology, v. 22, no. 8, p. 695-698.

Booth, D.B., Troost, K.G., and Hagstrum, J.T., 2004, Deformation of Quaternary strata and its relationship to crustal folds and faults, south-central Puget Lowland, Washington State: Geology, v. 32, no. 6, p. 505-508.

Brocher, T.M., Blakely, R.J., and Wells, R.E., 2004, Interpretation of the Seattle uplift, Washington, as a passive roof duplex: Bulletin of the Seismological Society of America, v. 94, no. 4, p. 1379-1401.

CH2M Hill, 2004a, Preliminary design geotechnical interpretive report, Route 9 site, Proposed Brightwater Wastewater Treatment Plant: unpublished consultant's report to King County Wastewater Division, Washington.

CH2M Hill, 2004b, Final design geotechnical recommendations report, Brightwater Regional Wastewater Treatment Plant: unpublished consultant's report to King County Wastewater Division, Washington.

Dott, R.H., Jr. and Batten, R.L., 1976, Evolution of the Earth, 2nd Edition, McGraw-Hill, p. 38-39

Flint. R.F., 1971, Glacial and Quaternary geology: John Wiley and Sons, p. 121-126.

Gower, H.D., Yount, J.C., and Crosson, R.S., 1985, Seismotectonic map of the Puget Sound region, Washington: U.S. Geological Survey Miscellaneous Investigations Map I-1613, scale 1:250,000.

Johnson, S.Y., Dadisman, S.V., Stanley, W.D., and Childs, J.R., 1999, Active tectonics of the Seattle fault and central Puget Sound, Washington – Implications for earthquake hazards: Geological Society of America Bulletin, v. 111, no. 7, p. 1042-1053.

Johnson, S.Y., Nelson, A.R., Personius, S.F., Wells, R.E., Kelsey, H.M., Sherrod, B.L., Okumura, K., Koehler, R., Witter, R., Bradley, L.-A., Harding, D.J., 2003, Maps and data from a trench investigation of the Utsalady Point fault, Whidbey Island, Washington: U.S. Geological Survey Miscellaneous Field Investigations MF-2420.

Johnson, S.Y., Potter, C.J., Armentrout, J.M., Miller, J.J., Flinn, C., and Weaver, C.S., 1996, The southern Whidbey Island fault: An active structure in the Puget

Lowland, Washington: Geological Society of America Bulletin v. 108, no. 3, p. 334-354.

Kelsey, H.M., Sherrod, B., Johnson, S.Y., and Dadisman, S.V., 2004, Land-level changes from a late Holocene earthquake in the northern Puget lowland, Washington: Geology, v. 32, no. 6, p. 469-472.

Nelson, A.R., Johnson, S.Y., Kelsey, H.M., Wells, R.E., Sherrod, B.L., Pezzopane, S.K., Bradley, L., Koehler, R.D., and Bucknam, R.C., 2003, Late Holocene earthquakes on the Toe Jam Hill fault, Seattle fault zone, Bainbridge Island, Washington: Geological Society of America Bulletin, v. 115, no. 11, p. 1388-1403.

Porter, S.C., and Swanson, T.W., 1998, Radiocarbon age constraints on rates of advance and retreat of the Puget Lobe of the Cordilleran Ice Sheet during the last glaciation: Quaternary Research, v. 50, p. 205-213.

Shannon & Wilson, 2004, Final Report, Probabilistic Seismic Hazard Analysis, Brightwater Project, SR-9 and Portal 41 Sites, King County Department of Natural Resources, Washington: Unpublished consultant's report dated June 30, 2004, 128 p.

Sherrod, B.L., Blakely, R.J., Weaver, C., Kelsey, H., Barnett, E., and Wells, R., 2005, Holocene fault scarps and shallow aeromagnetic anomalies along the Southern Whidbey Island fault zone near Woodinville, Washington, U.S. Geological Survey Open-File Report 2005-1136, 40 p.

Sherrod, B.L., Brocher, T.M., Weaver, C.S., Bucknam, R.C., Blakely, R.J., Kelsey, H.M., Nelson, A.R., and Haugerud, R., 2004, Holocene fault scarps near Tacoma, Washington, USA: Geology, v. 32, no. 1, p. 9-12.

Wells, D.W., and Coppersmith, K.J., 1994, New empirical relationships among magnitude, rupture length, rupture width, rupture area, and surface displacement, Bulletin of the Seismological Society of America, v. 84, p. 974-100.

Wells, R.E., Weaver, C.S., and Blakely, R.J., 1998, Fore-arc migration in Cascadia and its neotectonic significance: Geology, v. 26, no. 8, p. 759-762.

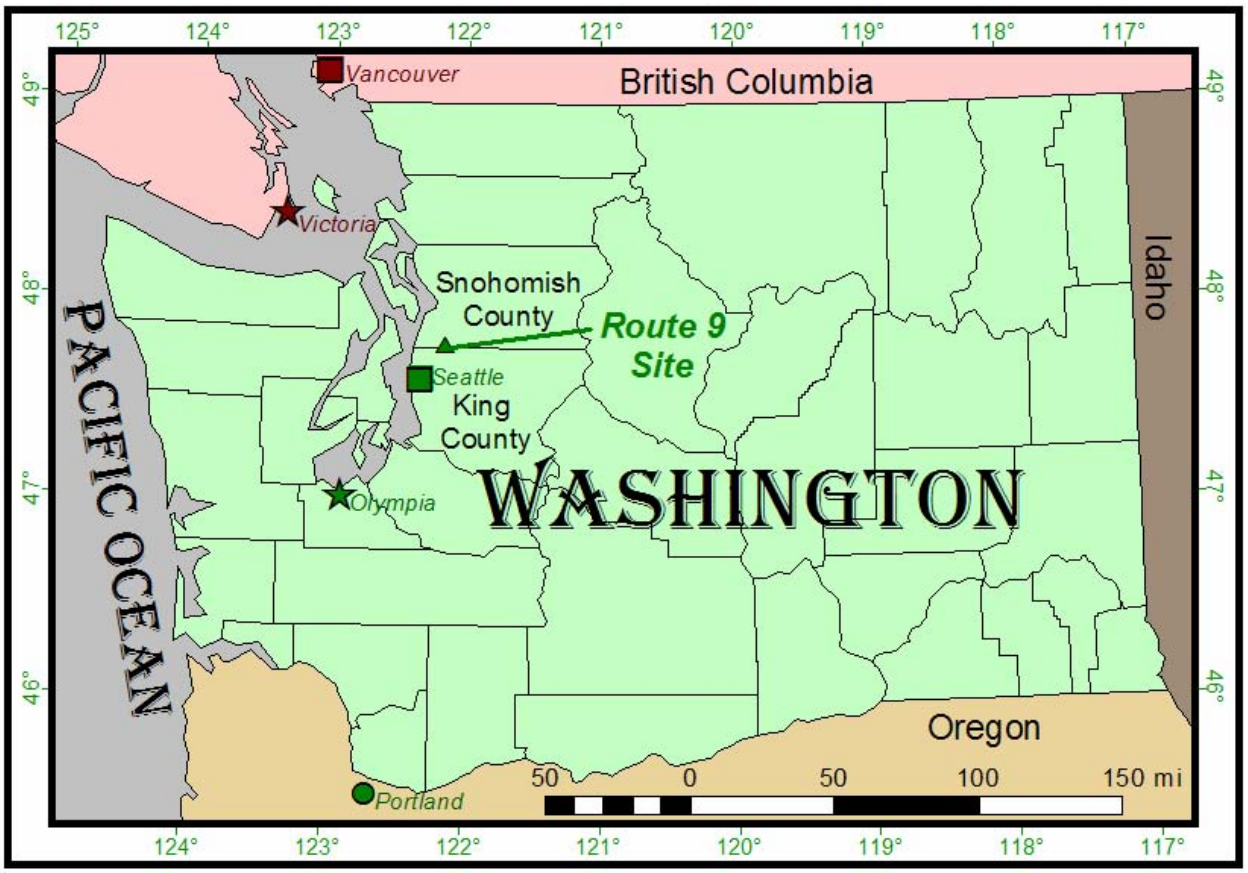

Figure 1. Location Map. Washington State Plane North Zone projection.

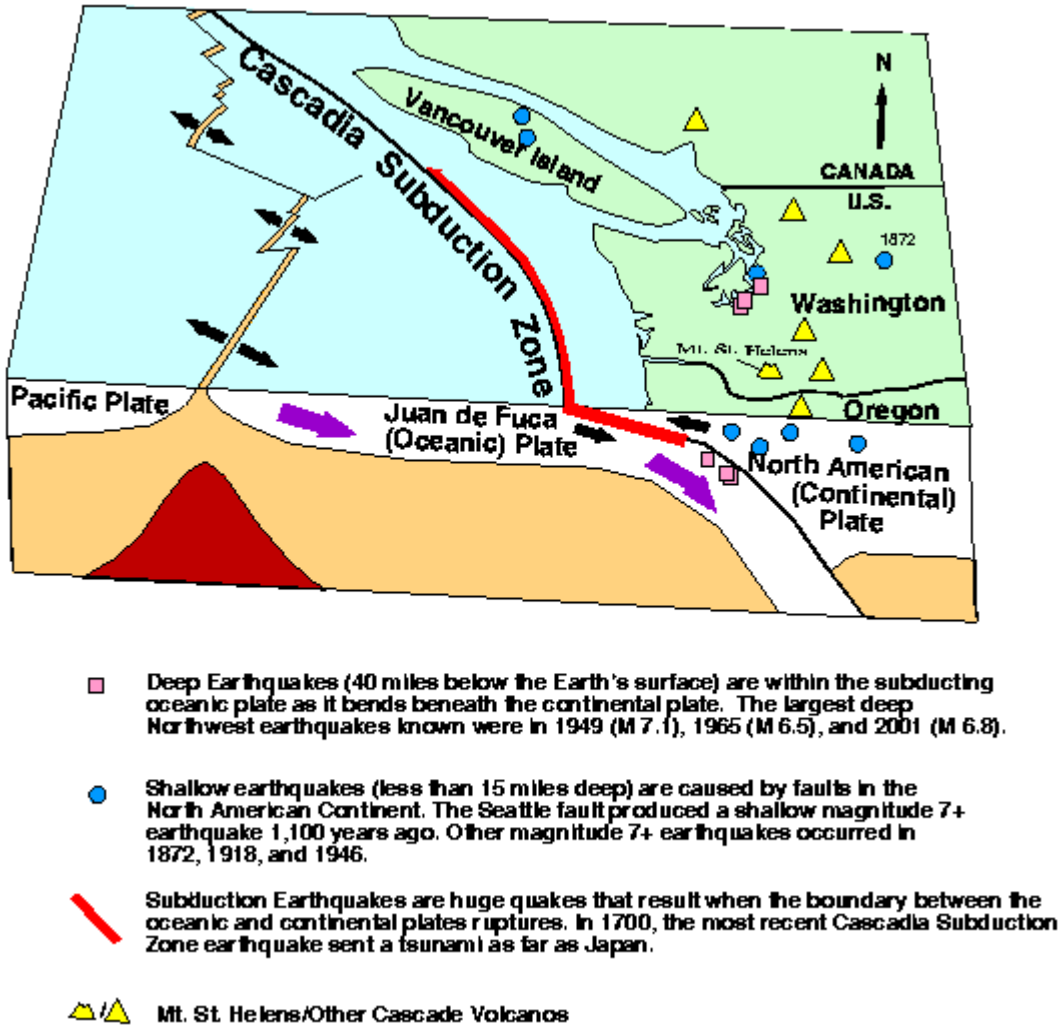

Figure 2. Plate-tectonic setting for earthquakes in western Washington and northwest Oregon. From Pacific Northwest Seismograph Network website (http://www.pnsn.org/INFO_GENERAL/eqhazards.html).

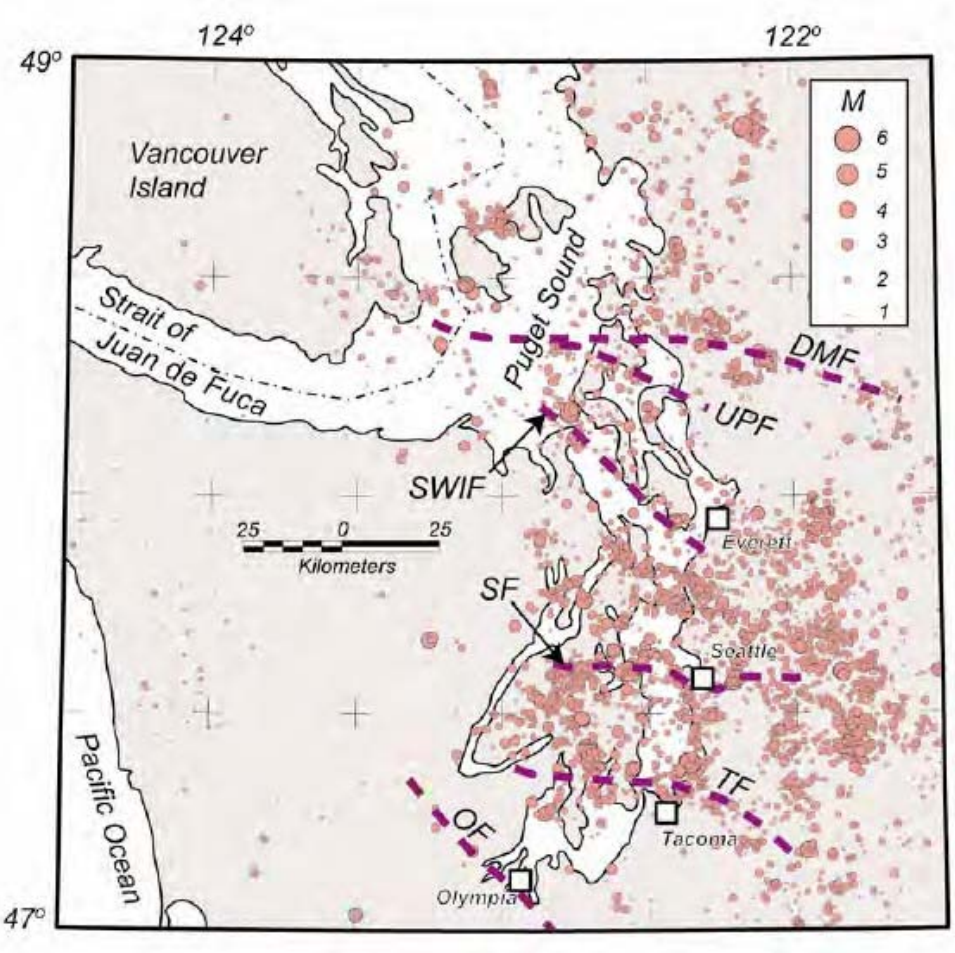

Figure 3. Crustal seismicity in the Puget Sound region from 1971 through 2003. From Blakely and others (2004) figure 3. Bold lines are aeromagnetic anomalies associated with recently discovered faults: DMF – Devils Mountain fault, UPF – Utsalady Point fault, SWIF – Southern Whidbey Island fault, SF – Seattle fault, TF – Tacoma fault, OF – Olympia fault.

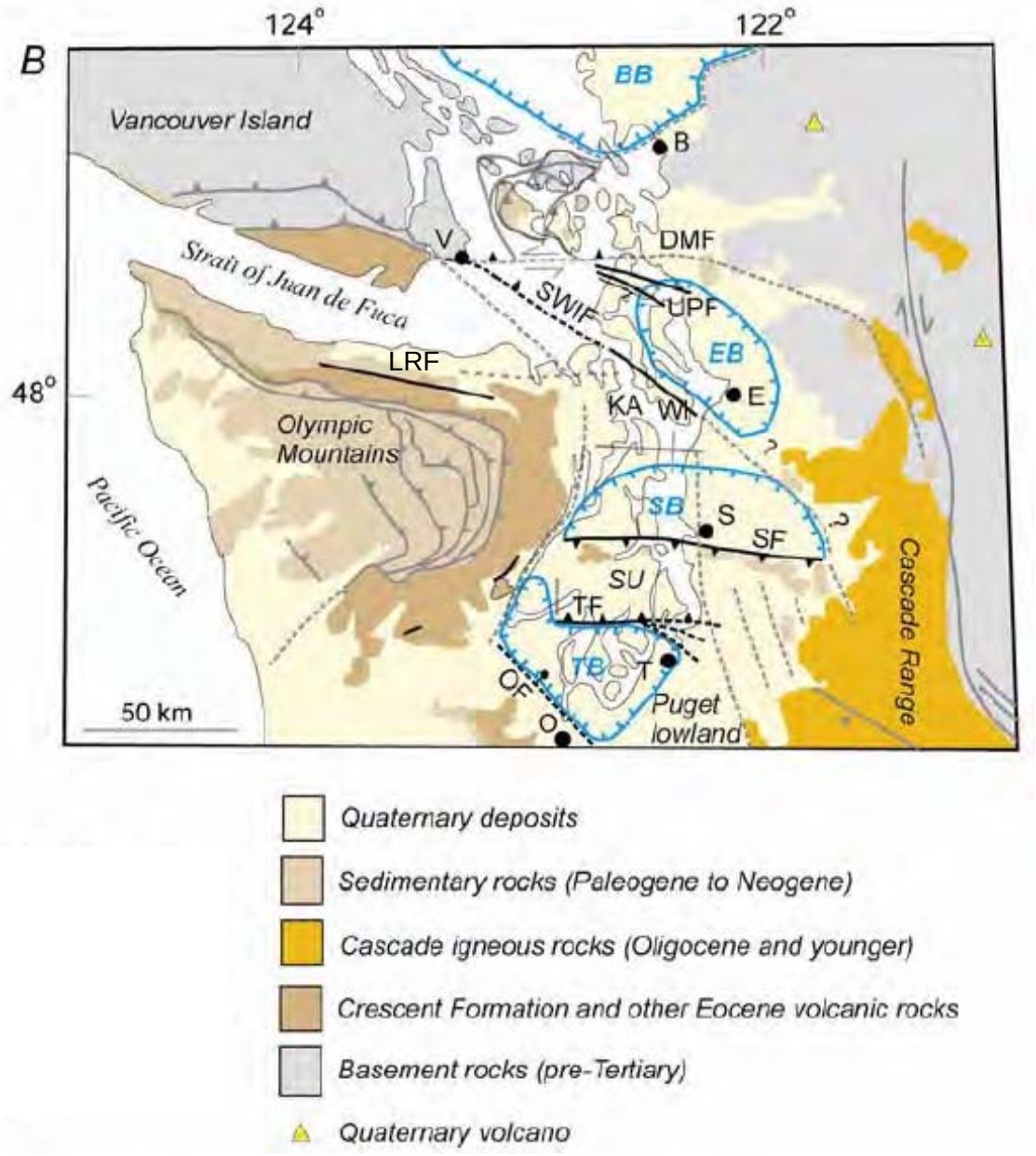

Figure 4. Generalized geology and tectonic map of the Puget Sound region. From Blakely and others (2004) figure 1B. Designations of recently discovered faults: DMF – Devils Mountain fault, UPF – Utsalady Point fault, SWIF – Southern Whidbey Island fault, LRF – Little River fault; SF – Seattle fault, TF – Tacoma fault, OF – Olympia fault. Basin designations: BB – Bellingham basin, EB – Everett basin, SB – Seattle basin, TB – Tacoma basin. Uplift designation: KA – Kingston arch, SU – Seattle uplift. Solid dots denote cities: B – Bellingham, V – Victoria, E – Everett, S – Seattle, T – Tacoma, O - Olympia

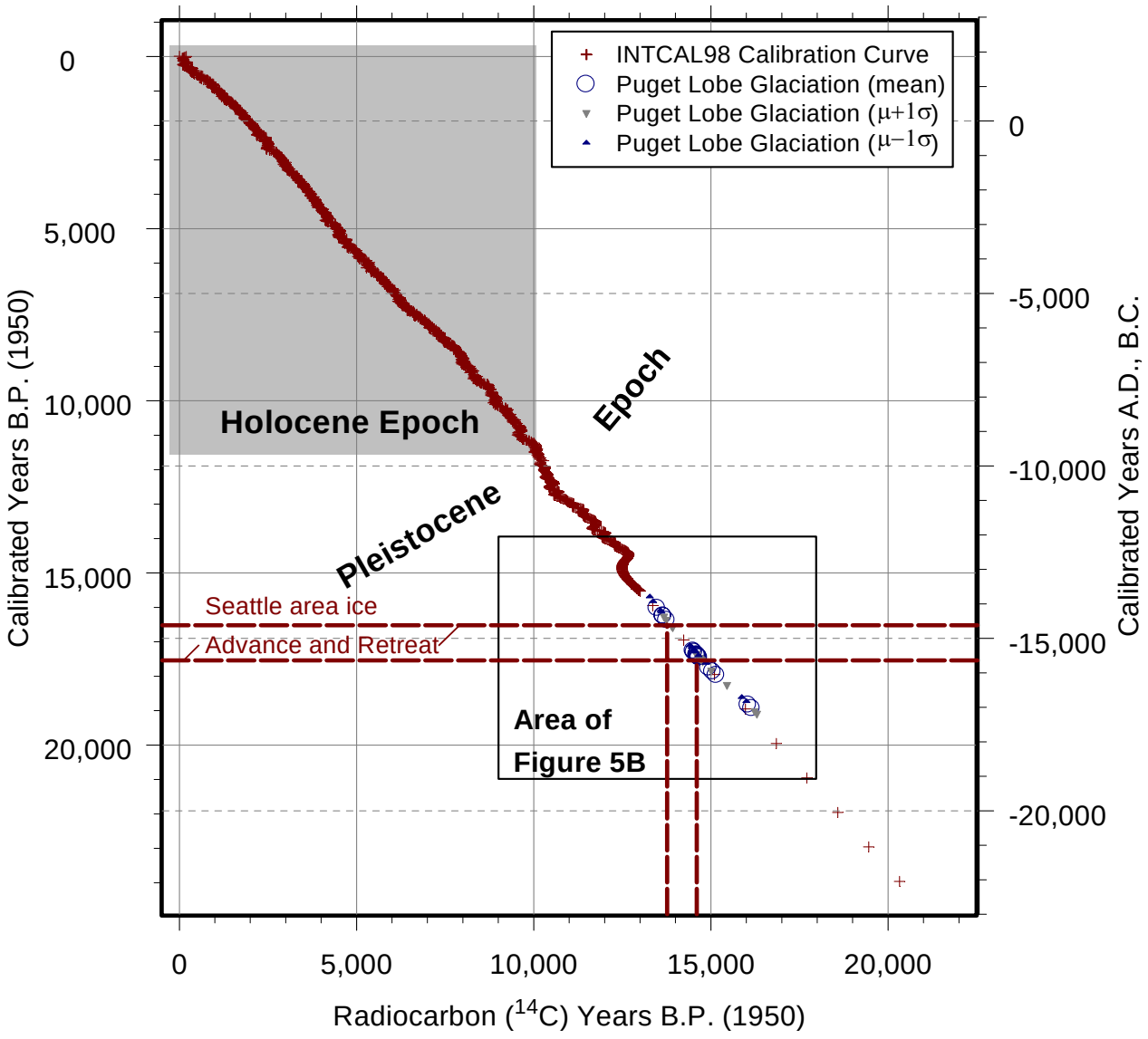

Figure 5A. Relations among radiocarbon and calibrated years before present and calendar years for the most recent approximately 25,000 years of earth history. INTERCAL98 calibration curve is from Stuiver, Reimer, and Reimer (2004, http://radiocarbon.pa.qub.ac.uk/calib/). Ages for advance and retreat of the Puget Lobe of the Cordilleran Ice Sheet are from Porter and Swanson (1998). μ denotes mean; σ denotes standard deviation. B.P. denotes 'before present' based on 1950 A.D. as 0 years B.P. Calendar years B.C. on the right-hand y axis are negative. Figure 5B shows in more detail the area inside the box.

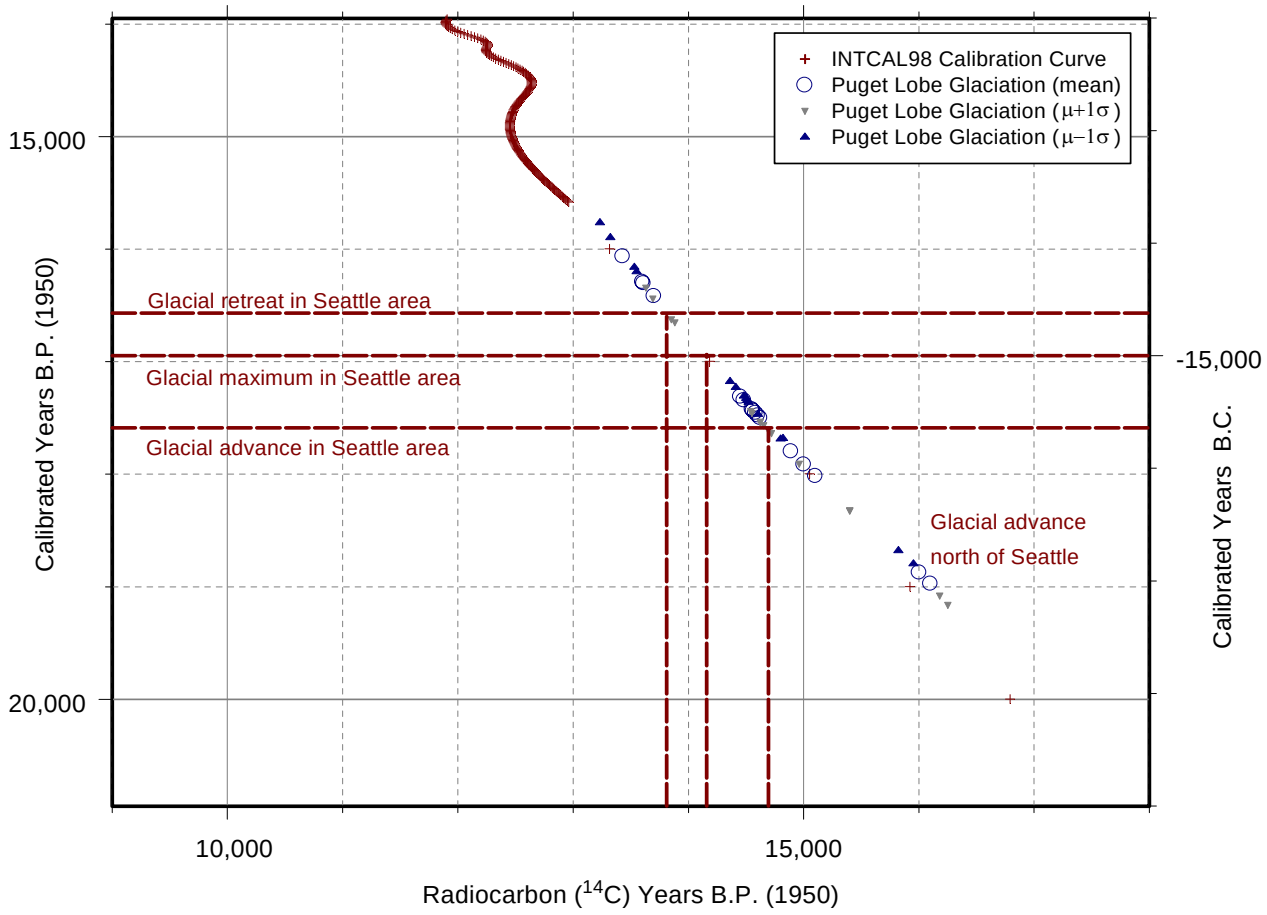

Figure 5B. Relations among radiocarbon and calibrated years before present and calendar years for the period during the most recent advance and retreat of glacial ice in the Puget Sound region. INTERCAL98 calibration curve is plotted from data obtained from the Radiocarbon web site (http://radiocarbon.pa.qub.ac.uk/calib/). Ages for advance and retreat of the Puget Lobe of the Cordilleran Ice Sheet are from Porter and Swanson (1998). μ denotes mean; σ denotes standard deviation. B.P. denotes 'before present' based on 1950 A.D. as 0 years B.P. Calendar years B.C. are negative on the right-hand y axis. Figure 5A shows the context of the most recent approximately 25,000 years of earth history.

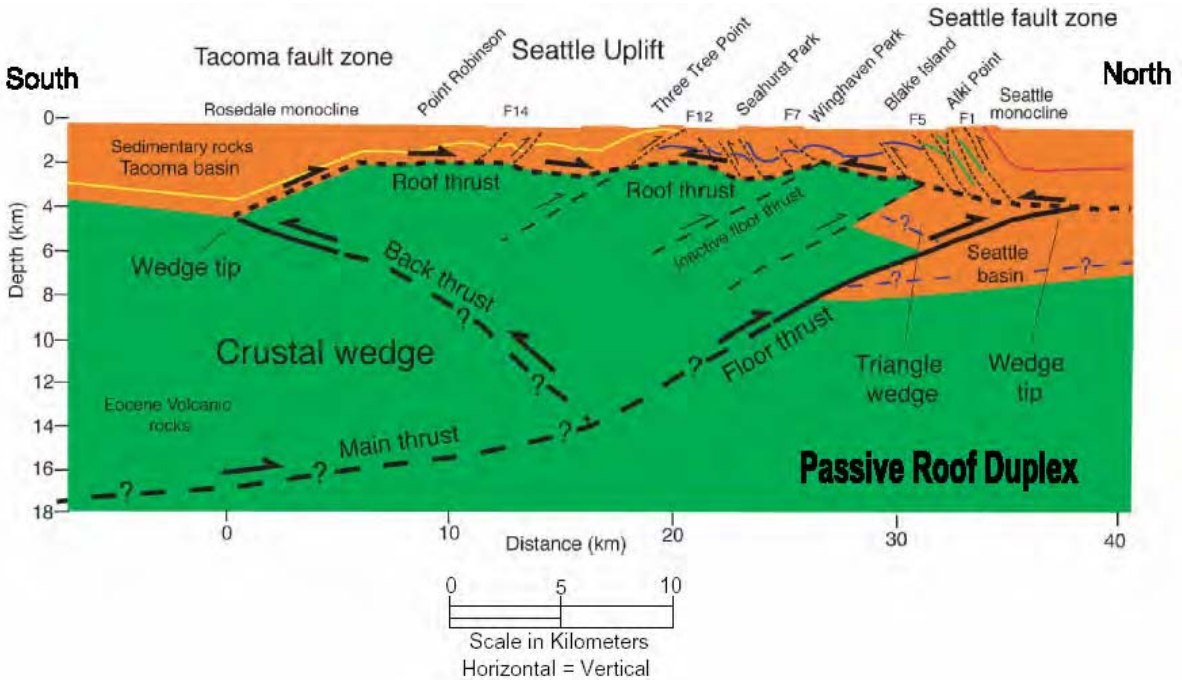

Figure 6. Tectonic framework for Seattle uplift. From Shannon & Wilson (2004, figure 3-7, attributed to Brocher and others, 2003, in press [actually published as Brocher and others, 2004]).

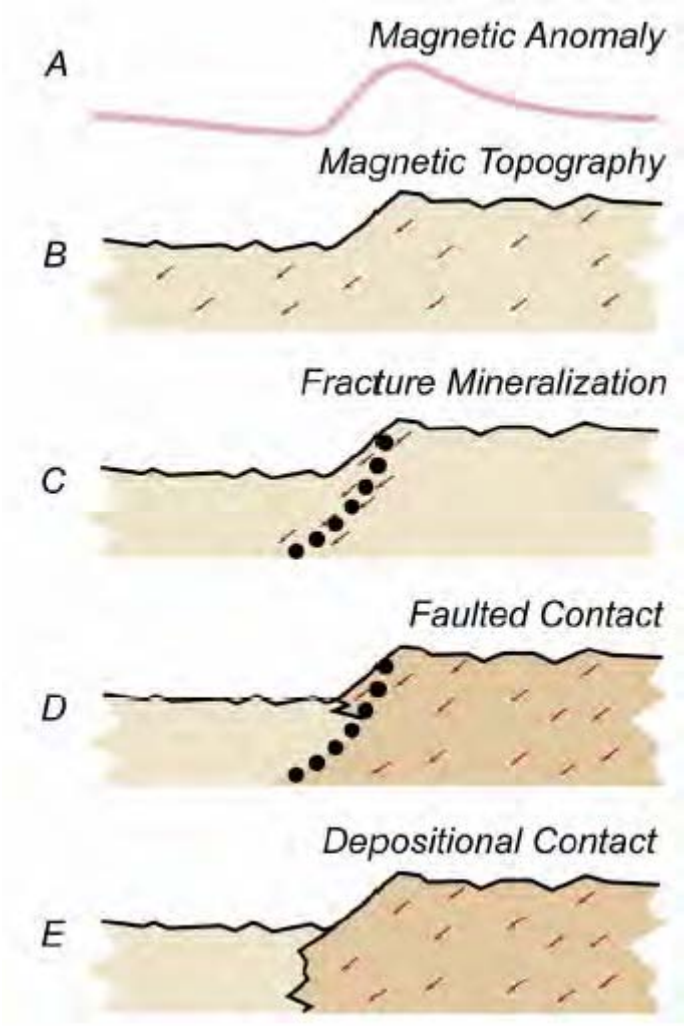

Figure 7. Alternative subsurface conditions that can create an aeromagnetic anomaly. From Blakely and others (2004, figure 12).

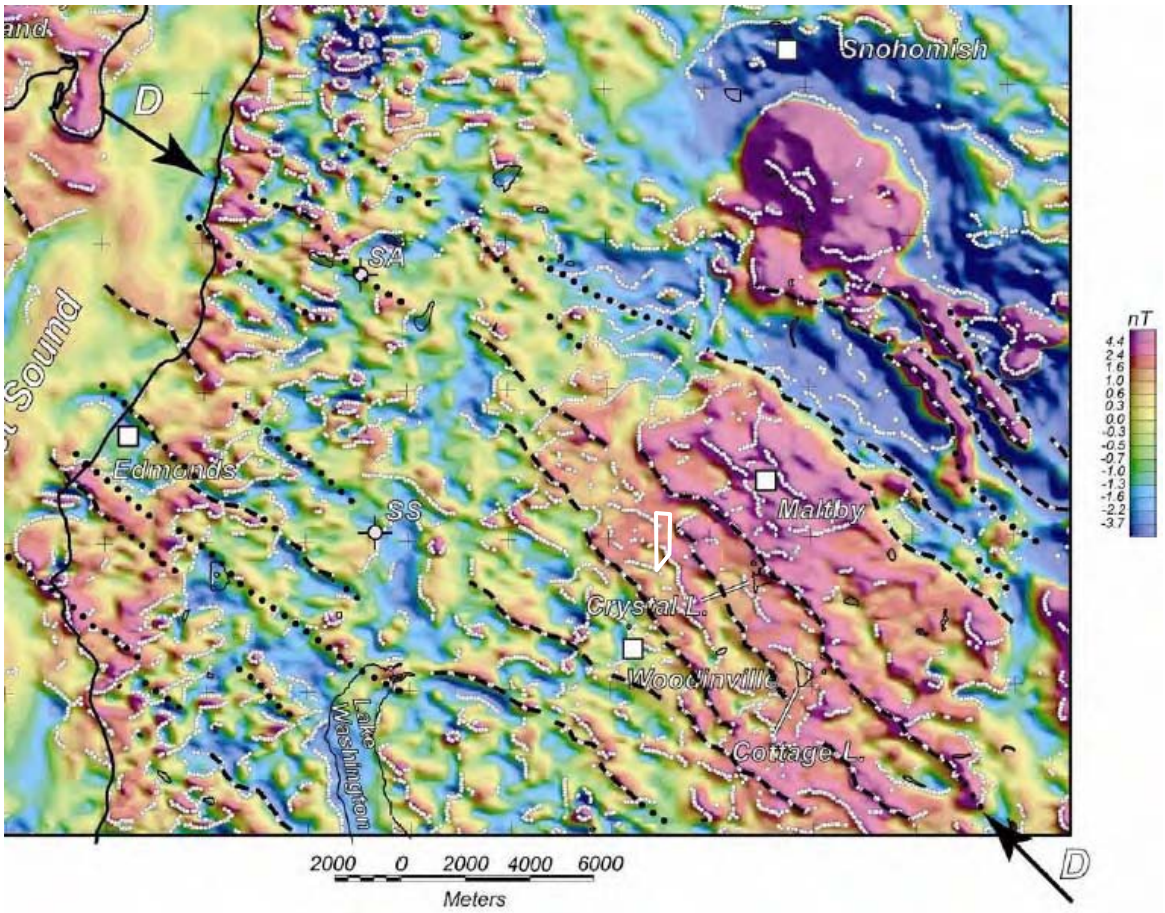

Figure 8. Residual aeromagnetic anomalies in the site area. From Blakely (2004, figure 10). White dots – magnetic contacts determined automatically, black dashed lines – lineaments associated with specific magnetic contrasts, black dotted lines – lineaments identified with lower confidence. Approximate Brightwater Route 9 site boundary (solid white line) added.

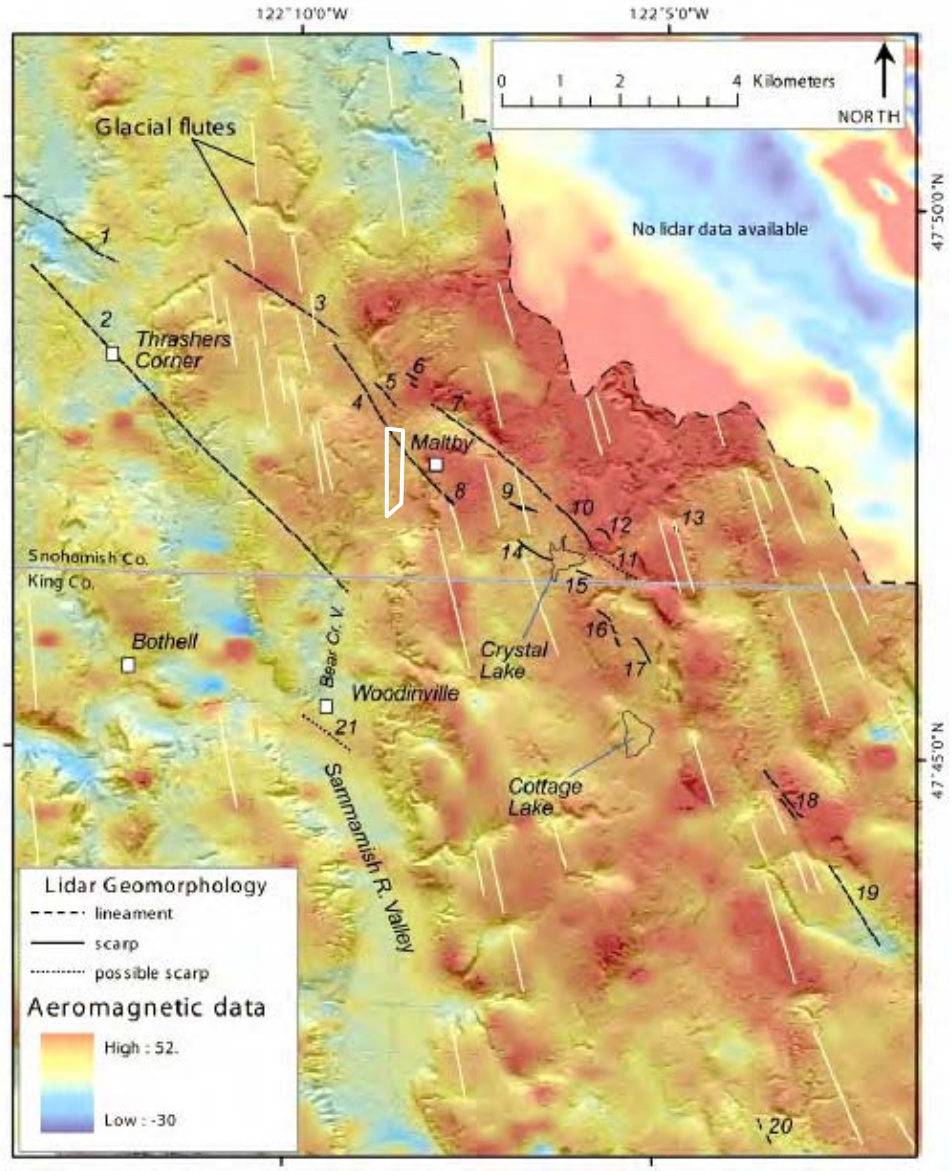

Figure 9. LiDAR map with aeromagnetic data near the Cottage Lake lineament. From Blakely (2004, figure 15A). Thin white lines indicate glacial flute directions. Approximate Brightwater Route 9 site boundary (solid white line) added.

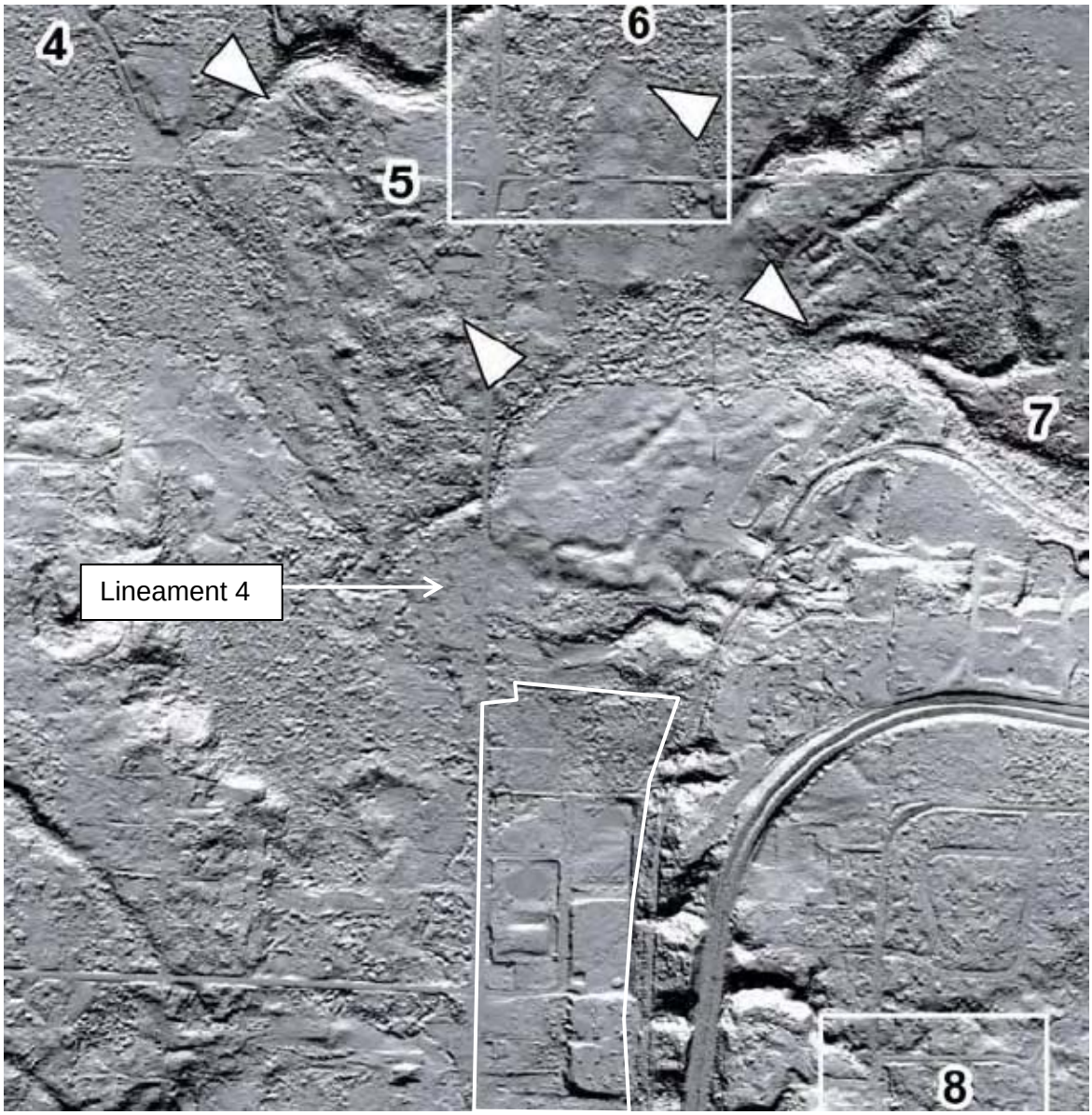

Figure 10. Lineament 4 on King County LiDAR data shown as hillshade relief map. From Blakely and others (2004, figure 17). Lineament 4 notation and Brightwater Route 9 site boundary (solid whit line) added.

Figure 11. Aerial photograph showing site land use as of 2000(?) and trench locations. Note: Trench 1 does not exist. Washington State Plane North Zone coordinates in feet.

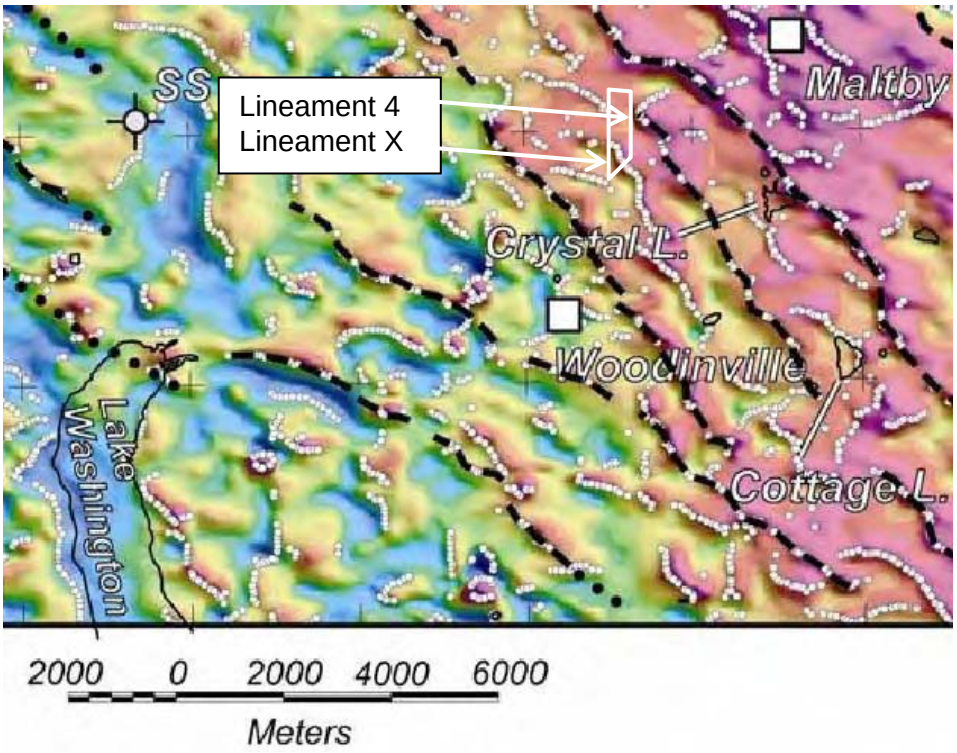

Figure 12. Detail of residual aeromagnetic anomaly map on Figure 8. From Blakely and others (2004, figure 10). Lineament 4 and Lineament X notations and Brightwater Route 9 site boundary (solid white line) added.

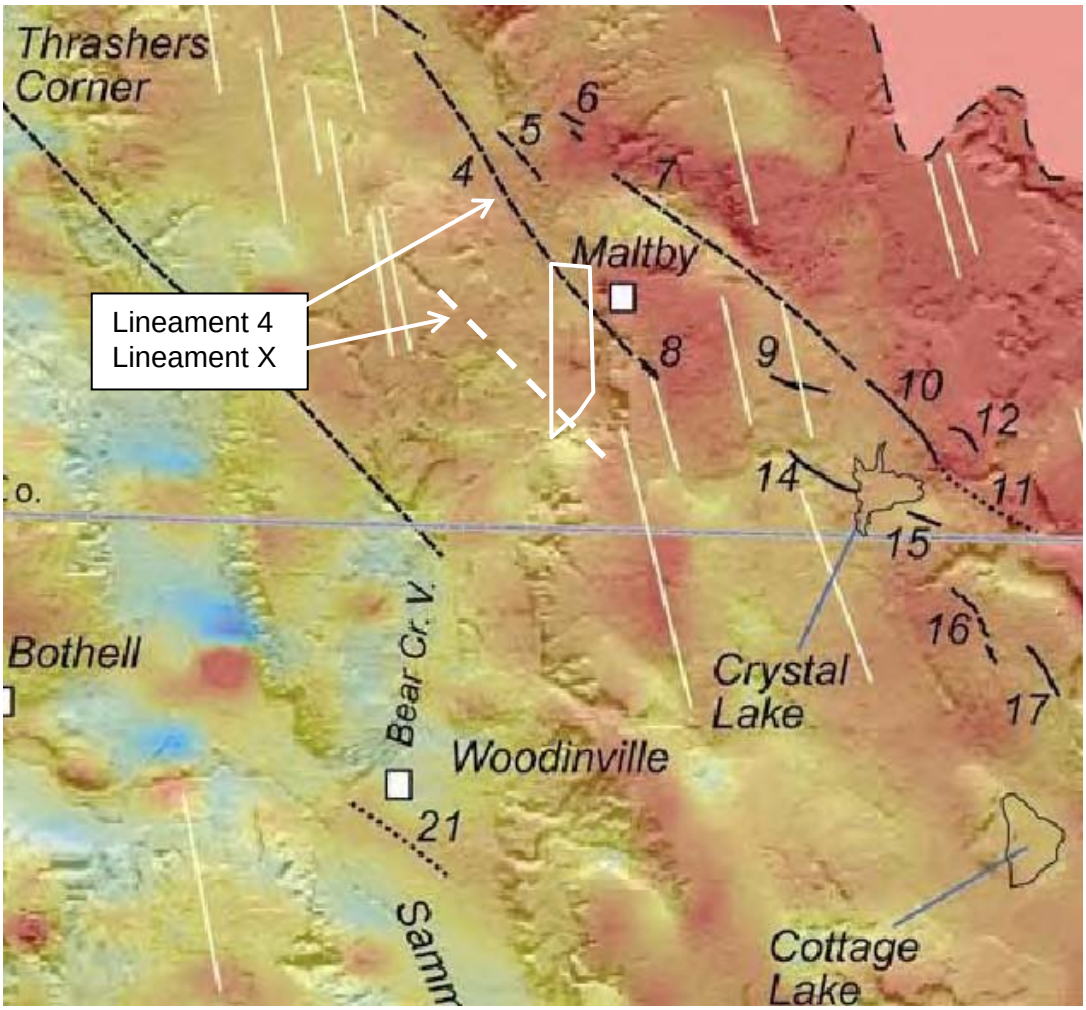

Figure 13. Detail of the LiDAR map with aeromagnetic data shown on Figure 9. From Blakely and others (2004, figure 15A). Lineament 4 and Lineament X notations and Brightwater Route 9 site boundary (solid white line) added.

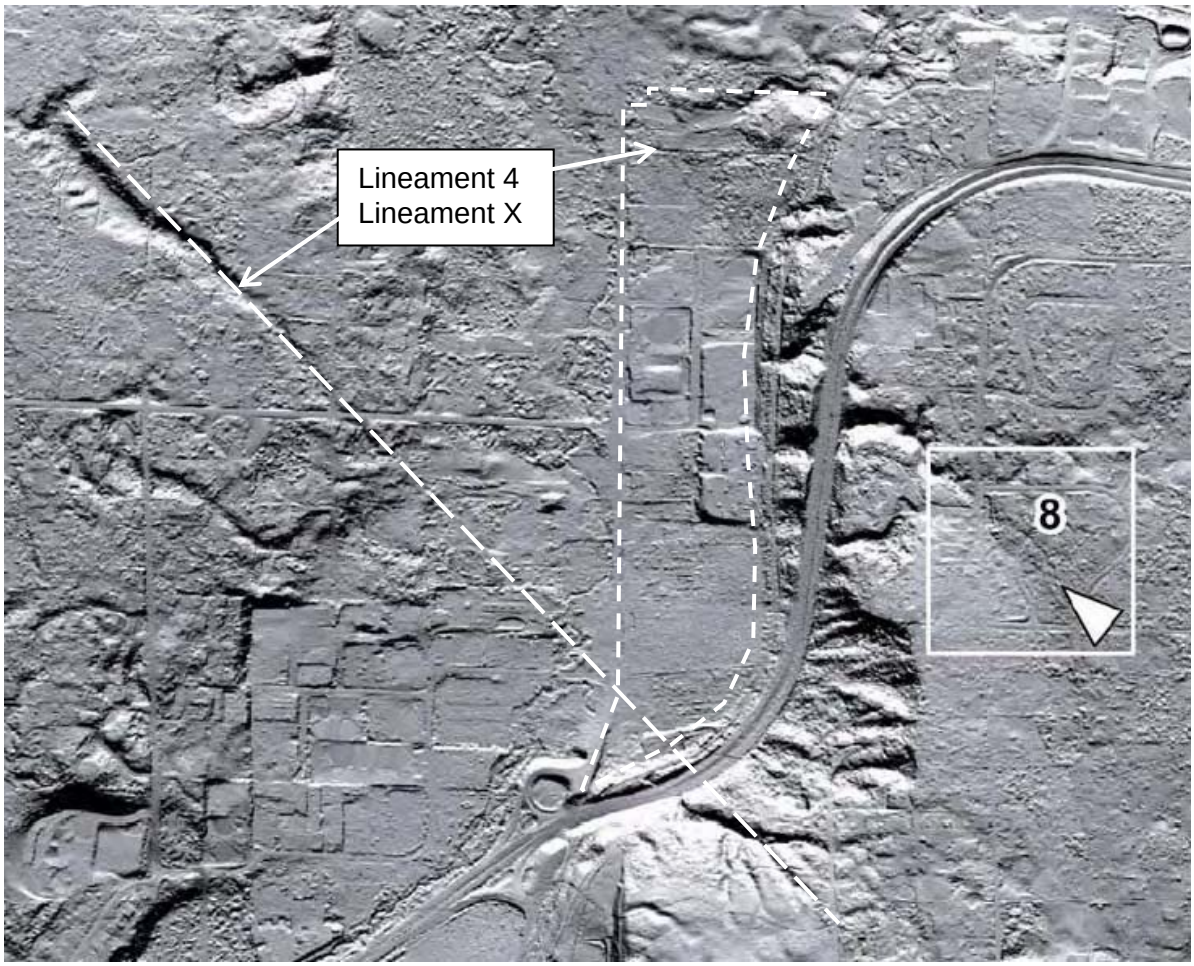

Figure 14. Lineament X on King County LiDAR data shown as hillshade. Base map from Blakely and others (2004, figure 17). Lineament X (long dashed white line), Lineament 4 and Lineament X notations, and Brightwater Route 9 site boundary (short dashed white line) added.

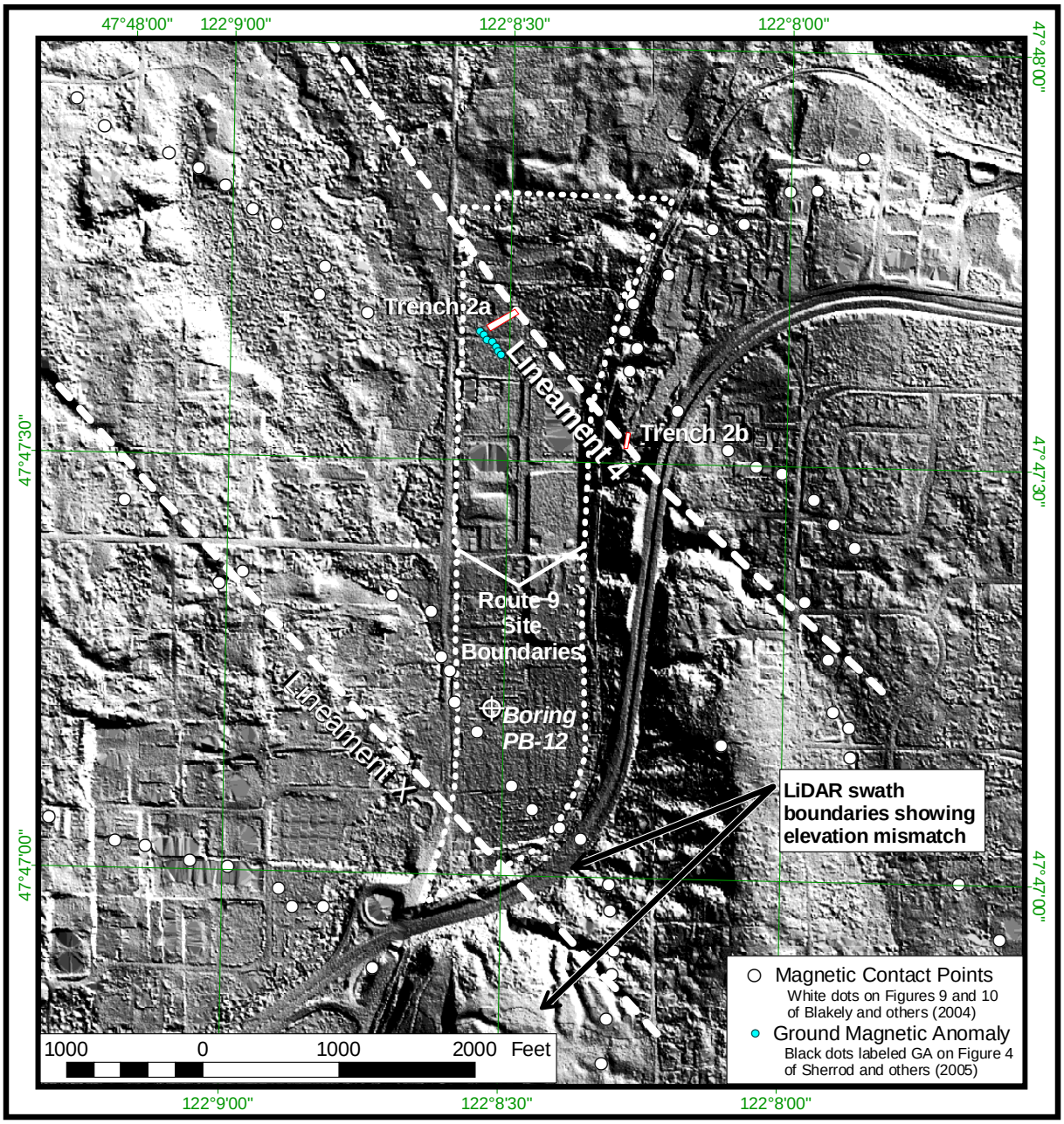

Figure 15. Lineament 4, Lineament X, magnetic contact points, and ground magnetic anomaly GA on King County LiDAR data shown as hillshade. Magnetic contact points plotted from data file provided by the USGS and are the same as the white dots on figures 9 and 10 in Blakely and others (2004). The ground magnetic anomaly point were scaled from figure 4 in Sherrod and others (2005). Boring PB-12 location from CH2M Hill (2004b). Brightwater Route 9 site boundary is in short dashed line. Washington State Plane North Zone projection.

Appendix A.A
Trenching Investigation of LiDAR Lineament 4

A.A.1 Introduction

This appendix contains the results of the trench investigation and geologic interpretation of two trench excavations across the suspected trace of Lineament 4 as identified by scientists with the U. S. Geological Survey (USGS). The data and interpretations presented herein provide support for the Surface-Fault-Rupture Hazard Evaluation. The trenching investigation consisted of the following elements:

- Initial geologic reconnaissance of the North Mitigation Area and an area east of the Route 9 site between the Burlington Northern and Santa Fe (BNSF) rail tracks and Route 522,
- Three-dimensional laser scan survey of one trench,
- Geologic mapping of exposures created in two shallow trenches,
- Preparation of field and Autocad formatted trench logs, and
- Interpretation of the stratigraphy and geologic structure exposed in the trench.

Members of the Brightwater Design Team participated in geologic reconnaissance, preliminary cleaning of the trench sidewalls, and field observations. AMEC Earth and Environmental, Inc., (AMEC) performed the detailed geologic mapping of the trench exposures and geologic interpretation presented in this report. Comments on draft versions of this report from the Brightwater Design Team members and USGS scientists have been incorporated through revisions to the text as deemed appropriate.

A.A.2 Geologic Reconnaissance and Surface Conditions at Trench Locations

AMEC engineering geologists visited the site to observe general site conditions prior to the time that trenches were excavated. Surface conditions were noted, including the general topographic setting, railroad cut exposures, and conditions related to the future trench excavations. Topographic profiles were measured along the trench locations using a tape measure and optical level, or a portable slope-angle measuring device.

The northwestern portion of the Brightwater treatment plant site area where the first trench (Trench No. 2a) was excavated is referred to as the North Mitigation Area. This area is characterized by gently sloping topography with local areas of intermittently to perennially ponded water that have been designated as wetlands. This terrain slopes gently westward toward the southerly draining Little Bear Creek, located about 50 to 200 feet west of Route 9. Little Bear Creek flows within a narrow and shallow bank that appears underfit with respect to the wider valley in which it is located. The wider valley is believed to have been created by erosion and deposition that occurred during the last glacial retreat in the area.

The topography ascends eastward above the site-parcel boundary at moderate slope angles toward Route 522. The BNSF rail line is located about midway up this west-facing slope. Rail line cuts along the east side of the rail line exposed Quaternary till and glaciolacustrine beds. These deposits are discussed under the section entitled Stratigraphic Framework. The second trench location (Trench No. 2b) was located along the nose of a topographic spur, located about 50 feet above (in elevation) the BNSF rail line. A portion of this spur is located within a narrow sliver of land that is part of the Route 9 Brightwater site.

A.A.3 Trench Investigation

A.A.3.1 Trench Excavation

Two exploratory trenches were excavated at the site on September 29 and 30, 2004 using a Komatsu PC 150 backhoe with extend-a-boom and 36-inch wide bucket. The location of the trenches were determined by the U.S. Geological Survey based upon recently acquired aeromagnetic and LiDAR data, surface reconnaissance and environmental site constraints. Geologists with the U. S. Geological Survey directed excavation of the exploratory trenches with assistance from members of the Brightwater Design Team.

The first exploratory trench, designated Trench No. 2a, was excavated within the North Mitigation Area. This trench was excavated to a depth of approximately 7 to 8 feet below ground surface (bgs), along a trench length of about 140 feet, and at an azimuth of 060°. Topographic profile measurements along the centerline of the trench prior to excavation indicated that elevation relief was about 6 feet between the higher eastern end and the lower western end (approximate elevations of 179 and 173 feet) respectively.

The second exploratory trench, designated Trench No. 2b, was excavated along the upper portion of a southerly-trending, topographic spur, located east of the Stock Pot Soups Building and BNSF rail line. This trench site was accessed via the GLY construction yard, located west of Route 522. Trench 2b was excavated to a depth of approximately 4 to 4½ feet bgs, along a trench length of 70 feet, and at an azimuth of 016°. Trench locations are shown on Figure A-1.

The sidewalls of Trench 2a were cut back by the Komatsu excavator for safety purposes to angles ranging from 28° to 45° (i.e., slope inclinations of 2:1 to 1:1 horizontal to vertical). An aluminum-framed canopy with plastic sheet covering was assembled over the majority of the trench to permit geologic work during the inclement weather. Groundwater seepage along the base of the trench was periodically removed using a portable sump pump at the southwestern end of the trench and discharged at the ground surface against hay bales to minimize soil erosion. Trench 2b was able to be excavated safely with vertical sidewalls because of its shallow depth.

Monitoring well FB-24, installed by CH2M Hill during previous work at the site, was partially exposed during excavation of Trench 2a at the North Mitigation Area. The well

was abandoned by Gregory Drilling of Redmond, Washington by removing the exposed 2-inch PVC casing and filling the screen section and casing to the ground surface with bentonite chips (Aspect Consulting, 2004). The chips were then hydrated with potable water. A well abandonment form was submitted to the Washington State Department of Ecology.

A.A.3.2 Geologic Logging

An AMEC engineering geologist, working independently of the USGS, mapped the geologic contacts between the various subsurface soil and stratigraphic layers encountered in the trenches. A horizontal (level string) line was established by AMEC along the northern sidewall of Trench 2a with horizontal stationing every five feet to facilitate horizontal and vertical location while geologic mapping in Trench 2a. The USGS later surveyed and installed a one-meter by one-meter string line grid (horizontal by vertical) along the southern and northern sidewalls in the eastern half of Trench 2a. The USGS also installed a one-meter by one-meter survey grid along the eastern sidewall of Trench 2b.

AMEC's engineering geologist classified geologic units and subunits visually using the Unified Soil Classification System, and where appropriate, described soil pedologic development using Soil Conservation Service terminology (Soil Survey Staff, 1975). The lithologies of the geologic units and subunits were described according to their predominant grain size, Munsell soil color, bedding thickness and character, and physical properties. The northern sidewall of Trench 2a and the eastern sidewall of Trench 2b were mapped at a scale of 1 inch = 5 feet using level lines installed by AMEC and USGS, respectively, for elevation and horizontal station control. In addition, a portion of the southern sidewall and a small section of the northern sidewall of Trench 2a were mapped at a detailed scale of 1 inch = 2 feet using the USGS grid lines.

Logs of Trenches 2a and 2b are presented at a scale of 1 inch = 5 feet on Plates 1 and 3, respectively, and the detailed logs of Trench 2a (at a scale of 1 inch = 2 feet) are shown on Plate 2. Each trench log includes a scanned image of the field log showing the geologic contacts and internal stratigraphy and for illustrative purposes, a second log depicting geologic contacts and selected individual beds minus the stratigraphic details of the field log. Lithologic descriptions and geologic structure data are also provided on the logs. Color reproductions of the field logs are presented on Figures A-2, A-3, A-4, and A-5. Views of 3-dimensional laser scanner data of Trench 2a are shown on Figures A-6, A-7, A-8, and A-9. Selected photographs of Trench 2a are presented on Figures A-10, A-11, A-12, A-13, and A-14.

The trenches were left open for about four weeks, during which time Brightwater Design Team members and geologists with the U.S. Geological Survey studied, photographed, and mapped the exposures. The trenches were backfilled with excavated earth materials under the observation of the USGS. The backfilling work was completed after AMEC's engineering geologist left the site.

A.A.4 Stratigraphic Framework

Geologic mapping and assignment of stratigraphic units in the Bothell, Maltby and Kirkland 7.5 minute quadrangles by J.P. Minard of the U.S. Geological Survey (1985a, 1985b, and 1983, respectively) provide a regional perspective of the Quaternary-age deposits in the vicinity of the Brightwater Route-9 site. This work was later compiled in the 1:100,000 scale "Geologic Map of the Surficial Deposits in the Seattle Quadrangle" (Yount et al., 1993). Most recently, geologists working under the Pacific Northwest Center for Geologic Mapping Studies (GeoMap NW), formerly known as the Seattle-Area Geologic Mapping Project (SGMP), have published a draft version of a composite geologic map of the Snohomish-King County area at 1:24,000 scale (Booth et al., 2004). This most recent geologic map is based upon prior mapping and new mapping in selected areas. Booth and others (2004) depict several Quaternary-age geologic units at the Brightwater Route 9 site including Vashon Recessional Outwash, Vashon Advance Outwash, and Lawton Clay. A geologic contact between Vashon Recessional Outwash deposits and Lawton Clay is shown on the Snohomish-King County Geologic Map (Booth and others, 2004) at about the 200-foot-elevation contour. The geologic map also delineates a narrow swath of younger alluvium bordering Little Bear Creek.

Glacial deposits in the vicinity of the Brightwater Route 9 site have a range of ages, but the most recent glaciation is called the Vashon Stade of the Fraser glaciation. During this glaciation, the Puget glacial lobe advanced from British Columbia toward the south to a point near Olympia, achieving a thickness greater than 3,000 feet in the project area (Thorson, 1980), and then receded rapidly back toward the north during a relatively short period of time. Deposits older than the Vashon Stade of the Fraser glaciation were either overridden by Vashon ice or scoured by advancing ice. Melt water from receding ice also eroded the Vashon and older deposits and left behind coarse- to fine-grained sediments (recessional outwash) that were deposited within fluvial to lacustrine environments. Vashon Recessional Outwash deposits were not overridden and compressed by glacial ice; consequently, they tend to be normally consolidated. They are typically less dense and softer than the older (pre-Vashon) glacial deposits.

Radiocarbon dates for organic samples in the central Puget lowland (Porter and Swanson, 1998) indicate that the Puget glacial lobe advanced to the latitude of Seattle by about 14,500 ^{14}C yr B.P. (17,590 cal (i.e., calibrated) yr B.P. 1950). The ice reached its maximum advance by about 14,000 ^{14}C yr B.P. (16,950 cal yr B.P.), then rapidly retreated northward, passing the Seattle area by about 13,600 ^{14}C yr B.P. (16,575 cal yr B.P. (Porter and Swanson, 1998)).

The geotechnical site characterization by CH2M Hill and Shannon & Wilson (CH2M Hill, 2004) provided a stratigraphic framework for interpretation of the trench exposures. The geotechnical site characterization included drilling numerous exploratory soil borings and test pits at the Brightwater site. One of the geologic sections prepared for the geotechnical site characterization intersected the eastern portion of Trench 2a and depicted alluvial sediments underlain at shallow depth by coarse and fine-grained recessional outwash deposits (CH2M Hill, 2004). Prior to the trench excavation, nine soil

borings were drilled along the trend of Trench 2a and subsequently converted into monitoring wells to provide data for design of potential trench dewatering (Aspect Consulting, 2004). Two of the nine borings were drilled near the western and eastern ends of the trench, whereas, the other seven were drilled beyond the eastern end of the trench. Although the wells were not used to dewater the trench, geologic logging of in-situ samples collected at frequent intervals resulted in a geologic section drawn from the western end to well beyond the eastern end of Trench 2a (Aspect Consulting, 2004). Vashon Recessional Outwash is shown underlain at variable depth by Vashon Ablation Till or weathered Vashon Diamicton on the geologic section (Aspect Consulting, 2004).

A.A.5 Trench Exposures

A.A.5.1 Trench 2a Geologic Units and Stratigraphy

Artificial Fill: Undocumented (Trench log symbol: af)

Artificial fill soils, apparently placed during prior grading operations, were observed throughout the upper portion of the trench. Fill materials were apparently not identified in the logs of recently drilled soil borings in the area of Trench 2a (Aspect Consulting, 2004). The geotechnical site characterization (CH2M Hill, 2004) reported that the Brightwater Route 9 site has been extensively re-graded. It is our understanding that prior site usage had included periods of logging and agriculture dating back to the early 1900's. It is assumed that no engineering observation of these fill soils was provided at the time of grading. The fill depth varied between approximately three and four feet below ground surface (bgs).

Fill soils encountered in the trench appeared to consist of more than one layer; however, mapping emphasis was not placed on logging details of the fill. The fill consisted primarily of medium to dark brown, fine sandy silt with few to some well-rounded gravel. Scattered glass fragments, minor amounts of metal, and pieces of sawed wood were encountered in the fill during excavation of the trench. The fill appeared generally loose to medium dense.

Wetland Deposits/ Organic Soil (Trench log symbol: Hw)

Organic-rich sediments deposits of inferred Holocene age were exposed beneath the artificial fill along the length of Trench 2a. The depth to these sediments ranged from approximately three to four feet bgs. Thickness ranged from approximately one foot at the western end of the trench to three feet toward the eastern end. These sediments were mapped as a single geologic unit overlying recessional outwash deposits.

This unit appeared to consist of two slightly differing lithologies. The upper portion consisted of black (Munsell soil color 5Y 2.5/1), organic/peat-rich silt with scattered roots that graded below to dark brown to black, clayey silt with trace coarse sand and some organic material. Sub-rounded to well-rounded gravels comprised less than about five percent of the unit, ranged from about ½- to 2-inch diameter, and appeared randomly

scattered. The contact between the fill and the wetland deposits appeared sharp and undulatory. Near the contact, the upper portion of the wetland deposits appeared darker and suggested a disturbed plow zone from prior agricultural activity. A sharp to locally gradational and undulatory to irregular contact separated the base of the wetland deposits from the underlying recessional outwash deposits.

The peat/organic-rich character of the upper portion of this unit suggests that it formed as a poorly-drained forest soil on the lower portion of the unit. It is inferred that the lower portion of the unit may be derived in part by alluvial processes, rather than being part of the wetland soil. This inference presumes that a possible source for the sediments in the lower portion of the unit is from the westward flowing drainages that emanate from the west-facing slopes bordering the eastern portion of the Northern Mitigation area and drain into Little Bear Creek. The proximity to Little Bear Creek suggests an alternate possibility that the sediments may have been deposited by Little Bear Creek during overflow of its banks or perhaps, at a former time when the Little Bear Creek had a different drainage configuration. However, this possible origin is considered unlikely due to the absence of interbedded sandy or silty lenses that are commonly found in overbank deposits.

Based on the lithologic changes cited above, there is a remote possibility that the lower portion is a weakly developed soil B-horizon that developed from the underlying recessional outwash deposits. However, neither soil structures that are characteristic of soil B-horizons nor an underlying C_{ox} (i.e., weathered parent material) were apparent. It is noted that alluvial deposits ranging from about 5 to 10 feet thick have been reported in previously drilled soil borings and test pits in the North Mitigation area (CH2M Hill, 2004).

A lenticular shaped deposit, inferred to be of colluvial-alluvial (symbol Hcol) origin, was exposed at the base of the wetland deposits east of Trench station 1+35. This poorly sorted, massive appearing deposit consisted of olive-gray (5Y 3/2), gravelly, fine- to medium-grained sand with silt. It appeared gradational with the underlying recessional outwash deposits, which are described in the following section.

Vashon Recessional Outwash Deposits (Trench log symbol: Qvrf)

A sequence of interlayered sand, sandy gravel, silt, and minor silty clay was exposed beneath the wetland-alluvial deposits to the base of the trench. The contact between the interlayered sediments and overlying wetland deposits appeared sharp and undulatory with many areas along the contact that exhibited irregular relief. In general, the sand and silt beds (i.e., layers) ranged in thickness from laminated (less than 3/8-inch thick) to thinly bedded (0.1 to 0.3-ft. thick) and the sandy gravel to gravel beds ranged from thinly- to medium thickly-bedded (0.1 to 1-ft. thick). Bedding appeared primarily planar parallel and continuous with some lenticular-shaped beds and minor channel lenses. Bedding contacts appeared generally sharp, although some beds exhibited gradational contacts.

Blow count data reported from drive samples collected in soil borings (CH2M Hill, 2004, and Aspect Consulting, 2004) near the area of Trench 2a indicates that the granular sediments encountered to the depths of Trench 2a are predominantly medium-dense. A probable recessional outwash origin for these interbedded sediments appears consistent with published geologic mapping (Booth and others, 2004), subsurface characterization and description from soil borings and test pits (CH2M Hill, 2004), and stratigraphic features observed in Trench 2a that are commonly associated with fluvially derived sediments. A Vashon age assignment for the recessional outwash deposits is based upon the prior mapping, geomorphic position along the valley floor, and apparent relative densities (medium dense sand and gravel) suggestive of normally consolidated sediments not overridden by ice.

The recessional outwash deposits exposed in Trench 2a were subdivided during the trench investigation into several mappable beds and subunits as shown on the trench log. Lithologic composition formed the primary basis for subdividing the outwash deposits. Brief lithologic descriptions of the individual subunits are presented below in general order of increasing geologic age. Detailed lithologic descriptions of all geologic units are provided on the trench log (Plates 1 and 2).

Subunit $3a_1$ was present as a mappable unit directly beneath the wetland deposits and stratigraphically above all other recessional outwash subunits. Consequently, it was interpreted to be the youngest of the recessional outwash subunits. It was comprised predominantly of orange-brown (10YR 4/6) fine- to coarse sandy gravel at the base, grading upward and laterally into fine- to coarse-grained sand with scattered gravels and local zones of silty, fine grained sand. The subunit appeared crudely bedded, lenticular shaped, and oxidized relative to the underlying subunits. The basal contact appeared conformable with the underlying beds west of trench station 1+10, except for localized erosional scour and/or cut-fill deposition. East of trench station 1+15, the basal contact formed an angular unconformity, above tilted recessional outwash deposits. The geometry and significance of this angular unconformity is discussed in the following section. An alternative origin for the sediments comprising this subunit is that they were deposited by an ancestral Bear Creek drainage, which would imply an age younger than recessional outwash deposition. The age of this subunit is unknown; however, research scientists from the University of Washington collected samples for thermoluminescence (TLM) age dating.

Subunit 3b was exposed beneath subunit $3a_1$ from the western end of the trench to station 1+10. The lithology consisted of olive gray (5Y 4/2 to 5Y 5/2), fine- to coarse-grained sand with thinly interbedded, silty, fine to medium grained sand, laminae of sandy silt, and very thin to thin lenses of sandy gravel. This interbedded subunit was about one to three feet thick. A tentative correlative subunit to this was mapped between station 1+17 and 1+21, beneath subunit $3a_1$. The correlative subunit, designated $3a_2$, consisted of fine- to coarse-grained sand with thin laminae of silty, fine-grained sand.

Complex geometric relationships were observed between station 1+11 and 1+17. Due to liquefaction features and minor fault offsets, it was difficult to correlate the stratigraphy

across this zone. Between station 1+11 and 1+16, the basal contact of a sandy gravel lens (subunit $3a_3$), inferred to be correlative with subunit $3a_1$, was locally steep, irregular and at a lower elevation relative to the basal contact of subunit $3a_1$ to the east and west. Further details of this zone are presented in a following section on Trench 2a geologic structure.

Subunit 3b was underlain by subunit $3c_1$ between station 0+45 and station 1+10. West of station 0+45, subunit $3c_1$ dipped gently beneath the trench bottom. This subunit consisted primarily of very thinly bedded to laminated, fine- to medium-grained sand, sandy silt, fine-grained sand, clayey silt, and minor silty clay. The silty clay and clayey silt beds were mapped as discrete beds on the trench log. Sub-horizontal beds in subunits 3b and $3c_1$ terminated laterally against tilted beds between station 1+00 and 1+10. The angular discordance between the sub-horizontal and tilted beds formed an angular unconformity. The strata directly beneath the unconformable contact, designated subunit $3c_2$, were compositionally similar to subunit $3c_1$.

Subunits 3d through 3L were mapped east of a narrow zone of faults located between station 1+11 and 1+13. The faults are described under the following section on geologic structure. Subunits $3d_1$ through $3d_3$ were delineated adjacent to the east side of the easternmost fault trace. Subunit $3d_2$ comprised a lens-shaped brecciated unit of angular clayey silt and fine sand fragments within a fine- to medium-grained sand matrix. The fragments were possibly dislodged from similar appearing strata within and adjacent to the narrow zone of faults. This geometric relationship is detailed on Plate 2. The breccia lens appeared overlain by massive, fine- to coarse-grained sand with scattered gravel, designated subunit $3d_1$ (perhaps, correlative with subunit 3b) on the trench log. The massive character of subunit $3d_1$ contrasted with the moderately-well bedded character of adjacent subunits. These two subunits appeared anomalous with respect to the layered bedding observed in all the adjacent subunits. The disrupted nature of subunit $3d_2$ and the massive appearance of subunit $3d_1$ are inferred to be a result of a liquefaction event that occurred during strong ground shaking. A liquefaction origin for these units is supported by the observation of similar, massive appearing sand zones at other locations within the trench, directly adjacent to or above sand dikes. The nature of the sand injection features are presented in a following section.

The stratigraphic relationship between the units located adjacent to the west and east sides of the fault was difficult to interpret; however the inference that subunits $3d_1$ and $3d_2$ are liquefied remnants of subunits 3b and 3c, respectively, is suggested by the following observations. The lithologic composition of the fragments in subunit $3d_2$ appeared similar to the finer strata (silt and clay beds) of subunit 3c. Secondly, the fragments appear to be dislodged from an adjacent sequence of very thinly interbedded fine sand, silt, and clay that are probably part of subunit 3c. Lithologic similarities between subunits 3b and $3d_1$ were also apparent. Lastly, the amount of stratigraphic offset appeared relatively minor across the faults, suggesting that dissimilar subunits are not juxtaposed across the faults.

Subunits 3e through 3L were labeled according to their progressively lower stratigraphic position (i.e., increased depth in the stratigraphic column). The top and bottom of these subunits were placed at significant changes in lithologic composition in order to facilitate understanding the geologic structure of this tilted bed sequence. Subunit 3e consisted of a thin, undulatory silt bed and an underlying silty clay lens. The silt bed and silty clay lens were underlain by a thin, lenticular bed of sandy gravel, designated as subunit $3f_1$. Both subunits were tilted westward and overlain unconformably by a lens of fine- to coarse-grained sand with laminae of silty, fine-grained sand. As a consequence of the unconformity, the up-dip ends of subunits 3e and $3f_1$ were erosionally truncated.

Subunits 3e and $3f_1$ conformably overlie a 6 to 9-inch thick bed of fine-to medium-grained sand with laminae of fine sand, designated as subunit $3f_2$. This subunit was successively underlain in an eastward direction by tilted subunits 3g, 3h, 3i, $3j_1$, $3j_2$, and $3j_3$. The predominant lithology comprising these subunits included sandy gravel, interbedded with fine- to coarse-grained sand, gravelly, fine to coarse-grained sand, and laminae of fine-grained sand. Geologic contacts mapped between these subunits were based on changes in the predominant grain sizes comprising each subunit. The eastern up-dip ends of subunits 3g through 3i were observed overlain unconformably (with angular discordance) by a sandy gravel unit that capped all older subunits between station 1+16 and station 1+36 along the northern sidewall. This ‘capping’ gravel appeared compositionally similar to subunit 3a that was mapped west of the faults and consequently is interpreted to be correlative. Details and interpretation of the unconformities exposed along the trench sidewalls are provided in the following section.

Two more subunits were mapped at the eastern end of the trench. The stratigraphic position of these subunits – 3k and 3L – relative to adjacent strata to the west was undetermined because of relatively poor exposures in the trench sidewall and difficult delineation of the fluvial bedforms in this area of the trench. Subunit 3k consisted of medium- to coarse-grained sand with thin laminae of fine sand and subunit 3L consisted of crudely bedded fine- to coarse-grained sandy gravel with gravels ranging from ½- to 4-inch diameter.

Sand Intrusions

Sand intrusions were observed crosscutting the recessional outwash deposits at seven separate locations along the northern sidewall, shown on the trench log, Plate 1. The intrusions appeared to terminate beneath the wetland deposits, except at station 0+73 where a narrow sand injection dike intruded both the recessional outwash deposits and the overlying wetland deposits. Sand intrusions were also observed at several locations along the southern sidewall, although no effort was made to correlate them across the trench due to the wet muck along the trench bottom.

The sand intrusions generally formed irregular-shaped dikes that in several instances branched upward into narrower injections. Several intrusions appear to have obliterated bedding adjacent to the sides and above the injection dikes, whereas others appeared to drag adjacent bedding upward on a scale of several inches. The trench log, however, only

shows the cross-cutting sand dikes and not the zones of obliterated strata which probably were liquefied at the time the sand dikes formed. The sand intrusions are interpreted to be features of liquefaction of granular outwash sediments in response to earthquake-generated strong ground shaking at the site. The absence of sand dikes that cross-cut each other or cross-cut older liquefied deposits precluded evaluation of whether the liquefaction features formed during a single event or multiple strong ground-shaking events.

A.A.5.2 Trench 2a Geologic Structure

Structural features interpreted to have formed by tectonic (coseismic) deformation were mapped along portions of the north and south sidewalls of Trench 2a. These secondary (i.e., post depositional) features consisted of folded strata, angular unconformities, and minor fault displacement. The structural interpretation of these features is discussed in the following section (Structural Interpretation) and the geologic structures mapped in Trench 2a are described below.

Recessional outwash subunits 3b and $3c_1$ were found to be sub-horizontal to gently dipping (apparent dips of about 2 to 5 degrees) between the western end of the trench and station 1+00. An apparent localized flexure was observed at station 0+50, where a strike of N. 11° W. and dip angle of 14° SW. was measured on a well-developed bedding surface between sandy silt and fine-to medium sand (within subunit $3c_1$). Subunits $3f_1$, $3f_2$, 3g, 3h, and 3i were tilted into a monoclinal flexure east of station 1+15. Three bedding surfaces measured within this flexure showed a range in strike of about N. 05° W. to N. 30° W. with dip angles ranging between 23 and 34° SW. Thus, the strike of beds within the monoclinal flexure was about perpendicular to the trench azimuth.

East of station 1+30, the apparent dip of subunit 3i flattened along the northern sidewall to subhorizontal and two underlying subunits, $3j_1$ and $3j_2$ appeared to dip gently eastward. The apparent eastward dips indicate that subunits $3j_1$ and $3j_2$ have been deformed into an open fold (i.e., fold geometry exhibiting gently dipping limbs). Strikes and dips of about N. 10° E. / 10° SE and N. 50° E. / 30° SE were measured on two laminae surfaces within subunit 3k near station 1+40. The southeast dipping laminae at the eastern end of the trench supports the interpretation that the monoclinal flexure is at least locally warped into an open-fold. The width of the zone of tilting and folding extended from about station 1+00 to at least the eastern end of the mapped portion of the trench sidewall at station 1+45.

A similarly appearing monoclinal flexure was exposed in the southern sidewall (Plate 2), where delineation of the stratigraphy and structure was hindered by sand intrusions and krotovina (i.e., small-animal burrows in-filled with soil). The hinge point (i.e., angular change or inflection in dip from subhorizontal to moderately dipping) of the monoclinal flexure was observed at about station 1+04 along the base of the southern sidewall and station 1+02 along the northern sidewall. A trend of approximately N. 25° W (155° azimuth) was measured along the hinge axis by sighting the two hinge points on either sidewall. Only one bedding attitude was measured along the southern sidewall. A

bedding surface between the top of a silt bed and the base of a fine-to medium-grained sand layer had a strike of N. 04° E. and dip angle of 22°NW.

Two angular unconformities were exposed along the eastern half of the northern sidewall. They were mapped on the trench log and are shown by dashed green lines on Plate 1. Only one of the unconformities was clearly evident on the southern sidewall, perhaps due to the shallow level of exposure. One unconformity was exposed along the northern sidewall between station 1+00 and 1+10. Stratigraphic evidence for a possible eastward continuation of the unconformity was obscured by sand dikes and liquefied sediments between station 1+10 and 1+15. The unconformable contact was delineated by subhorizontally bedded sediments of subunit $3c_1$ and overlying subunit 3b that onlap (i.e., terminate laterally) eastward against inclined strata of subunit $3c_2$. The structural interpretation of this geometric relationship is that the sediments below the unconformity became tilted prior to depositional onlap of adjacent horizontally bedded strata resulting in an angular-buttress unconformity. Other possible explanations for the angular-buttress unconformity are presented in the following section.

The second angular unconformity was exposed between station 1+15 and 1+40. This unconformable contact is undulatory and defined by erosional truncation of the up-dip ends of subunits 3e through 3i by fine to coarse sandy gravel of subunit $3a_1$. The sandy gravel appeared crudely bedded and undeformed above the unconformity. Therefore, the deformation of the underlying tilted beds occurred prior to deposition of the capping sandy gravel. A possible third unconformity beneath subunit $3a_2$ appears to bevel the up dip ends of subunits $3d_3$, 3e, $3f_1$, and $3f_2$. This unconformable surface may transgress laterally eastward into the previously described second angular unconformity. The apparent difference between the two would be the lithologic composition of the strata directly above the unconformity. Only one period of tectonic deformation is required by the geometric relationships of the unconformities based on the observed dip of the subunits. A second period of tectonic deformation could be inferred if the unconformable contact observed beneath subunit $3a_2$ actually underlies and is beveled off by the unconformity beneath subunit $3a_1$.

The tilted strata are offset by four closely spaced faults with variable displacement. The faults are exposed in the northern sidewall between station 1+11 and 1+12. A fault trend of approximately N. 65° W was determined by aligning a brunton compass over the trace of the faults in the inclined sidewall. No piercing points were observed which precluded determination of fault slip. The sense of offset based on displaced silty clay and silt layers appeared to be east side up (apparent reverse separation) in each instance. However, a component of lateral slip would appear to be required across one of the faults due to significant differing thickness of strata on either side of the fault. The vertical offset appeared to range from about an inch to at least 6-inches. No gouge was observed along either of the faults. The projected trace of these faults across the trench to the southern sidewall intersects a portion of the southern sidewall that has been obscured by sand intrusion and burrowing rodent activity.

A.A.5.3 Trench No. 2a Structural interpretation

Both tectonic deformation and various depositional and glacial processes are known to cause angular discordance between sedimentary layers. The following discussion presents various non-tectonic processes that can form angular discordance in sedimentary layers and the necessary stratigraphic and geomorphic evidence that would be required to support such a non-tectonic origin. This is compared to the geometric relationships (i.e., sedimentary structures and geologic contacts) observed in the trench and the surrounding geomorphology.

One of the possible non-tectonic explanations for the presence of tilted beds in glacial environments is that they may have formed as foreset beds in deltaic complexes. Numerous examples of deltaic complexes that prograded into sloping basins have been reported by geologists working in the various glaciated portions of the United States (Flint, 1957, Kolteff, 1974, Selby, 1985, and Bloom, 1998). Porter and Swanson (1998) indicate the location of seven deltaic complexes on a map of the Puget Lowland that shows the distribution of meltwater lakes during glacial recession.

It is common for deltaic deposits built into lakes to be comprised of coarse bed-load sediments; foreset beds are therefore commonly moderately dipping (Flint, 1957). Examination of published photographs of various outwash delta exposures reveals that dip angles of foreset beds probably are as steep as the angle of repose of the sediments (i.e., sandy gravels may dip as steeply as 35 to 40 degrees). Foreset beds in deltas are commonly overlain by gently dipping topset beds and underlain by bottomset beds of the basin floor. The down dip portion of foreset beds may abruptly terminate against the bottomset beds or have a tangential contact.

The tilted beds exposed in Trench 2a are located within a gently sloping valley bottom, which does not appear consistent with the location of other deltaic deposits that have been identified in the Puget Lowland area. Most of the known deltaic deposits that have been identified in the Puget lowland are features of significant topographic relief that exhibit large-scale delta foresets on the order of tens of feet (e.g., Galster and Laprade, 1991, Troost, 1999), in contrast to the lack of surface relief of the relatively small monoclinal fold exposed in Trench 2a. For example, a geologic section of the Sequalitchew Delta near Dupont, Washington indicates that the delta foresets extend from an elevation of approximately 220 feet to mean sea level at Puget Sound (Troost, 1999). Smaller scale deltaic deposits have been recognized in the Puget Lowland (McCormack, 2004), although details of their stratigraphy have not been made available.

The uppermost portion of the monoclinal fold exposed between station 1+05 and 1+10 consists of thinly interbedded fine-grained sand, sandy silt and silty clay. These beds appeared, based on their limited exposure, to be continuous from their tilted position down dip to relatively subhorizontal. In other words, within the depth of exposure, horizontal bottomset beds were not observed beneath the monoclinally folded strata, albeit the trench exposure was relatively shallow. No strata interpreted to be topset beds were exposed within the trench sidewalls. The dip of the strata measured within the tilted beds of the monoclinal fold is within the upper range of foreset beds, however, the shape

of the inflection point between the tilted and sub-horizontal portion of the monoclinal fold appeared abrupt and angular, rather than the more common gradual and curviplanar geometry reported in deltaic deposits. Moreover, fine-grained silts and clays are not common at the upper portion of a deltaic deposit because these sediments would more likely be carried in suspension beyond the delta front and then settle out in a lower energy environment. For the reasons cited above, the geometry of the fold and the bedform characteristics do not support a deltaic origin.

A second non-tectonic explanation for the tilting of beds exposed in Trench 2a is the possibility that the sediments in Trench 2a are somehow related to ice-contact sediments, such as kames or kame terraces. For example, kame sediments may have draped into a kettle or perhaps, interbedded strata collapsed into a kettle. Typical kettle topography is characterized by oval-shaped depressions or lakes scattered across recessional outwash deposits. Kames are associated with kettles and typically consist of poorly sorted and poorly bedded sand and pebble to cobble gravel, in which foreset bedding and slumping are common (Troost, 2003). Kame terrace deposits are composed of glaciofluvial sand and gravel deposited between a valley wall and active or stagnant ice. They typically include steeply dipping stratified sand and gravel with diamicton lenses (Troost, 2003).

Geomorphic evidence of kame and kettle topography is not apparent at the low lying portion of the Brightwater Route 9 site. The placement of fill at the site may have masked the possible presence of kettles. However, features of kettle topography in vicinity of the site are neither apparent on the 7.5 Minute Bothell Quadrangle Topographic Map (USGS, 1967), nor on LiDAR imagery available from King County. Internal stratification and the bedding surfaces within the tilted beds were primarily planar parallel in shape. Slumped structures were not observed within the planar parallel, tilted beds. Gravel beds appeared poorly to moderately sorted and with little to absent clast imbrication. Some of the sand beds appeared to be normally graded upwards. The above cited stratigraphic description of the tilted strata is not considered typical of kame deposits.

Collapse of internally stratified deposits into a kettle is another possible process to account for the observed angular discordance between the subunits. This possibility would appear to presume that the horizontally bedded sediments (subunits 3b and 3c) were deposited horizontally against the slumped deposits after collapse. This process may be questioned by considering the bed geometry at the far eastern portion of the north sidewall. Here, the subparallel to planar sand and gravel beds appear to be gently folded toward east at dip angles of about 10° to 30°. If these beds are continuous with the westward dipping monoclinal strata, which appears probable, then they are likely involved in folding of the monoclinal structure, in contrast to a change in dip direction due to soft sediment slumping.

In conclusion, the sedimentological contacts, deformational structures, and stratigraphy exposed in the trench, as outlined above, favor a tectonic origin for the angular-buttress unconformity. Geologic interpretation of stratigraphy and structure exposed in Trench 2a supports at least two periods (or events) of tectonic deformation. The first tectonic event tilted and deformed subunits $3c_2$ through 3k into an apparent open fold. An angular-

buttress unconformity then formed as sediments of subunits 3b and $3c_1$ onlapped progressively eastward against the previously tilted subunit $3c_1$. This tectonic event is interpreted to have occurred during deposition of recessional outwash. The maximum age of this event is estimated to be no older than about 13,600 ^{14}C yr B.P. (16,575 cal yr B.P.) which is the reported age of recessional sediment samples collected form the base of a sediment core obtained from Lake Washington and Lake Carpenter (Porter and Swanson, 1998). A minimum age for this event would likely be pre-Holocene, since glacial retreat was rapid and recessional outwash sedimentation probably ceased soon after significant ice retreat. As noted previously, the University of Washington has collected some recessional sediment samples for potential TLM dating (Kathy Troost, personal communication, 2004).

A second tectonic event is indicated by the several minor faults exposed within a 6- to 12-inch wide zone along the northern sidewall between station 1+11 and 1+12. The individual fault traces appeared to variably offset a thinly interbedded section of silty clay, silt, and fine-grained sand. These beds were tilted eastward at about 23° to 33°. The two eastern fault traces appeared to bifurcate (splay) upward. The dip of strata appeared relatively uniform adjacent to either side of the faults and also between the individual fault splays with only minimal, small-scale warping of two silty clay beds. The observations that the minor displacement faults offset relatively uniformly tilted strata coupled with only minimal small-scale warping adjacent to the fault splays suggest that most of the tilting and folding likely preceded displacement of the strata. However, it is recognized that the tilting and folding of the strata may have been caused by displacement along a fault below the explored depth of the trench. If this is the case, then the faults exposed in the trench may be splays of a deeper buried fault.

A splay of the eastern fault trace appeared to have truncated a splay of an adjacent fault splay as shown on the detailed geologic trench log, Plate II. The fault trace geometry appeared inconclusive as to whether the faults that were exposed in the trench occurred during one or more tectonic events. Subunits $3d_1$ and $3d_2$ are interpreted to be disrupted and liquefied sediments that formed adjacent to the minor faults. The basal contact of the wetland deposit was exposed at an abruptly lower depth directly above these liquefied deposits suggesting that the wetland deposits may have been warped downward by collapse during liquefaction. If the displacement along the faults exposed in the trench occurred during an earthquake event that also caused the apparent liquefaction and warping of the base of the wetland deposit – organic soil, then the second tectonic event (fault displacement and contemporaneous liquefaction) is younger than the age of the lower portion of the wetland deposit, which may be early Holocene in age. Alternatively, the liquefaction event may have occurred after fault displacement, in which case three deformation events are conceivable.

A.A.5.4 Trench 2b Stratigraphy

Earth materials encountered in Trench 2b consisted of colluvium (highly weathered till?) underlain by fine sediments interpreted to be of glaciolacustrine origin. A lenticular deposit of till was exposed over a lateral distance of about 15 feet along the eastern

sidewall. A thin layer of organic topsoil (soil A-horizon) formed a thin mantle over all the units exposed in the trench. Lithologic descriptions of the subsurface earth materials logged in Trench 2b are presented below. The trench log (Plate 2) presents a more detailed description of lithology and illustrates stratigraphic details of the geologic units.

Organic soil-A horizon (Trench Log symbol: 1A)

Organic topsoil formed a three to five-inch thick mantle over all the underlying earth materials exposed in Trench 2b. This soil-A horizon consisted of dark brown, fine sandy silt with abundant root and bark fragments. The topsoil appeared loose and moist.

Colluvium / Highly weathered till (?) (Trench Log symbol: Qcol)

A unit considered to be of colluvial origin was exposed beneath the soil-A horizon from the northern end of the trench to about station 0+52. The base of the colluvium appeared sharp to gradational and undulatory. This unit consisted of light yellow-brown (2.5Y 5/5.5), gravelly, sandy silt with scattered roots throughout. The well-rounded gravels ranged typically from ¼- to ¾-inch diameter to maximum of 2-inch diameter. The lithologic composition appeared similar to an underlying, lenticular deposit of till; however, it was relatively loose to only medium dense. Therefore, this unit is possibly till that is highly weathered and disturbed by near-surface bioturbation and creep.

Pre-Vashon(?) Till-Diamicton (Trench Log Symbol: Qpogt)

A lens of olive-gray (5Y 6/4), silty, fine-grained sand with some scattered medium to coarse-grained sand and fine gravel was exposed between station 0+20 and 0+30. This till-like diamicton unit is probably older than the Vashon Till, based on its apparent relative density and degree of weathering. Bedding appeared crudely stratified and poorly sorted. The northern end of the lens interfingered with glaciolacustrine deposits and the southern end pinched out beneath the colluvium (highly weathered till?). This stratigraphic relationship suggests that the diamicton and glaciolacustrine units may be of similar age.

Pre-Vashon(?) Glaciolacustrine Deposits (Trench Log Symbol: Qpogt)

Sediments of probable glaciolacustrine origin were exposed throughout the length of the trench. Three subunits were mapped within this deposit. The predominant lithology from the northern end of the trench to station 0+50 consisted of olive-gray, stiff to hard, clayey silt with thin lenses of light orange-brown, sandy silt. This subunit was designated 4a on Plate 3.The degree of bleaching and weathering suggests it is pre-Fraser. The layers in this subunit were difficult to trace laterally due to complex interfingering and pervasive shearing. Massive, yellow-gray (5Y 5/4) silt with trace fine gravel was mapped as a second glaciolacustrine subunit between station 0+50 and the southern end of the trench. This subunit (4b on Plate 3) appeared stiff and locally, contained clasts (rip-ups) of the underlying subunit. The silt subunit was underlain discordantly by dark-gray to brown silty clay with a hard consistency (semi-friable mudstone) containing thin, fine-grained

sand stringers. This subunit is designated 4c on Plate 3. The silty clay (mudstone) exhibited a blocky fracture pattern. Many of the fractures appeared discontinuous. The following section summarizes geologic structure features observed in Trench 2b.

A.A.5.5 Trench 2b Geologic Structure

The structure in Trench 2b appeared extraordinarily complex at a small scale. Delineating the structure within the glaciolacustrine unit was difficult due to the discontinuous strata and lack of mappable beds. Thinly bedded glaciolacustrine strata appeared to dip from subhorizontal to about 15° to 30° northward throughout most of the trench. Fine-grained sand stringers within the mudstone subunit were observed to dip at shallow angles to the south toward the southern portion of the trench.

The glaciolacustrine sediments were cut by numerous shallow dipping to subhorizontal shears, many of which had undulating surfaces. The trench log depicts several of these shears, although not all the shears observed along the trench sidewalls are shown. At least two of the subhorizontal shears appeared to truncate a second set of closely spaced shears, which exhibited moderate southerly dips and minor normal offset. The sense of displacement on the shears was difficult to ascertain due to the generally discontinuous strata and complex interfingering. The base of the till-like diamicton appeared to be offset several inches by a shallow- to moderate-south dipping fault with an apparent reverse-component of slip. Normal sense of stratigraphic offset was also observed at one location, where two subhorizontal shears truncated several minor normal (i.e., sense of offset) faults.

The shallow dipping to subhorizontal shears may be related to glaciotectonic shearing caused by ice loading. These subhorizontal shears appear to truncate a set of south dipping shears in some places, which may be related to a prior episode of soft sediment deformation of the lacustrine deposits. The subhorizontal shears at many places appeared in-filled with glacially overconsolidated, fine sand. This suggests that the deformation predates the retreat of the Vahon ice sheet and thus places the deformation prior to about 16,500 cal yr B.P. The most recent deformation may be associated with the apparent reverse offset of the till deposit, which may be tectonic in origin, although this deformation also likely pre-dates the retreat of the Vashon ice sheet.

A.A.6 References

Aspect Consulting, 2004, Summary of Trench Boring Investigations: Unpublished consultant's report submitted to CH2M Hill as part of the Brightwater Wastewater Treatment Plant Site Characterization.

Bloom, A. L., 1998, Geomorphology, A Systematic Analysis of Late Cenozoic Landforms, Prentice Hall, New Jersey.

Booth, D. B., Cox, B. F., Troost, K. G., and Shimel S.A., 2004, Composite geologic Map of the Sno-King area: University of Washington, Seattle-Area Geologic Mapping Project (SGMP), Scale 1:24,000.

CH2M Hill, 2004, Preliminary design geotechnical interpretive report, Route 9 site, Proposed Brightwater Wastewater Treatment Plant: unpublished consultant's report to King County Wastewater Division, Washington.

Flint, R.F., 1957, Glacial and Pleistocene Geology, John Wiley and Sons, Inc., New York

Galster, R.W., and Laprade, W.T., 1991, Geology of Seattle, Washington, United States of America: Association of Engineering Geologists Bulletin, v. 28, no. 3, p. 235-302.

Koteff, C. 1974, The morphological sequence concept and deglaciation of Southern New England, in Glacial Geomorphology, Ed., D. R. Coates, Binghampton, New York, Publications in Geomorphology, State University of New York.

McCormack, D., Personal communication with engineering geologist, Aspect Consulting, January, 2005

Minard, J.P., 1983, Geologic Map of the Kirkland Quadrangle, Snohomish and King Counties, Washington, U. S. Geological Survey Map, MF 1343: U. S. Geological Survey, Denver CO, Scale 1:24,000.

Minard, J.P., 1985a, Geologic Map of the Bothell Quadrangle, Snohomish and King Counties, Washington, U. S. Geological Survey Map, MF 1747: U. S. Geological Survey, Denver CO, Scale 1:24,000.

Minard, J.P., 1985b, Geologic Map of the Maltby Quadrangle, Snohomish and King Counties, Washington, U. S. Geological Survey Map, MF 1746: U. S. Geological Survey, Denver CO, Scale 1:24,000.

Porter, S.C., and Swanson, T.W., 1998, Radiocarbon age constraints on rates of advance and retreat of the Puget Lobe of the Cordilleran ice sheet during the last glaciation: Quaternary Research, v. 3, p. 251-261.

Selby, M. J. 1985, Earth's Changing Surface, An Introduction to Geomorphology, Clarendon Press, Oxford

Thorson, R. M., 1980, Ice sheet glaciation of the Puget Lowland, Washington, during the Vashon stade (last Pleistocene): Quaternary Research, v. 13, p. 303-321.

Troost, K.G., 2004, personal communication, University of Washington, November, 2004

Troost, K.G., 2003, Stratigraphic Framework in Quaternary and Engineering Geology of the Central and Southern Puget Sound Lowland, Professional Engineering Practices Liaison (PEPL) Program, University of Washington.

Troost, K.G., 1999, The Olympia nonglacial interval in the southcentral Puget Lowland, Washington: Seattle, University of Washington, Department of Geological Sciences, M.S. thesis, 123 p.

Yount, J. C., Minard, J. P., and Dembroff, G. R., 1993, Geologic map of surficial deposits in the Seattle 30' by 60' quadrangle, Washington: U.S. Geological Survey Open File Report 93-233, scale 1:100,000.

Table A-1. Geologic Unit Designation and Lithologic Descriptions for Trench 2A

Symbol	Geologic Unit and Lithologic Description
(1) af	**Artificial Fill (Undocumented)** Fine sandy Silt (ML_s) with few to some well-rounded gravel, scattered glass fragments, rare metal debris and wood chips, composed of several layers, medium to dark brown (Munsell soil color 7.5YR 3/3), appeared generally loose to medium dense, sharp and undulatory basal contact with underlying deposits.
(2a) Hw	**Wetland Deposits / Organic Soil** Organic-rich Silt, low to moderate plasticity, (OL/PT), black (5Y 2.5/1), trace to some scattered gravels, typically ½ to 2-inch diameter and moderately well to well rounded, scattered roots, appeared generally soft to firm, graded below to clayey silt with less organic content, dark brown. The contact between the fill and the top of the wetland deposits / organic soil appeared sharp and undulatory. Near the contact, the upper portion of the wetland deposits appeared darker and suggest a disturbed plow zone from prior agricultural activity. A sharp to locally gradational and undulatory to irregular contact separated the base of the wetland deposits from the underlying recessional outwash.
(2b) Hcol?	**Colluvium** Gravelly, fine- to medium-grained Sand with Silt, (SM), olive-gray (5Y 3/2), poorly sorted, massive appearing and lenticular-shaped deposit, appeared gradational with the underlying recessional outwash deposits.
(3) Qvrf	**Vashon Recessional Outwash Deposits** Moderately well-bedded (layered) sequence of Sand, sandy Gravel, Silt, and minor silty Clay; exposed beneath the wetland deposits / organic soil to the base of the trench. The contact between the outwash deposits and overlying wetland deposits appeared sharp and undulatory, commonly with irregular relief. In general, the sand and silt beds (i.e., layers) ranged in thickness from laminated (less than 3/8-inch thick) to thinly bedded (0.1 to 0.3-ft. thick) and the sandy gravel to gravel beds ranged from thinly- to medium thickly-bedded (0.1 to 1-ft. thick). Bedding appeared primarily planar parallel and continuous with some lenticular-shaped beds and minor channel lenses. Bedding contacts appeared generally sharp, although some beds exhibited gradational contacts.

Table A-1. Geologic Unit Designation and Lithologic Descriptions (continued)

The recessional outwash deposits were subdivided into several mappable beds and subunits defined primarily by lithologic contrast. Descriptions of the individual subunits described below are in general order of increasing geologic age.

($3a_1$) Fine- to coarse sandy Gravel at the base (GP), grading upward and laterally into fine- to coarse-grained Sand with scattered gravels (SW-SP) and local zones of silty, fine-grained Sand (SM), orange-brown (10YR 4/6). Subunit appeared medium dense and moist, crudely bedded, lenticular shaped, and oxidized relative to the underlying subunits. The basal contact appeared conformable with the underlying beds west of trench station 1+10, except for localized erosional scour and/or cut-fill deposition. East of trench station 1+15, the basal contact formed an angular unconformity, above tilted recessional outwash deposits.

($3a_2$) Fine- to coarse-grained Sand (SW-SP), with thin laminae of silty, fine-grained Sand (SM), olive brown (2.5Y 4/4); subunit appeared localized between station 1+17 and 1+21, beneath subunit $3a_1$, possibly correlative to subunit 3b

(3b) Fine- to coarse-grained Sand (SW-SP) and silty, fine-to medium-grained Sand (SP-SM), olive gray (5Y 4/2 to 5Y 5/2), interbedded with: Silty, fine- to medium- grained Sand (SM), laminae (⅛ to 1/16" thick) of sandy Silt to Silt with trace clay (ML), gray to olive gray (5Y 4/1 to 5Y 4/2), and very thin to thin lenses of sandy Gravel (GP), gravels range from ½ to 2½-inch diameter; bedding is wavy, parallel, moderately-well developed; locally bedding is destroyed adjacent to sand dikes (by liquefaction).

($3c_1$) Fine- to medium-grained Sand with trace silt (SP) and fine- to coarse-grained Sand (SW), olive gray (5Y 4/2 to 5Y 5/2), interbedded with: Silty, fine-grained Sand (SM), sandy Silt (ML), clayey silt (ML/CL), and minor silty clay (CL), gray to olive gray (5Y 4/1 to 5Y 4/2), lenticular, wavy, thinly to very thinly bedded (½ to 1-½-inch thick), well-developed bedding; locally bedding is destroyed adjacent to sand dikes (by liquefaction); Silty clay and clayey silt beds shown as discrete beds on the trench log. The beds in this unit and overlying subunit 3b terminated laterally (onlap) between station 1+00 and 1+10 against an unconformable contact.

Table A-1. Geologic Unit Designation and Lithologic Descriptions (continued)

($3c_2$) Fine- to medium-grained Sand (SP), interbedded with: Sandy Silt (ML), fine-grained Sand (SP), clayey Silt (ML/CL), silty Clay (CL), thinly to very thinly bedded; locally bedding appeared both destroyed and brecciated adjacent to sand dikes; this subunit directly underlies angular unconformity and are compositionally similar to Subunit $3c_1$.

($3d_1$) Fine- to coarse-grained Sand with scattered gravel (SP), massive, probably liquefied, (possibly correlative with subunit 3b)

($3d_2$) Lens-shaped, brecciated unit consisting of angular clayey Silt and fine-grained Sand fragments within a fine- to medium-grained sand matrix. The fragments appeared to have been dislodged (probably liquefied) from adjacent strata assigned to subunit $3c_2$.

($3d_3$) Silty, fine-grained Sand with lenses of medium- to coarse-grained Sand (SP), vaguely bedded.

(3e) Thin, undulatory silt bed (ML) and underlying silty Clay lens (CL), silt bed was erosionally truncated in up-dip direction by overlying subunit $3a_1$.

($3f_1$) Thin, lenticular bed of sandy Gravel (GP); erosionally truncated in up-dip direction by overlying subunit $3a_1$.

($3f_2$) 6 to 9-inch thick bed of fine-to medium-grained Sand with trace silt (SP) and parallel laminae of fine-grained Sand, light olive brown (2.5Y 4/6); appeared medium dense, erosionally truncated in up-dip direction by overlying subunit $3a_1$.

(3g) Fine- to coarse sandy Gravel (GW), light olive brown (2.5Y 5/6); gravels range from ½ to 4-inch length, sub-rounded to well rounded, poorly to moderately sorted (bimodal distribution?); erosionally truncated in up-dip direction by overlying subunit $3a_1$.

(3h) Fine-to coarse-grained Sand (SW) with laminae of silty, fine- to medium grained Sand (SP-SM), and thin, gravelly, fine- to coarse grained sand lenses, light olive brown (2.5Y 4/4); appeared medium dense, thinly bedded, well bedded, planar-parallel; erosionally truncated in up-dip direction by overlying subunit $3a_1$.

(3i) Gravelly, fine- to coarse grained Sand (SW) to sandy Gravel (GP) at base: gravels range from ½ to 1-inch with coarser gravel up to 5-inch length at base; erosionally truncated in up-dip direction by overlying subunit $3a_1$.

($3j_1$) Fine-to coarse-grained Sand (SW) with laminae of silty, fine- to medium grained Sand (SP-SM), and thin, medium to coarse grained sand bed at base; thinly bedded, well bedded, planar-parallel.

Table A-1. Geologic Unit Designation and Lithologic Descriptions (concluded)

($3j_2$) Fine- to coarse-grained sandy Gravel (GP) with trace silt in matrix, gravels ranging from ½- to 3- inch length.

($3j_3$) Fine-to medium-grained Sand (SP) with thin lenses of sandy Gravel (GP); gravels ranging from ½- to 4- inch length.

(3k) Fine-to coarse-grained Sand (SW) with laminae of fine- grained Sand (SP); similar to subunit 3h in lithologic composition, however, correlation uncertain due to erosional truncation by overlying subunit $3a_1$.

(3L) Fine- to coarse-grained sandy Gravel (GP) with trace silt in matrix; gravels ranging from ½- to 4- inch length, (porphyritic volcanic and gneissic clasts), crudely bedded; similar to subunit 3g in lithologic composition, however correlation uncertain due to erosional truncation by overlying subunit $3a_1$.

(3m) Gravelly, fine- to coarse-grained Sandy (SP): mottledyellow and olive brown; gravels ranging from ½- to 2- inch diameter; appeared medium dense to dense, poorly sorted, crudely bedded; probably correlative with subunit $3a_1$; lower portion appeared to have been liquefied

Notes:

Sand intrusions are shown as irregular-shaped dikes that in several instances branched upward into narrower injections. Several intrusions obscured adjacent bedding and others appeared to drag adjacent bedding upward on a scale of several inches.

Research faculty from the University of Washington collected several samples of various subunits for potential thermoluminescence (TLM) age dating.

Figure A-1c. Aerial photograph showing site land use as of 1990. Digital ortho-quarter-quad; UTM Zone 10 coordinates.

Figure A-1a Part of the Bothell, Washington, quadrangle. UTM Zone 10 coordinates.

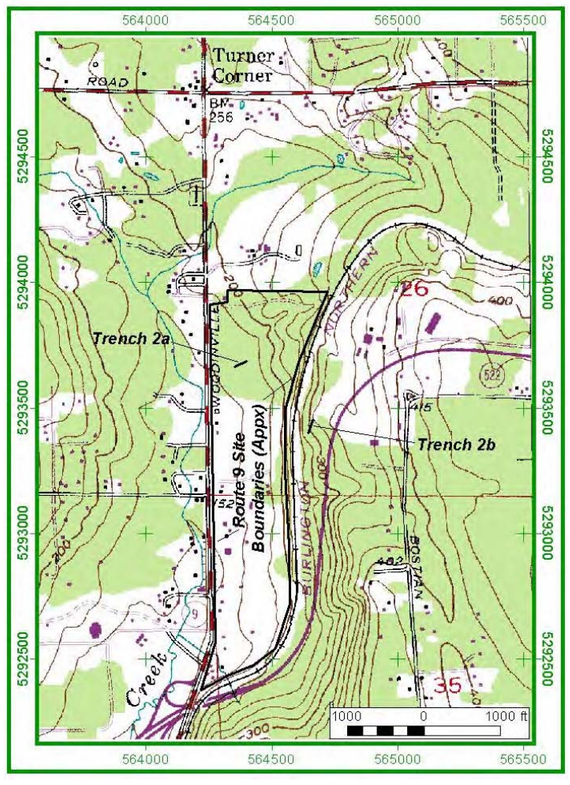

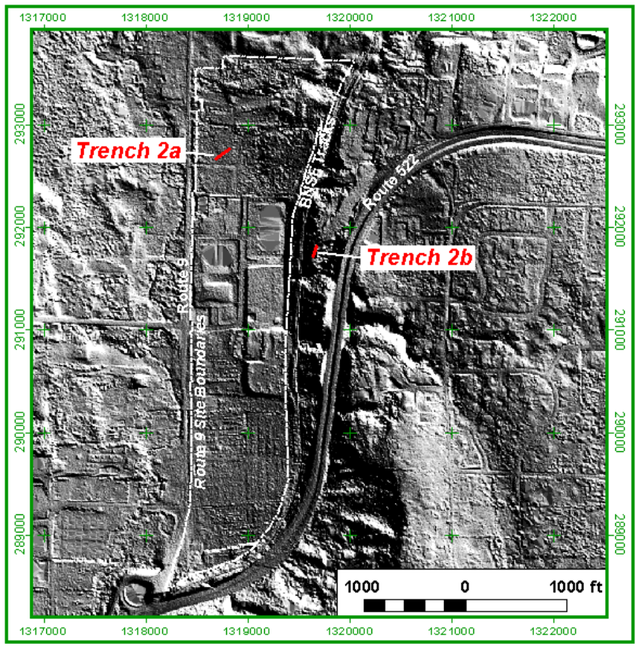

Figure A-1. Locations of Trenches 2a and 2b at the Brightwater Route 9 Site.

Figure A-1d. Aerial photograph showing site land use as of 2000(?) and trench locations. Washington State Plane North Zone coordinates.

Figure A-1b. LiDAR topography as morning-sun hillshade showing trench locations. Puget Sound Lidar Consortium data. Washington State Plane North Zone coordinates.

Prepared by AMEC under Job No. 4-212-102100

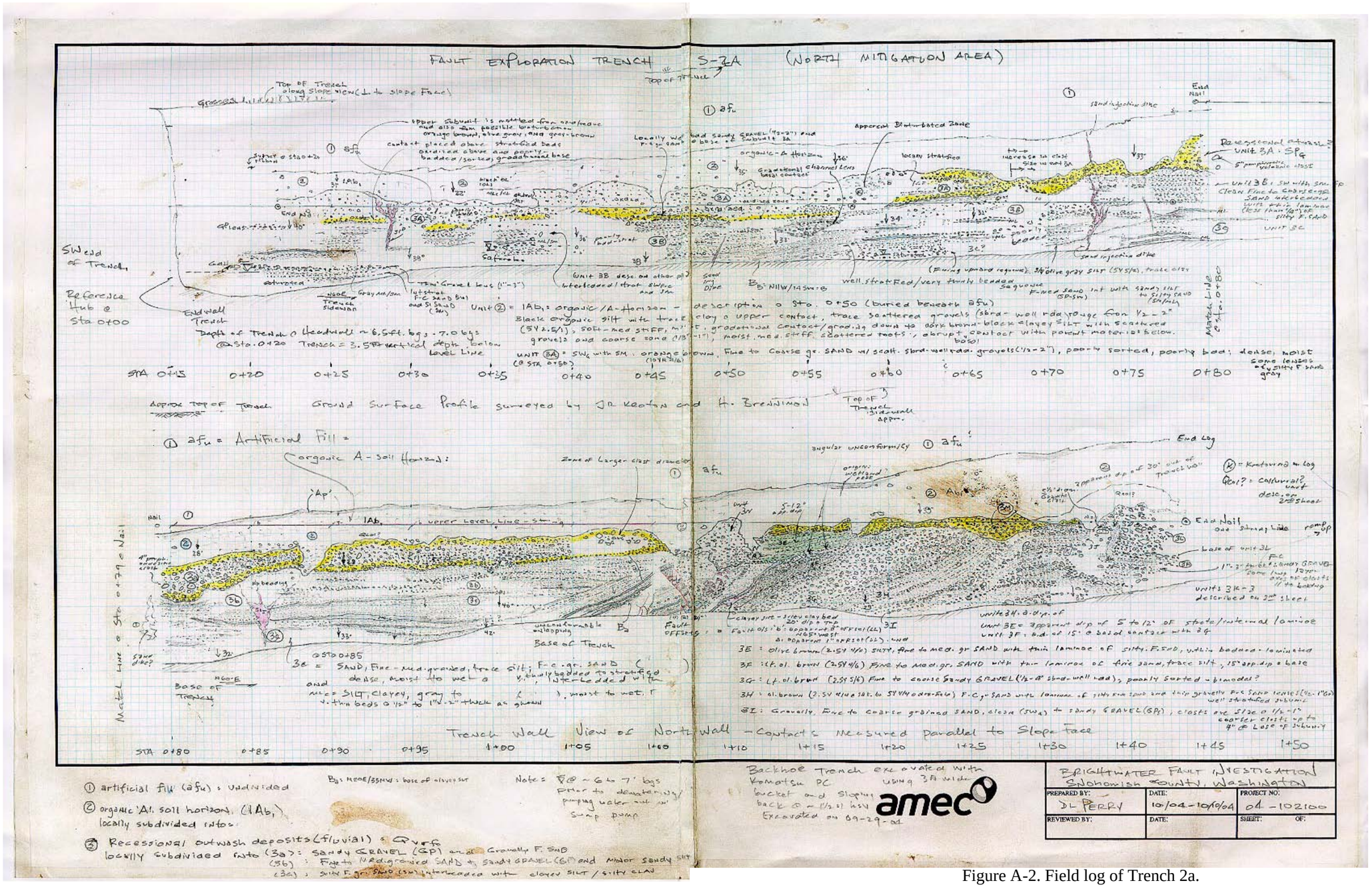

Figure A-2. Field log of Trench 2a.

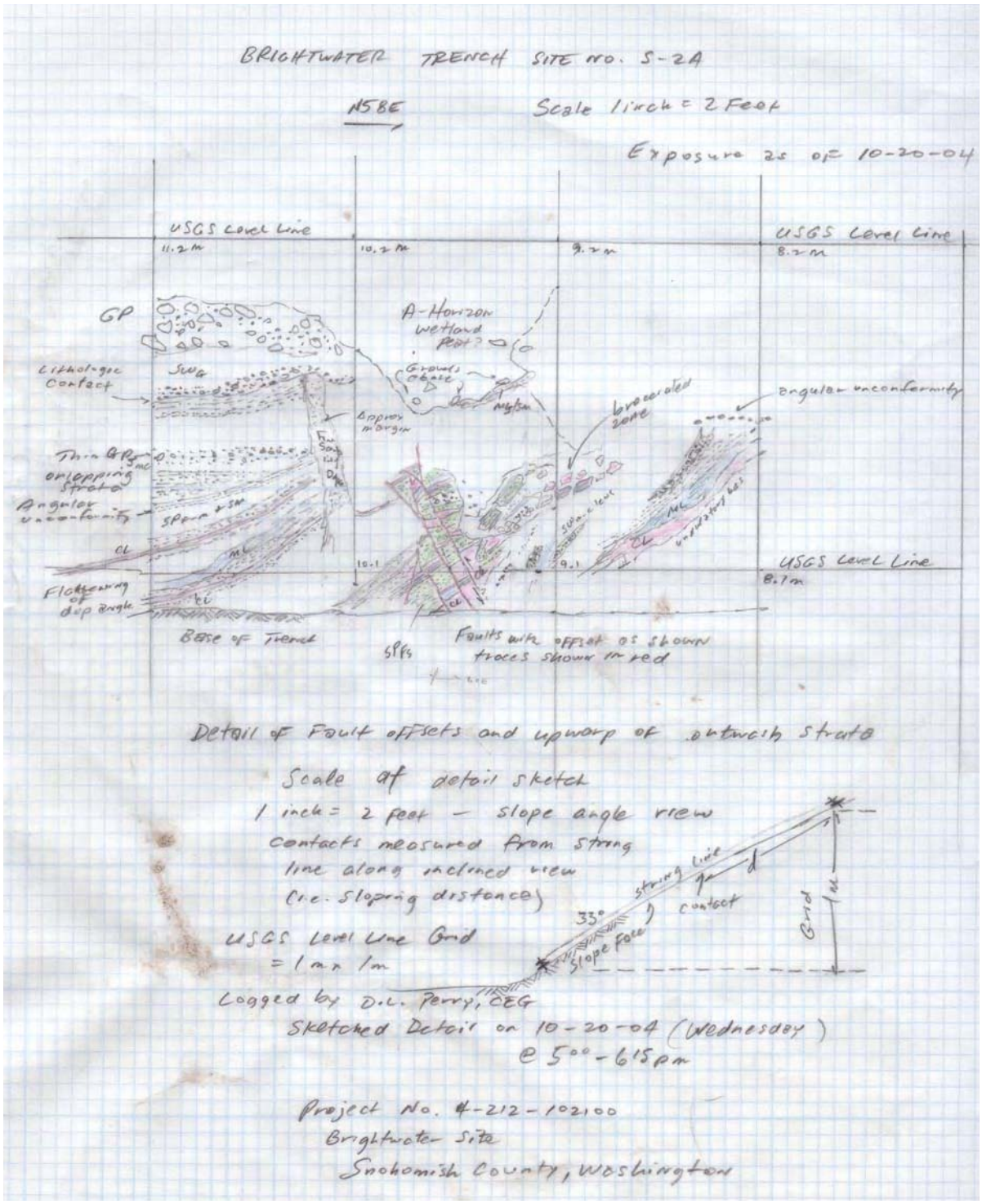

Figure A-3. Field log detail of part of Trench 2a.

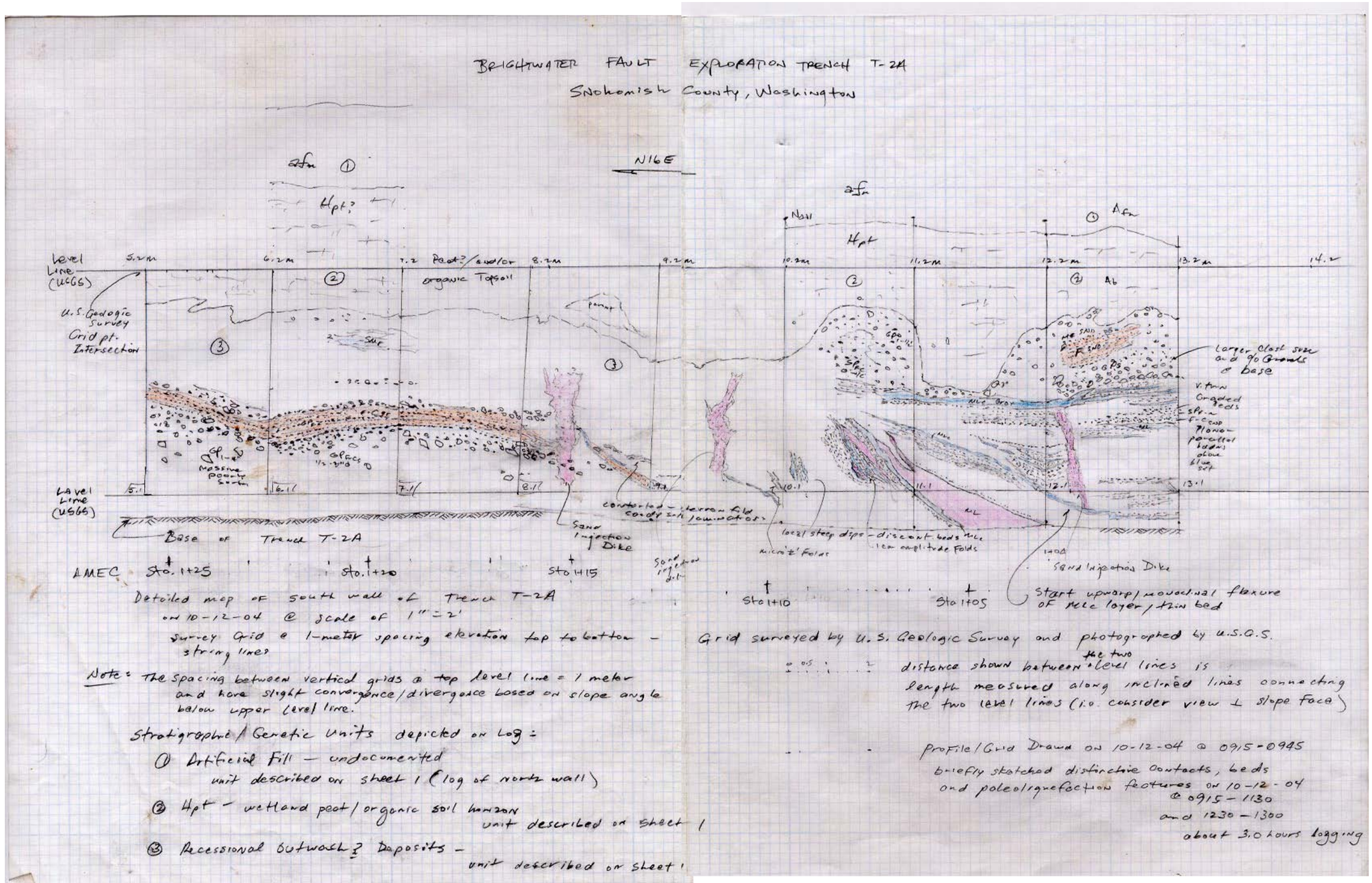

Figure A-4. Field log detail of part of south side of Trench 2a.

BRIGHTWATER FAULT

EXPLORATION TRENCH T-2b

Located along ridge spur

N16E

Base of Trench

Fault/Shear: ¼" wide shear appears to offset base of Till unit throw about 4" reverse (bifurcates) as shown oxid-reduction halo around shear many rocks

4" metabasalt clast

crude stratification @ base of Till unit Organics

low angle shears dip southward offset at north dipping strata - laminae

soil around root (1¼" Ø)

roots

blocky Fracturing #physical parting surfaces subparallel to bedding w clayey silt

sloop subvert. jt? fracture

blocky fracture pattern

Faintly laminated, less disrupted bedding

4" decomposed granite clast

colluvial wedge

yellow-gray SILT with trace Fine gravel, very stiff-hard moist massive appr. structure

sharp knee amplitude & type fold

Gravelly clayey silt/silty clay

MLs - soft, fine sand

low angle shears

dark gray silty clay stone/mudstone

olive brown blocky mudstone/clay stone overlying brown F gr. SOnd beds blocky fracture pattern moderately indurated moist - hard

Scale: 1 inch = 5 feet
Grid pattern = 1 meter x 1 meter
Mapped East Sidewall of Trench

Note: Survey Grid & 1 meter x 1 meter installed by USGS

Trench profile drawn 10-11-04 @ 1030-1145

ON 10-11-04: Logged @ 1230-115 pm - description of litho units
330-530 pm - contacts / details
by D.L. Perry, CEG

-0 Ft
-5 Ft
-10 Ft
-15 Ft

Lithologic Unit Descriptions 0 to ~0+18 meters

Unit ① - topsoil/organic horizon A (Thin Mantle)
Dark brown fine sandy SILT with abundant roots and bark fragments moist, loose (MLs)

Unit ② Light Yellow Brown Gravelly SILT, gravels are sbrd-well rnd clasts average ¼-3/4" diameter up to 2" rare; soft/loose, moist, scattered rootlets throughout (GM)
- Alternate Origins = Weathered Till unit separate from underlying subunit, or, perhaps, in-situ weathering of unit below

Unit ③ Mottled olive-gray and yellow brown slightly clayey SILT with trace scattered gravels up to ¾" stiff, to hard, moist contains irregular-shaped lenses of

UNIT ④ - Olive Gray-brown with orange mottling very Silty Fine gr. SAND with med-coarse grains scattered t/o and sbrd-well rnd. gravels from ¼-1" inch diameter; some larger clasts directly below (in lower unit?), poorly sorted, crudely stratified (Glacial Till origin?)

MF 2423 - Waterman point - Pay Wells - Local shear offset by thrust faults?

Brittle fractures - Up Glacial and Downglacial directional shears
don't see plucking out and smearing of clasts in up glacial direction towards
strong fabric to south Pay Wells observes - brittle deformation
thrusting to south

BRIGHTWATER FAULT INVESTIGATION		
PREPARED BY: D.L. PERRY	DATE: 10-11-04	PROJECT NO: 04-212-1021
REVIEWED BY:	DATE:	SHEET: OF:

amec

Figure A-5. Field log of Trench 2b.

Figure A-6. View produced by 3-D laser scan survey looking vertically down at Trench 2a.

Figure A-7. View produced by 3-D laser scan survey looking west at northern sidewall of Trench 2a.

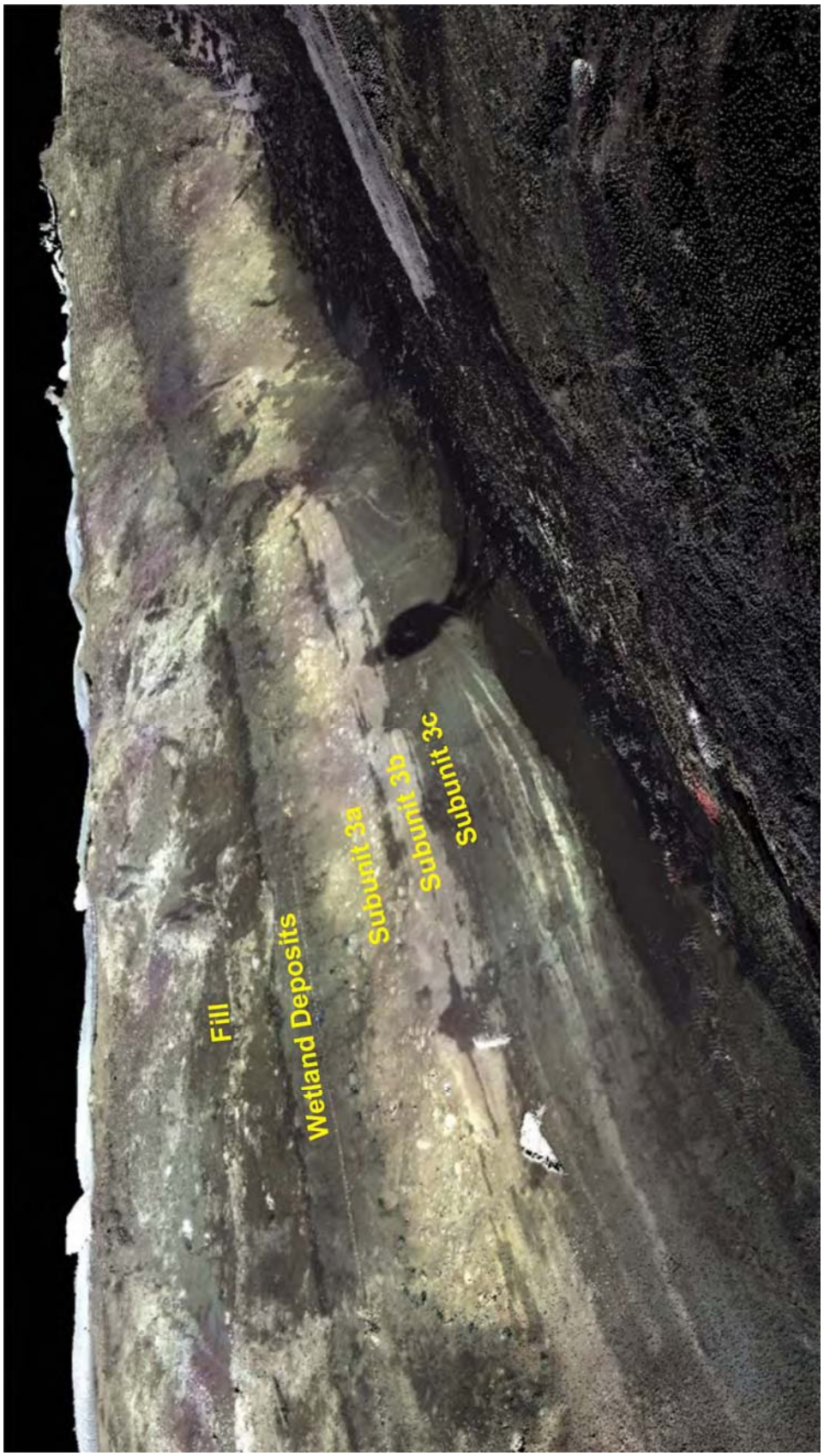

Figure A-8. View looking at northern sidewall of Trench 2a showing subhorizontally bedded sediments of subunits 3b and 3c beneath capping sandy gravel subunit 3a. Contact beneath outwash and wetland deposits delineated by colored tags beneath horizontal string line.

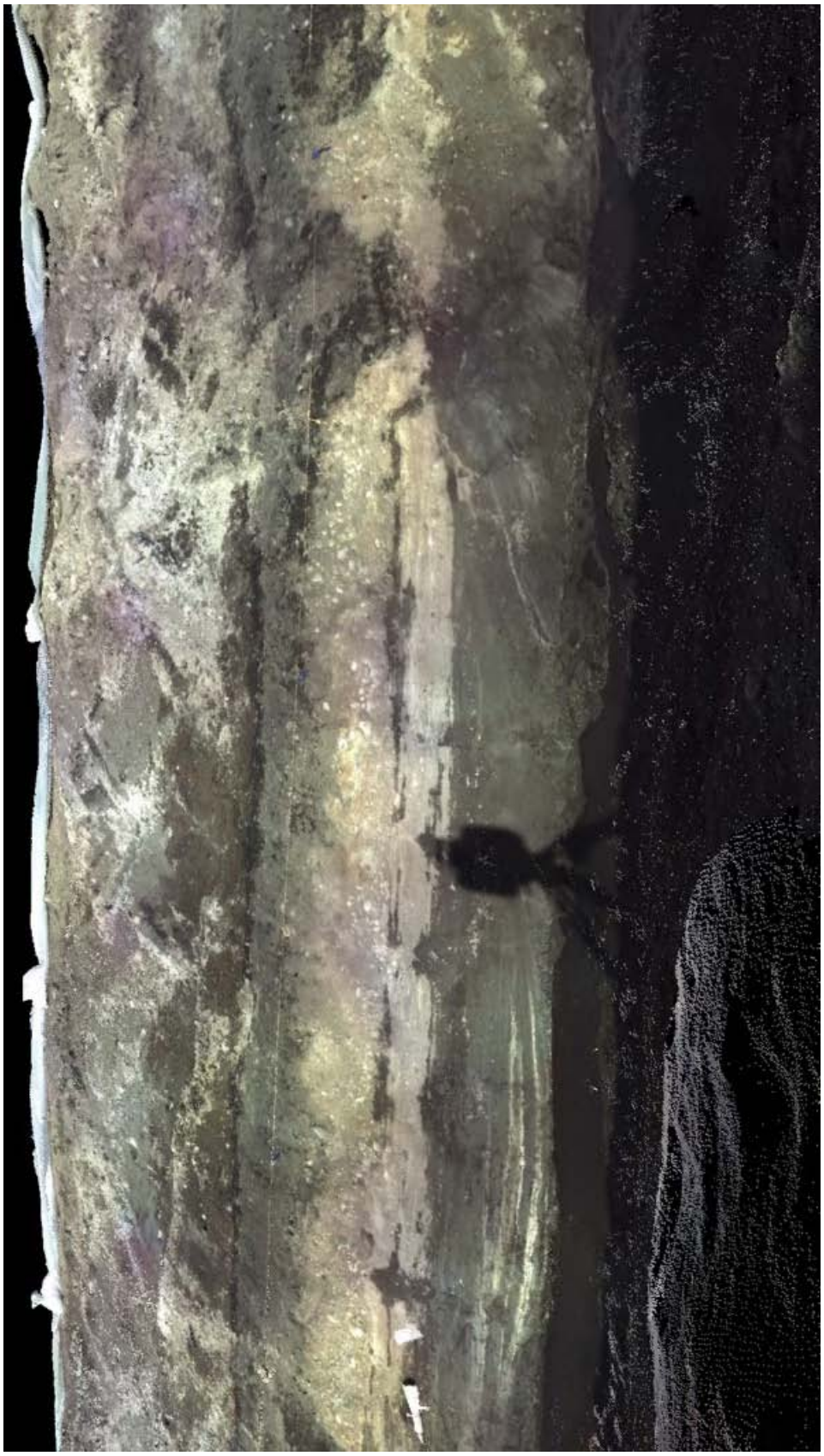

Figure A-9. View looking at northern sidewall of Trench 2a showing angular unconformity.

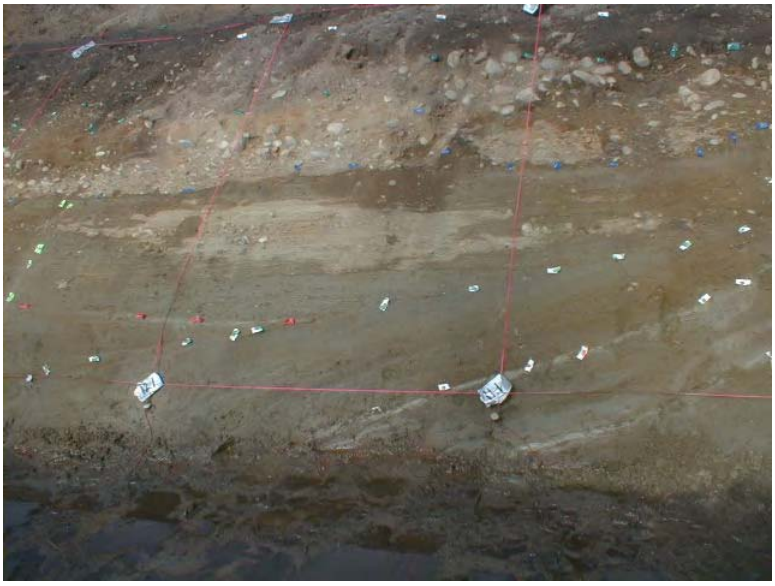

Figure A-10. Angular unconformity exposed in northern sidewall of Trench 2a. View of photo is between station 1+00 and 1+10. The U.S.G.S. survey grid lines (red string lines) are spaced at about 1-meter vertically and horizontally. The white tags at left part of photo delineate the unconformable contact between tilted outwash beds (of subunit 3c) and sub-horizontal strata that on-lap onto the tilted beds in an eastward (to the right in view) direction. Station locations are indicated on Plate 1. (PIC00037)

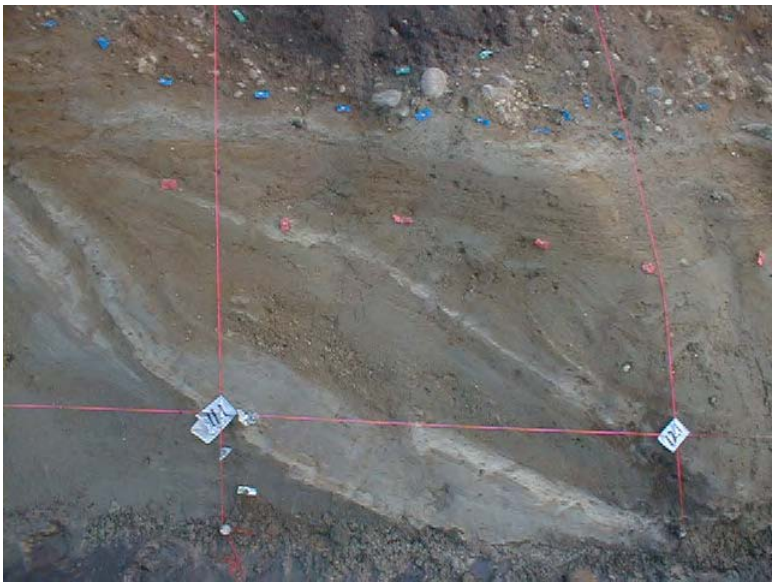

Figure A-11. The same angular unconformity as Figure A-10 exposed in the southern sidewall of Trench 2a. View between the U.S.G.S. survey grid lines is from station 1+03 and 1+06. Unconformity is delineated by white tags at base of sandy gravel subunit 3b. (PIC00027)

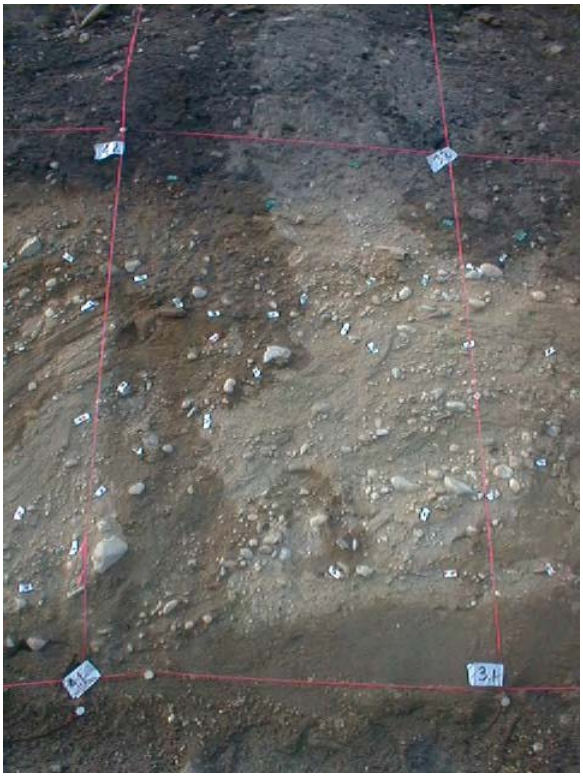

Figure A-12. Angular unconformity exposed in northern sidewall of Trench 2a between station 1+16 and 1+23. At this location, unconformity marks boundary between tilted outwash strata (subunits 3d3, 3e, and 3f) that are erosionally truncated in the up-dip direction by gently dipping subunit 3a2. Tilted beds are dipping westward at about 30 to 35 degrees. (PIC00014)

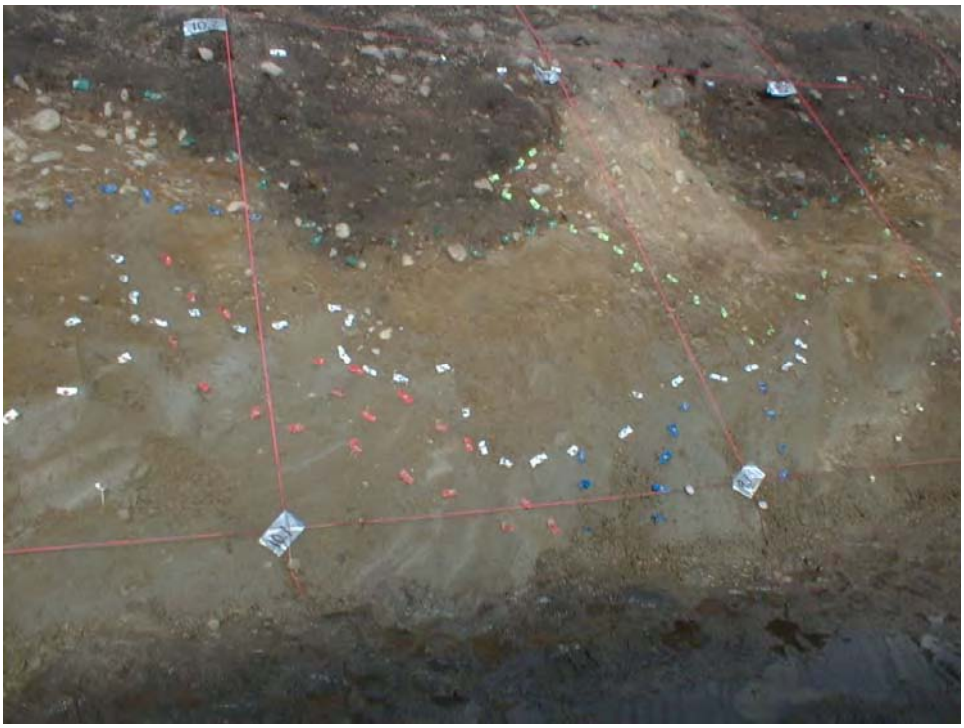

Figure A-13. Faults with apparent minor offset of tilted strata exposed in northern sidewall of Trench 2a between station 1+12 and 1+13. Offsets delineated by red tags in lower half of view. (PIC00033)

Figure A-14. Close up view of part of Figure A-13 photograph showing fault offsets. (PIC00034)

Appendix A.B

Reinterpretation of Seismic Refraction Data Collected in April 2004

Seismic Lines 1 through 7, completed in April 2004, were reinterpreted and the results reexamined in light of the subsurface information developed from a series of borings drilled in the North Mitigation Area during planning of the trench excavated across Lineament 4. Seismic Lines 1 through 7 are each 120 feet long and were completed with partial overlapping to provide a seismic interpretation of a subsurface profile of part of the project site. The locations of Seismic Lines 1 through 7 are indicated on Figure B-1. The original interpretations had focused on the deeper portions of the seismic refraction and refraction microtremor (ReMi) profiles in an attempt to characterize to as great a depth as practical. Neither shallow seismic refraction quartershots nor ReMi dispersion information at frequencies higher than 25 Hz were interpreted in April 2004. The reinterpretation work presented in this appendix includes all of the seismic refraction shots for Lines 1 through 7 and ReMi results to frequencies up to 50 Hz to interpret the shallow portion of the subsurface profile. Also, a new version of the ReMi software that became available in September 2004 permitted splitting the ReMi data into half lines for interpretations with shallow variations across each seismic line. Some of the ReMi reinterpretations utilized this feature. Non-linear optimization interpretations of the seismic refraction data utilizing the SEISOPT2D software program were also completed. These provided depth of investigation interpretations, served as a check on the intercept-time interpretations, and provided a check for maximum interpreted p-wave velocities.

A summary of interpretation results for the shallow subsurface profile as interpreted from Lines 1 through 7 is summarized on Figure B-2. Reinterpreted seismic refraction profiles are shown on Figures B-3 through B-9, whereas reinterpreted ReMi profiles are shown on Figures B-10 through B-16. In general, a layer of low velocity material is interpreted along the lines to depths ranging from about 2 to 7 feet. This material horizon has a range of compression wave (p-wave) velocities of about 500 to 1,200 feet per second (f/s) and shear wave (s-wave) velocities of about 320 to 700 f/s. Such material velocities are consistent with surficial soils and fill deposits above the water table.

Beneath the low-velocity surface layer, interpreted p-wave velocities increase abruptly to a range of 2,800 to 7,300 f/s, with typical values in a range of 3,000 to 5,400 f/s. S-wave velocities remain in the range of about 500 to 1,000 f/s to typical depths of 11 to 20 feet. This large increase in p-wave velocity without a concurrent increase in s-wave velocity is consistent with the presence of a water table with full saturation in the subsurface horizon. A possible localized shallow subsurface seismic contact zone is located at the overlapping portion of Lines 5 and 6, however, insufficient information exists to assess whether the seismic contact reflects a real geologic contact or feature.

At depths of about 15 to 20 feet in several of the lines, the p-wave velocities increase to about 7,000 f/s to over 9,000 f/s. This velocity increase may be at a shallower depth with somewhat lower velocities at the overlap between Lines 5 and 6. Again, these high p-wave velocities are influenced by full saturation in the subsurface below the groundwater table. S-wave velocities, however, increase to a wide range of values from about 1,400 f/s to 4,700 f/s. The higher interpreted s-wave velocities, greater than about 3,000 f/s, indicate the presence of high modulus materials considering the anticipated setting of glacial outwash and till. Consistent depths between p-wave and s-wave horizon interface interpretations at Lines 1 and 3 through 6 indicate that material properties do change at those interpreted contacts and are not simply an artifact of the groundwater table. However, at Lines 1, 5 and 6, the increase in s-wave velocity is not nearly as prominent as the increase in p-wave velocity. The apparent high p-wave velocity horizon at Line 7 is not corroborated in the s-wave results.

Below about 20 feet in depth, p-wave refraction interfaces could no longer be interpreted. P-wave depth of investigation interpretations indicated that the effective p-wave depths of investigation are about 18 to 26 feet in Lines 1 through 7.

The s-wave profile at Line 4 included an interpreted velocity reversal below a roughly 10-foot thick high p- and s-wave velocity horizon. Whether such an interpretation is an artifact of the interpretation process or represents an actual subsurface condition is not known. The velocity reversal is in the proximity of the apparent interpreted contact that becomes shallow at the overlap of Lines 5 and 6. The other high p- and s-wave velocity horizon was interpreted below a depth of about 15 feet at Line 3. The high s-wave velocity interpretations especially are potentially inconsistent with the glacial outwash and till materials, since these high s-wave velocities are more consistent with rock than soil in a saturated condition. Perhaps one explanation might be that extreme loading by ice resulted in overconsolidated horizons with such high seismic velocities. Alternatively, those particular interpretations may not accurately reflect subsurface conditions.

Other apparent small, localized shallow areas of high p-wave velocities (greater than 6,000 f/s beginning at depths less than 7 ft) without corresponding high s-wave velocities are interpreted in Lines 1, 3, 4 and 5. Possible explanations for these high p-wave velocities may include localized subsurface geometries or lateral material velocity changes with arrival time patterns that mimic seismic refraction higher velocity contacts. These high velocity zones (about 6,100 to 7,300 f/s) are often flanked laterally on at least one side by a much lower p-wave velocity area (about 2,800 to 3,500 f/s), and the average of those two zones is in an expected p-wave velocity range for soils below the water table.

The interpreted p- and s-wave seismic velocity profile for the shallow subsurface is complex. Details of the profile are undoubtedly influenced by decisions and assumptions made during the interpretation process.

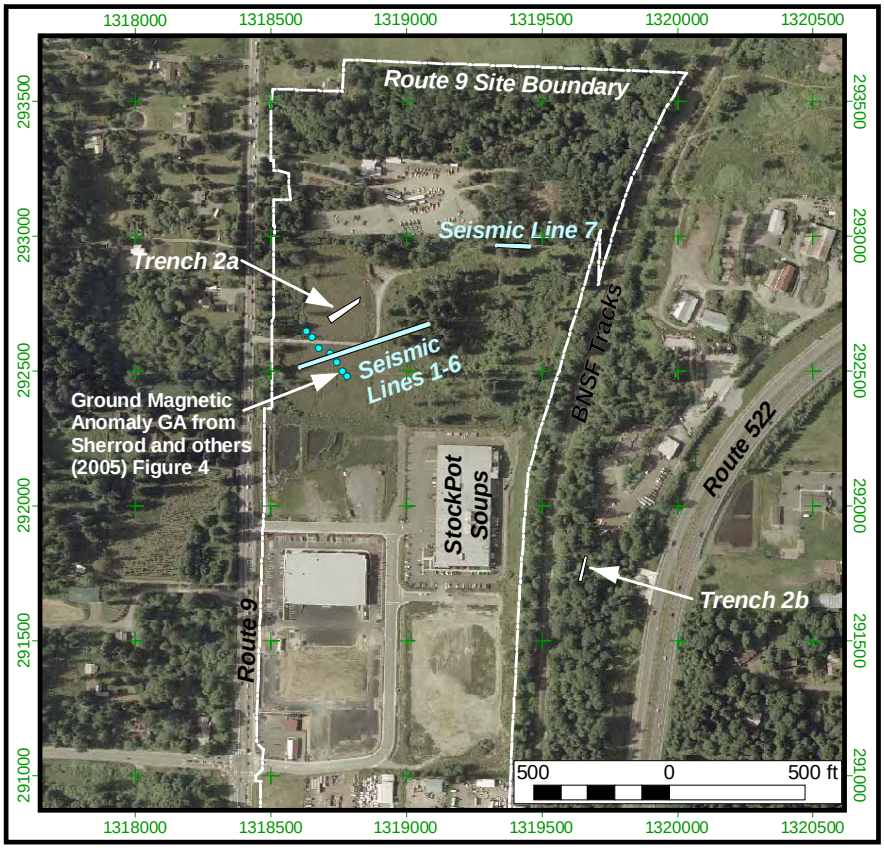

Figure B-1. Approximate locations of Seismic Lines 1 through 7 from April 2004.

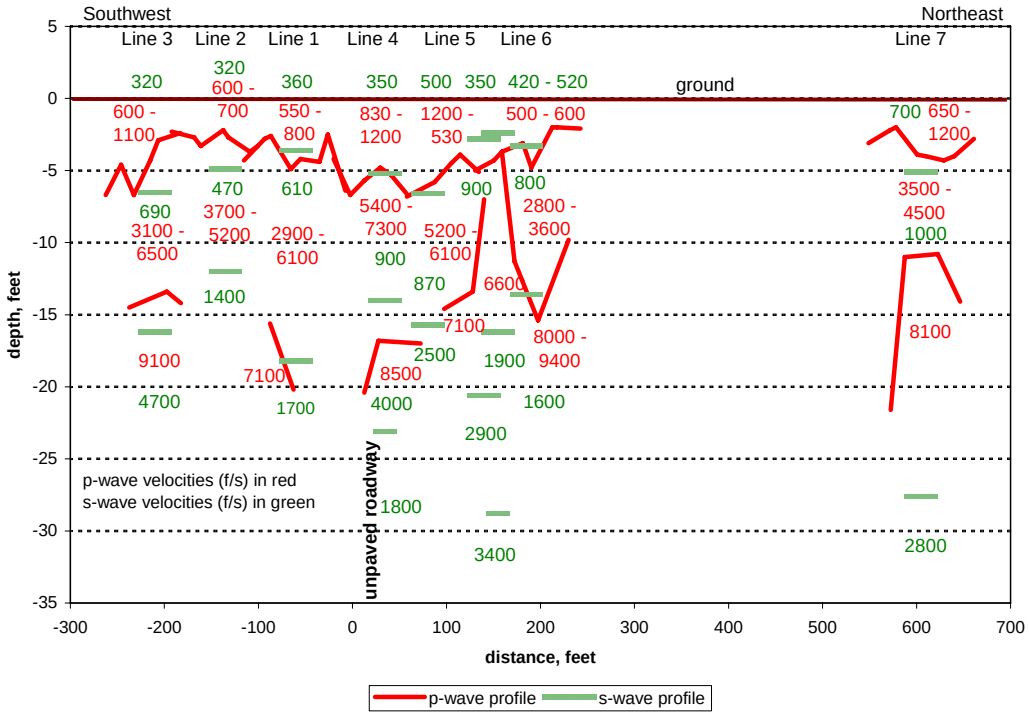

Figure B-2. SW - NE Shallow Subsurface Profile (Reinterpreted).

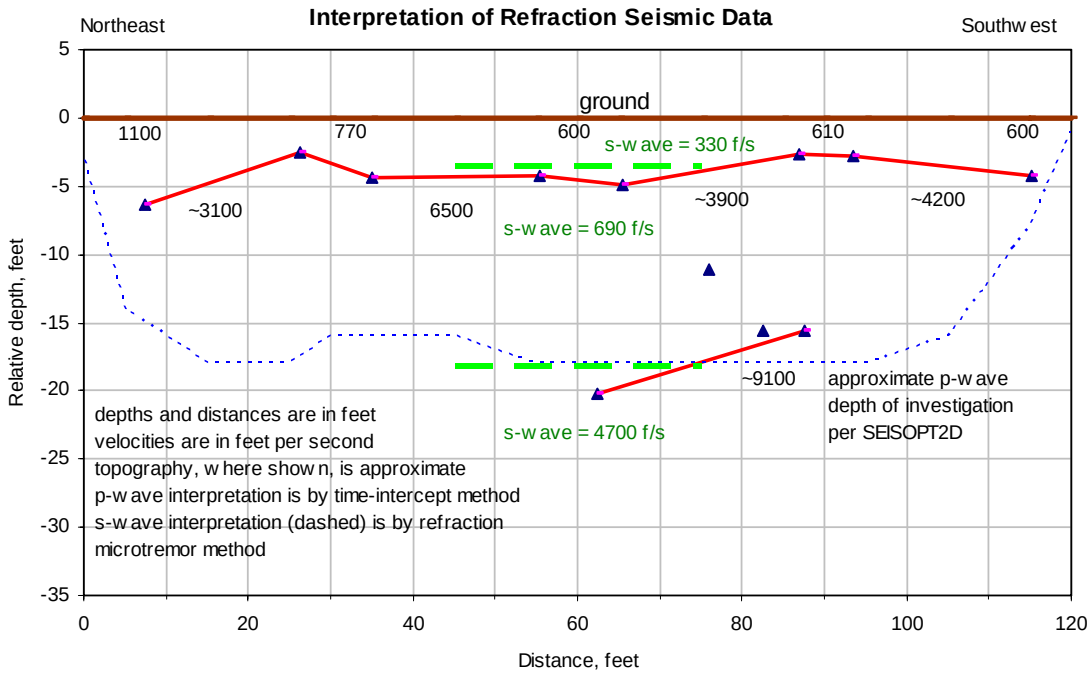

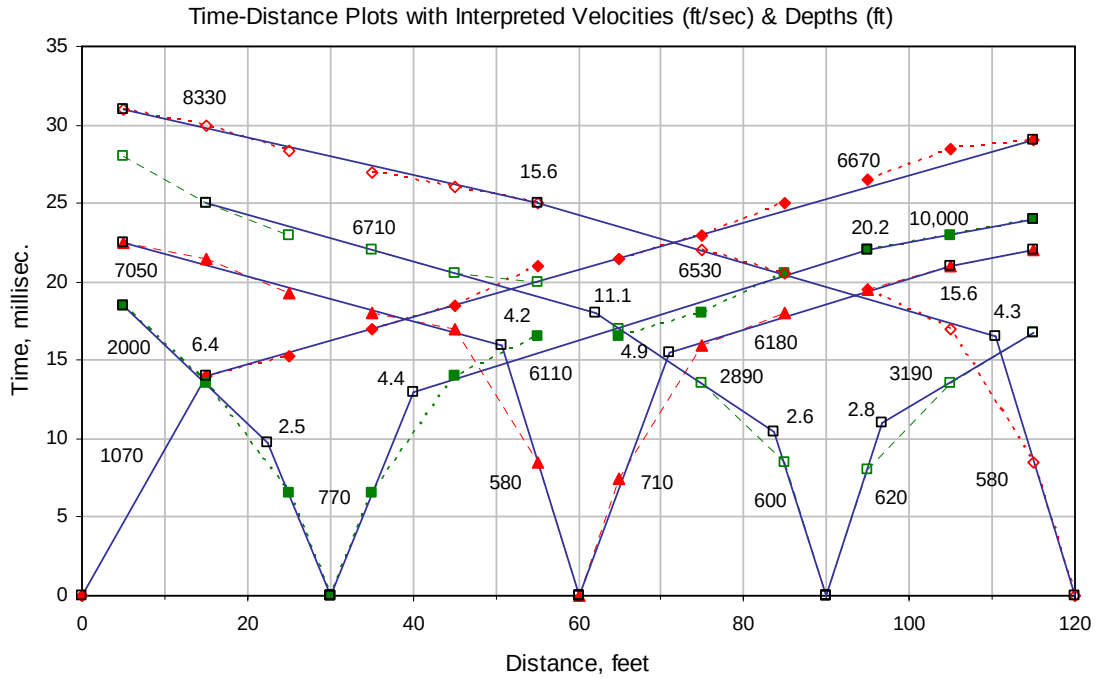

Figure B-3. Seismic Refraction Line 1 (Reinterpreted).

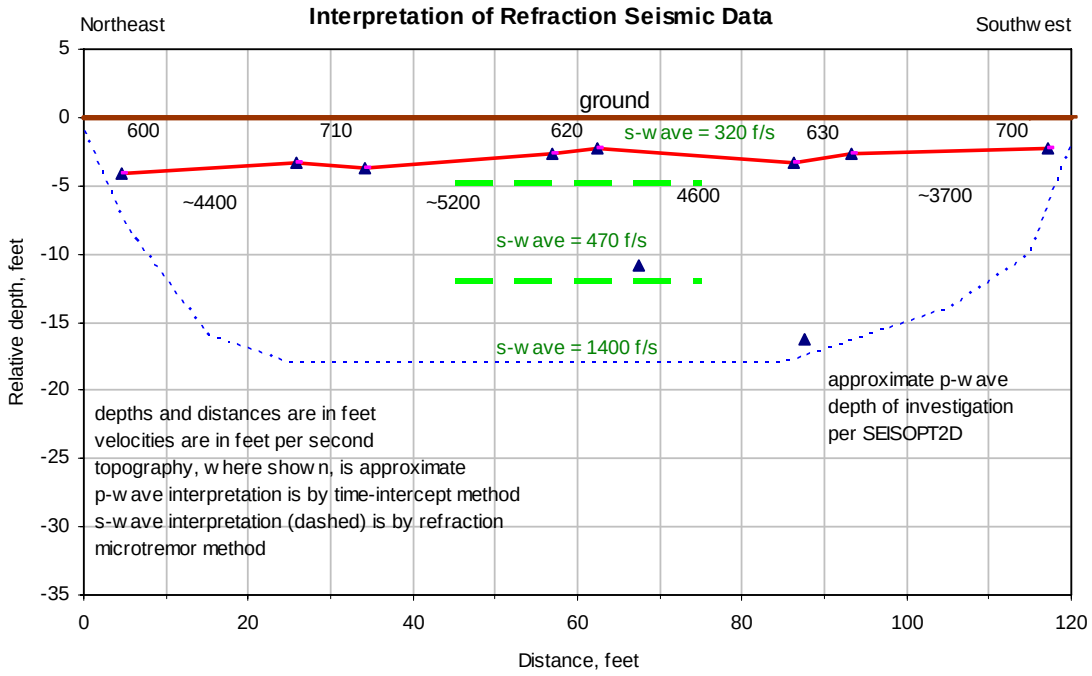

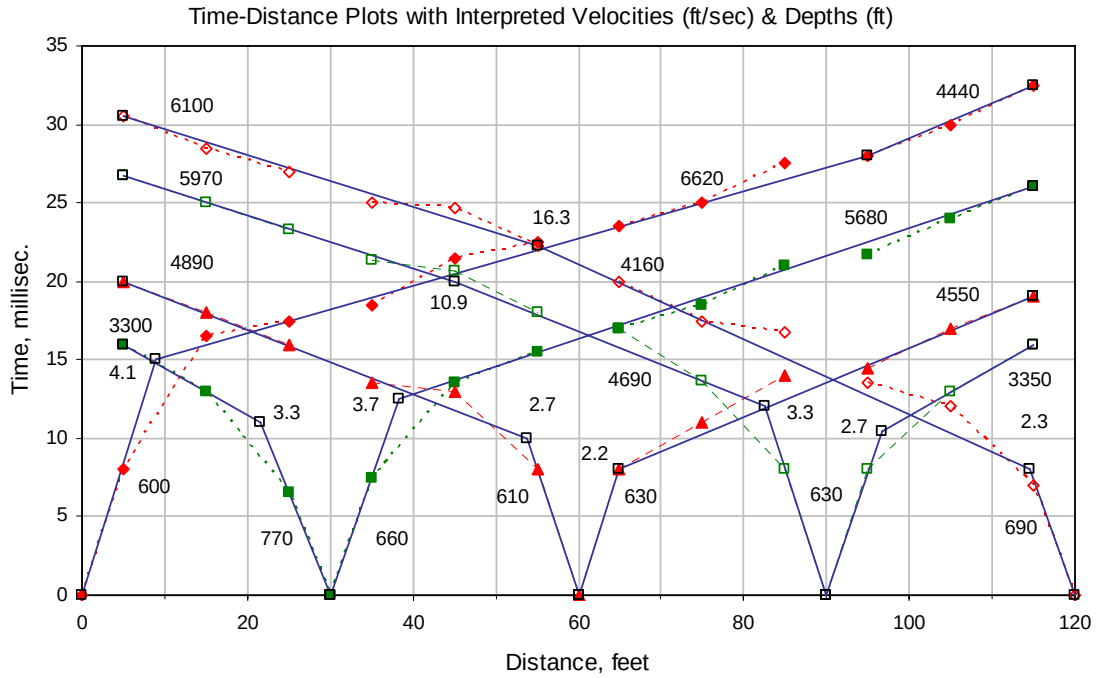

Figure B-4. Seismic Refraction Line 2 (Reinterpreted).

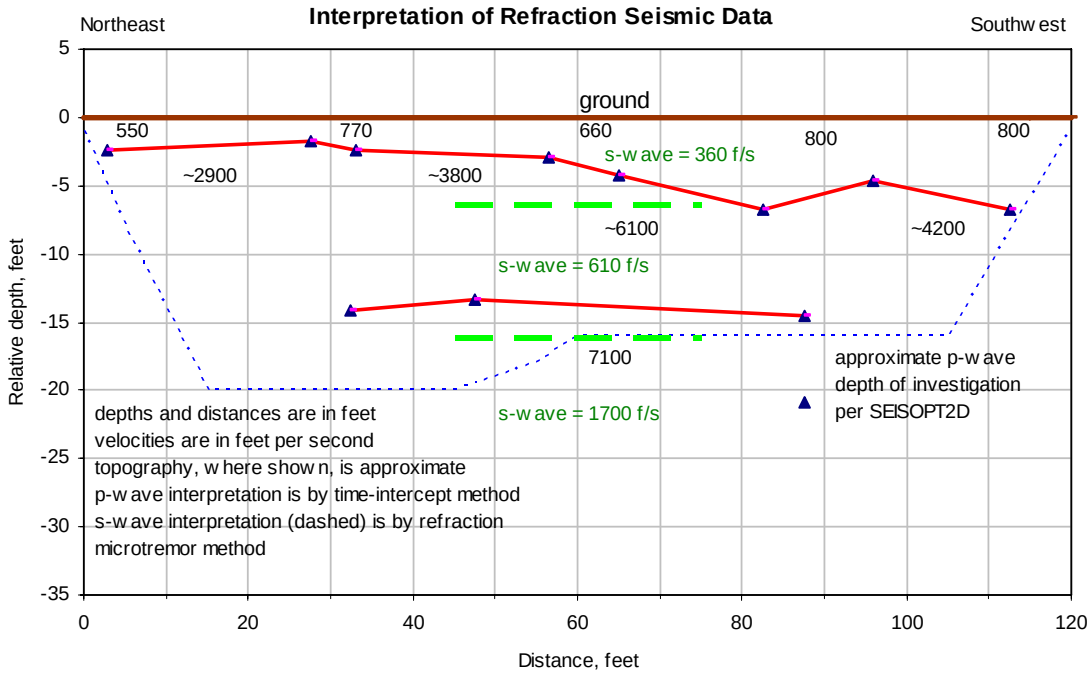

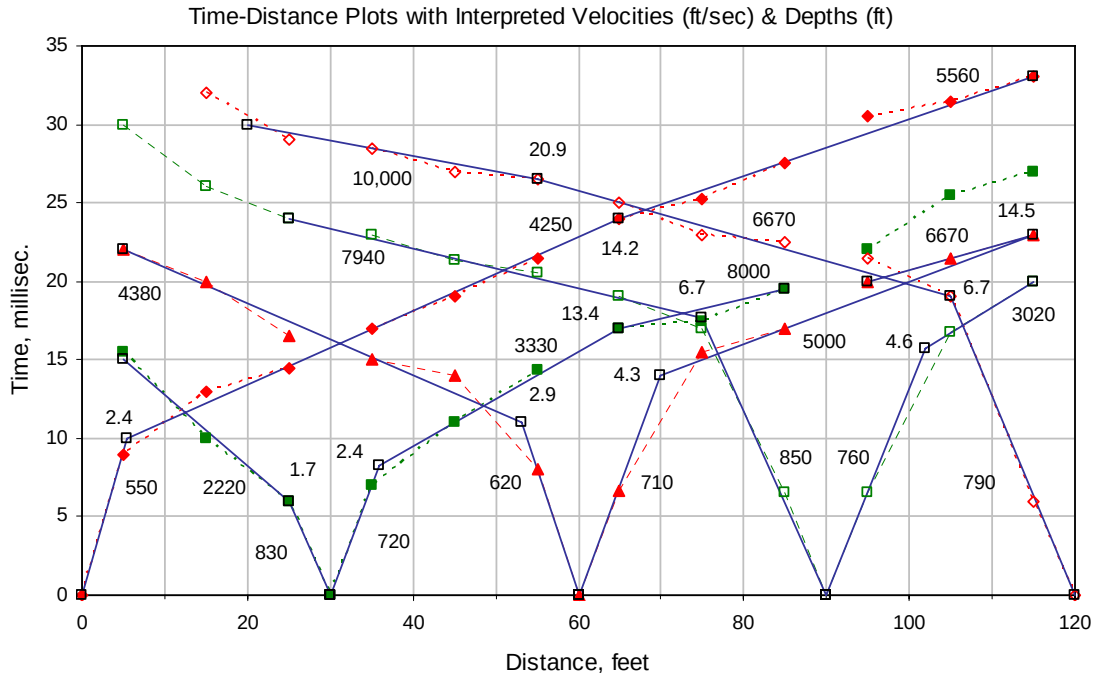

Figure B-5. Seismic Refraction Line 3 (Reinterpreted)

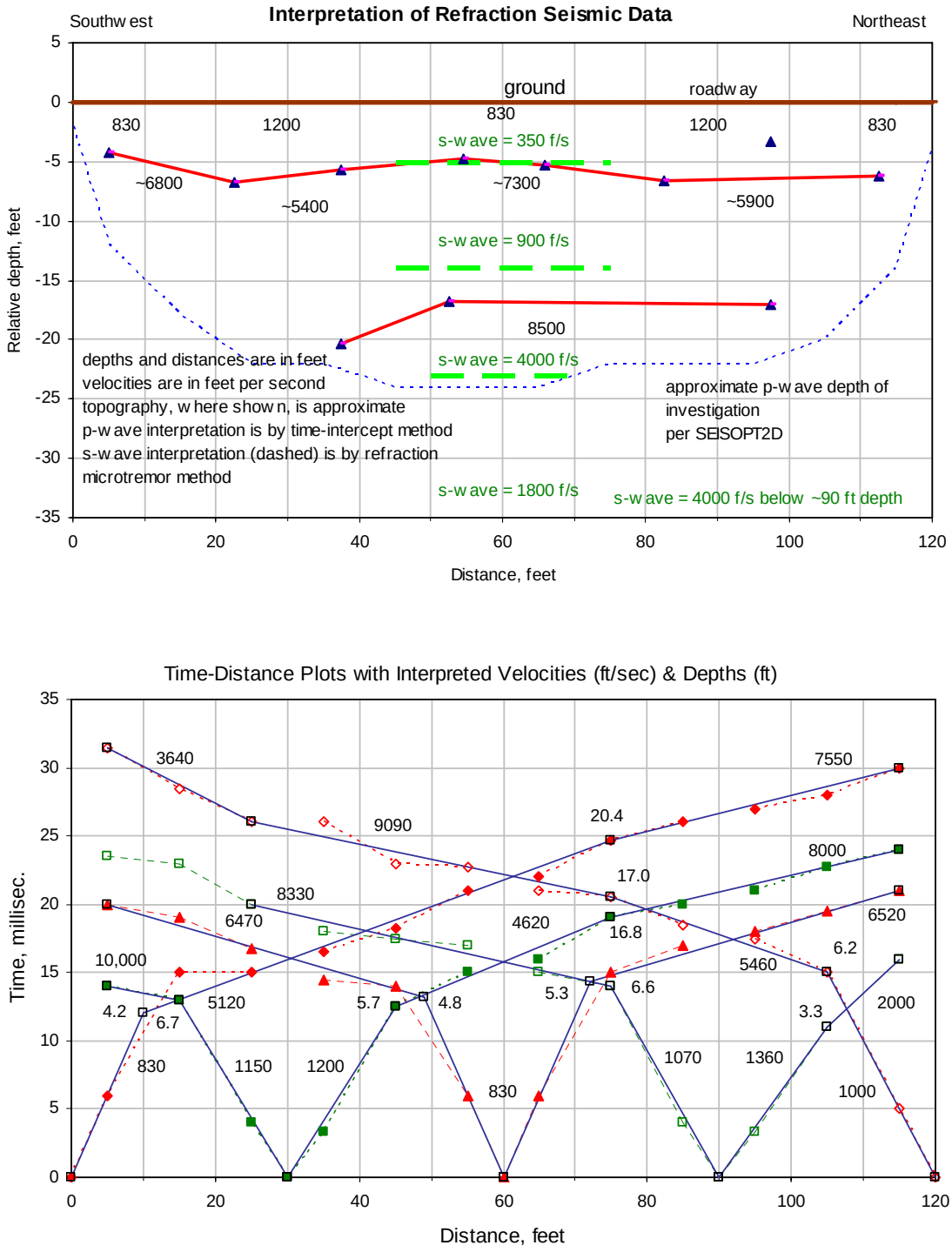

Figure B-6. Seismic Refraction Line 4 (Reinterpreted).

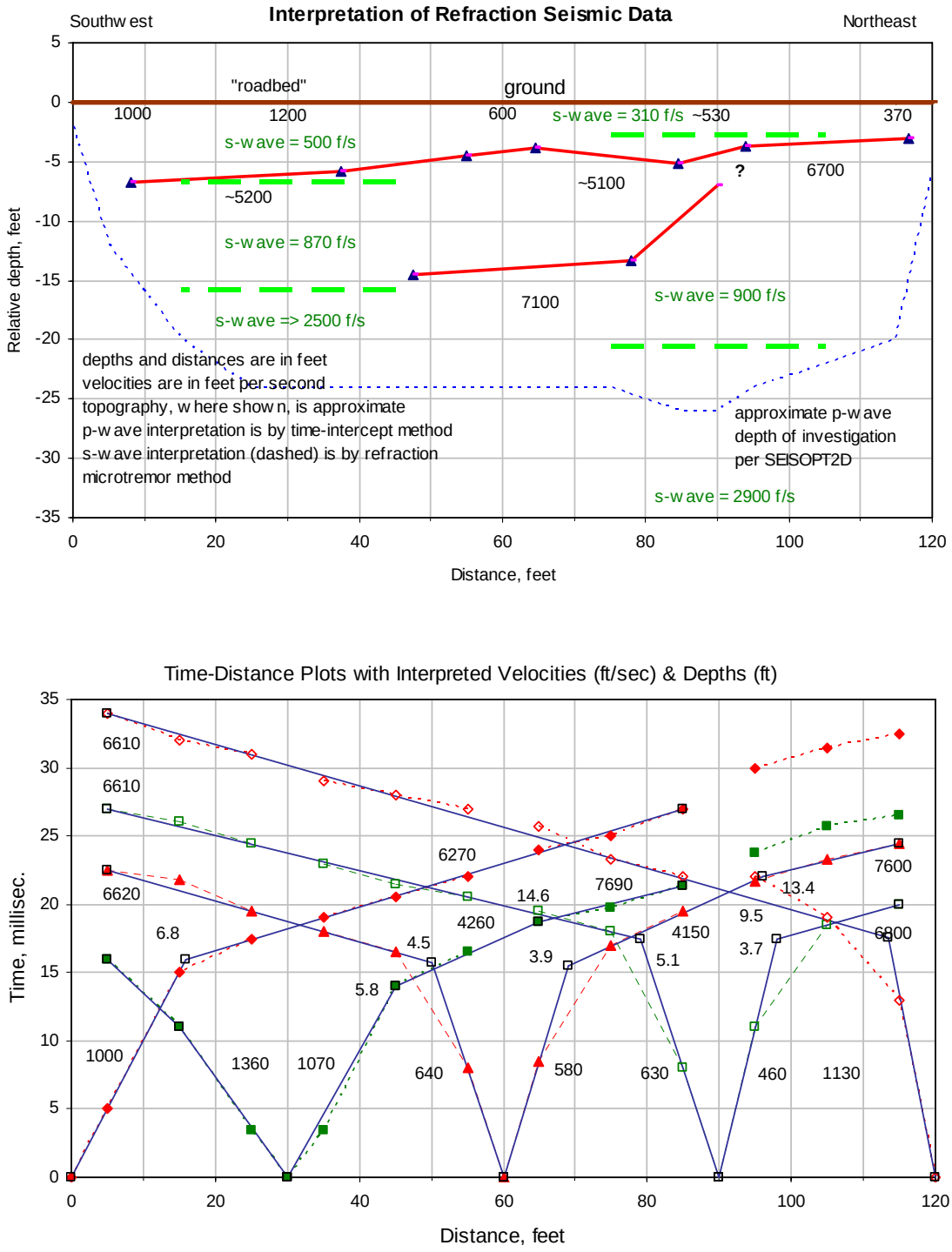

Figure B-7. Seismic Refraction Line 5 (Reinterpreted).

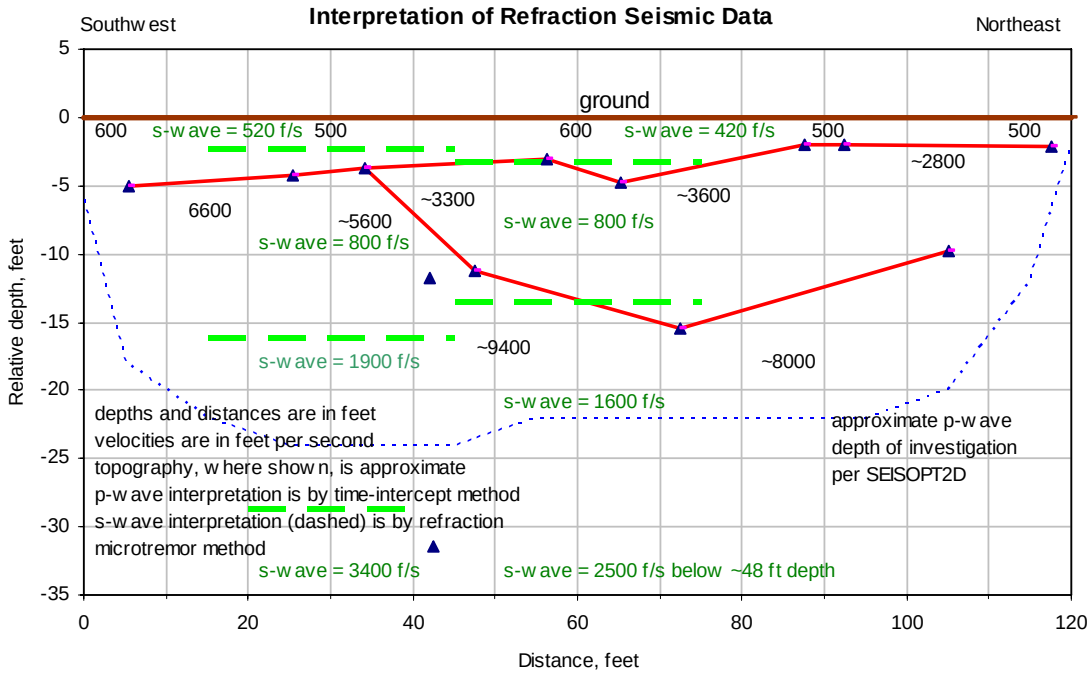

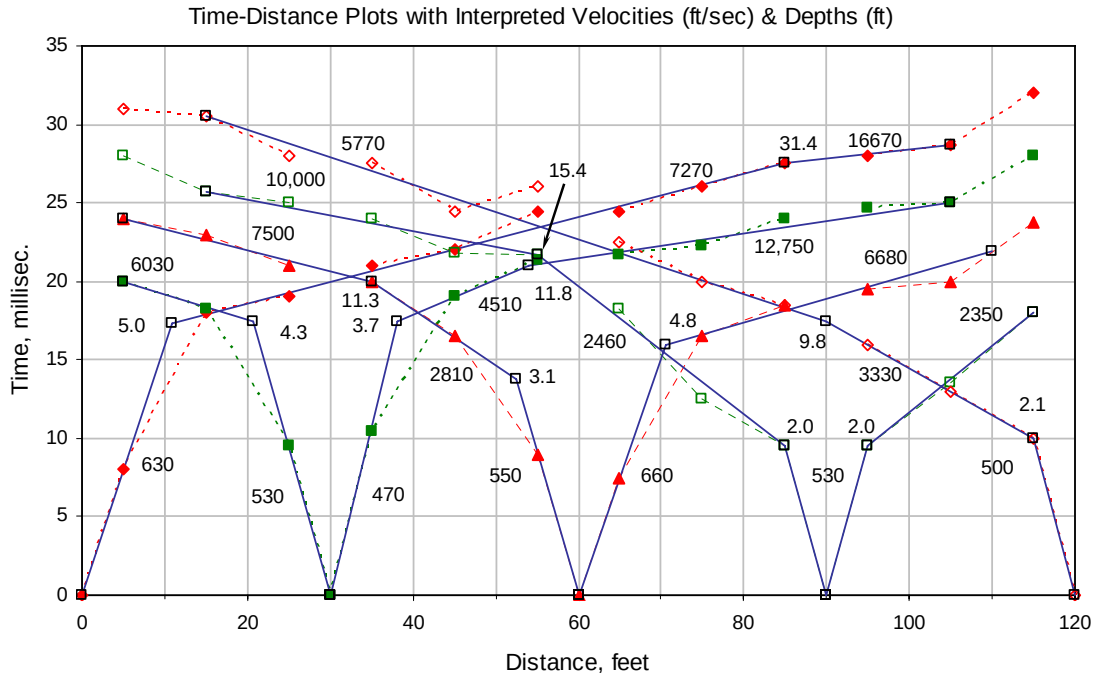

Figure B-8. Seismic Refraction Line 6 (Reinterpreted).

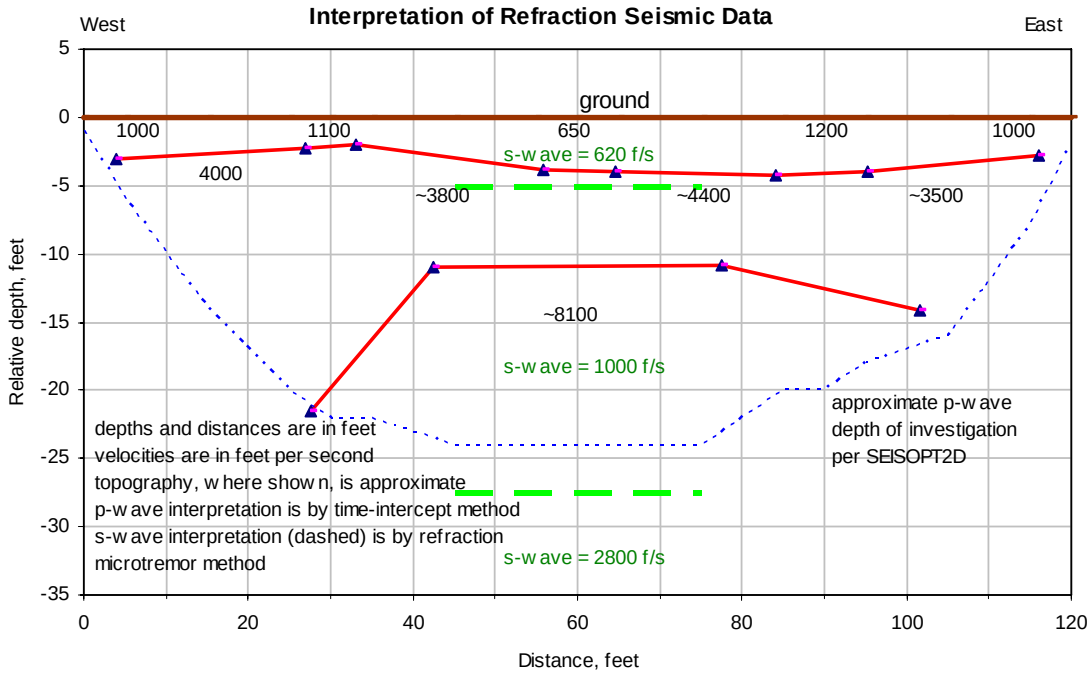

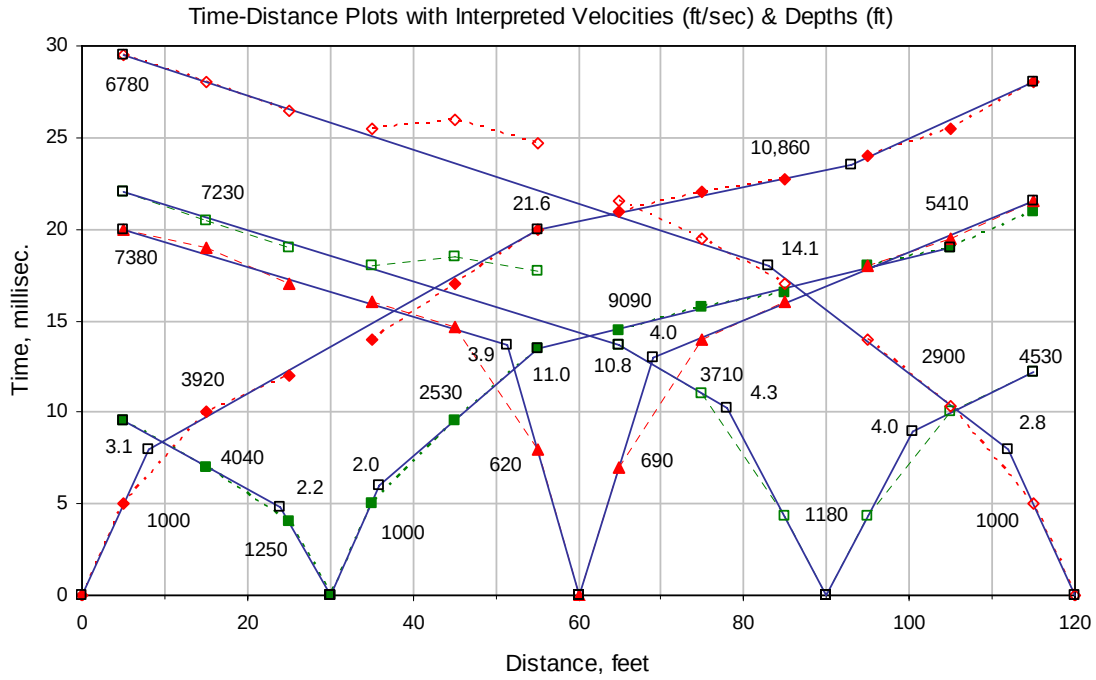

Figure B-9. Seismic Refraction Line 7 (Reinterpreted).

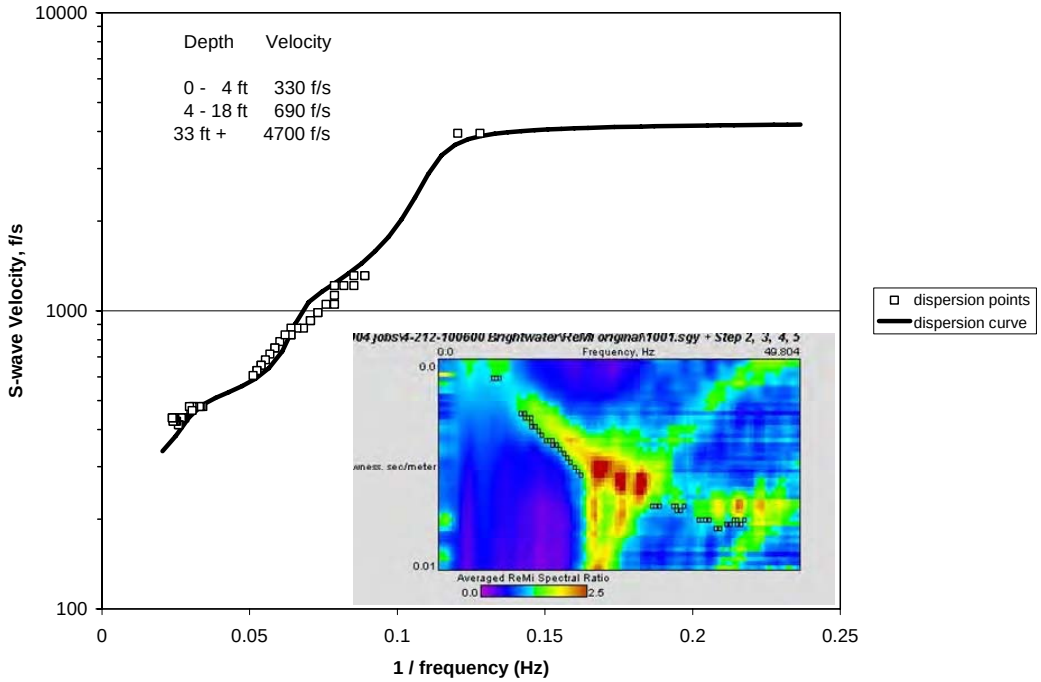

Figure B-10. Refraction Microtremor Line 1 (Reinterpreted).

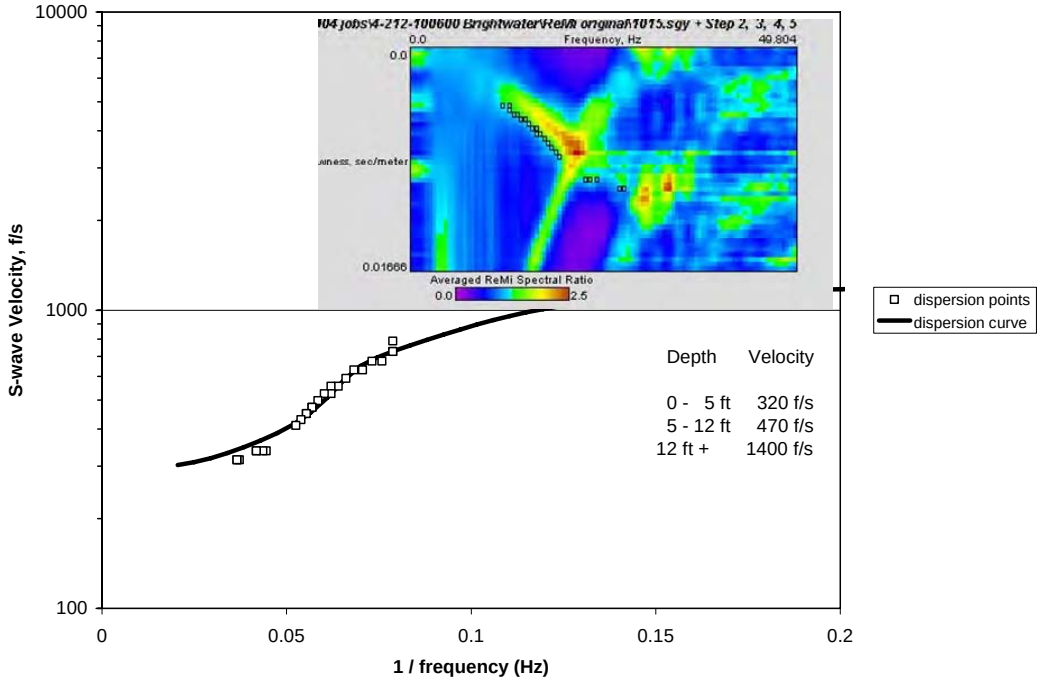

Figure B-11. Refraction Microtremor Line 2 (Reinterpreted).

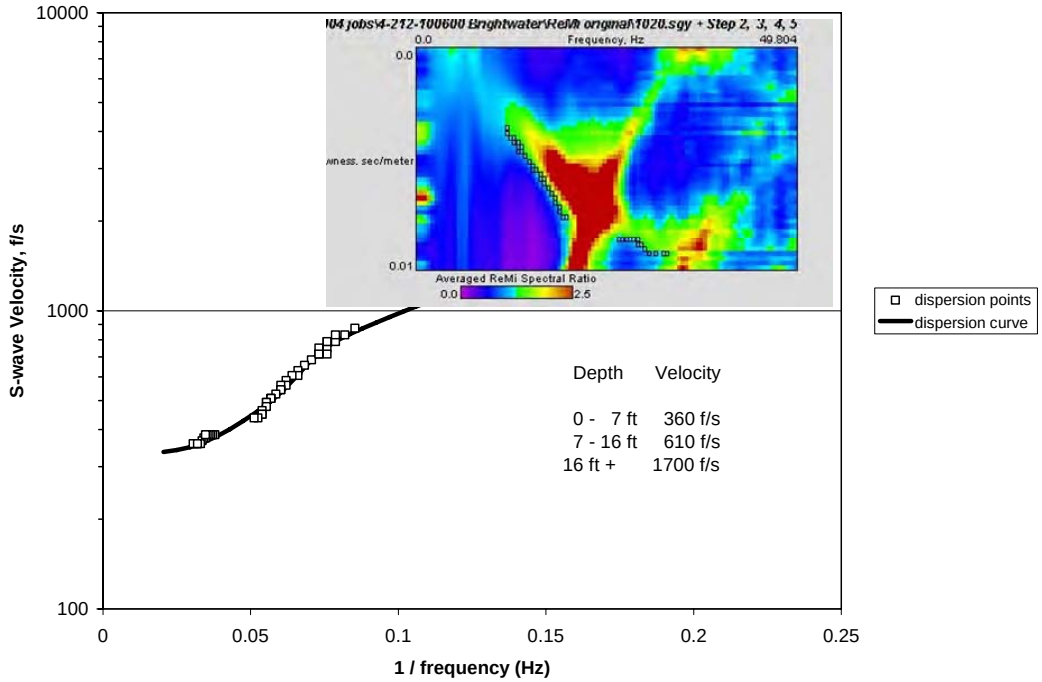

Figure B-12. Refraction Microtremor Line 3 (Reinterpreted).

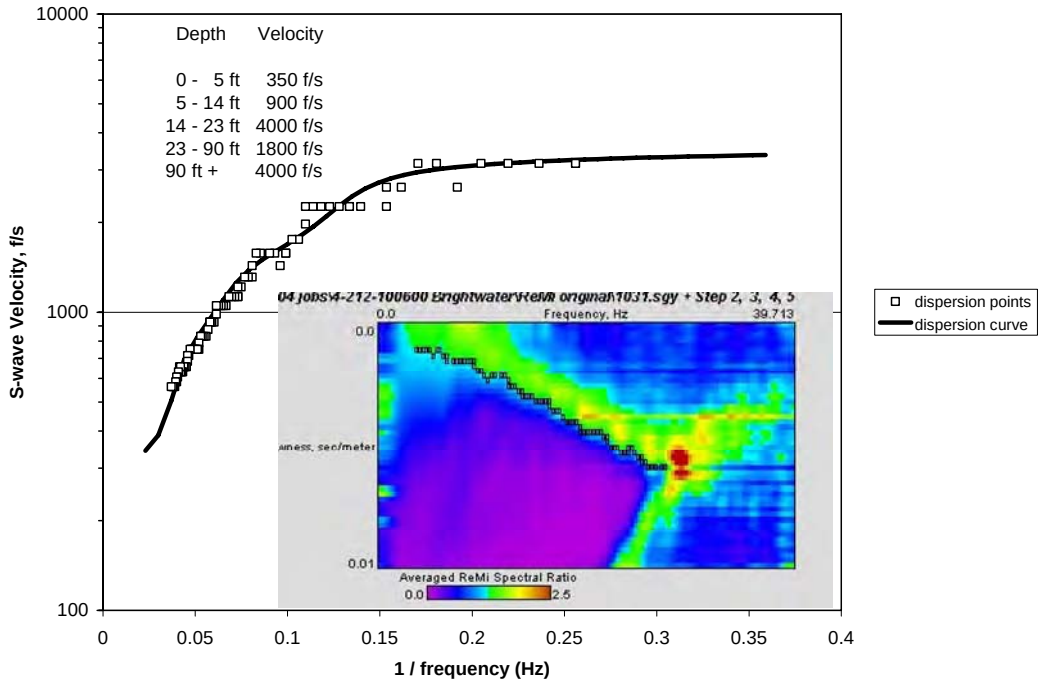

Figure B-13. Refraction Microtremor Line 4 (Reinterpreted).

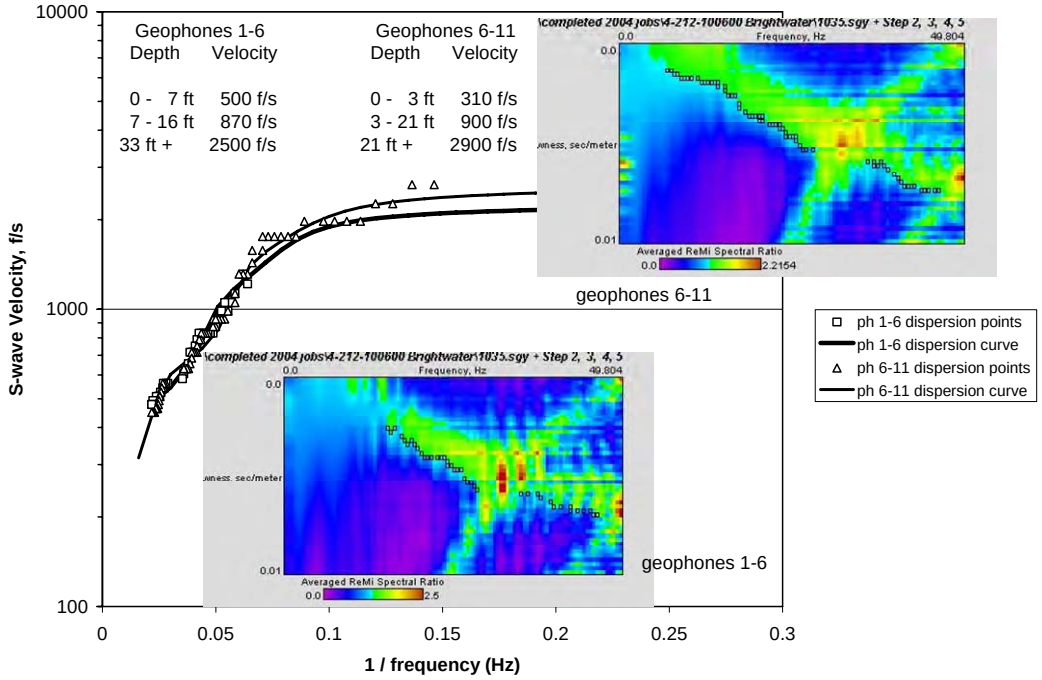

Figure B-14. Refraction Microtremor Line 5 (Reinterpreted).

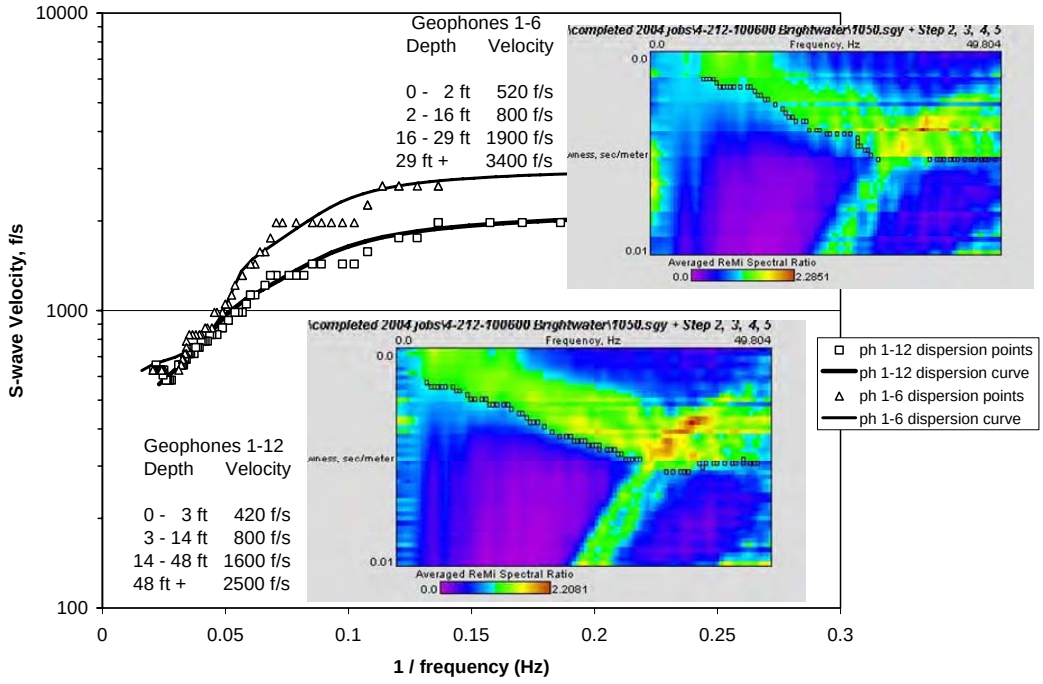

Figure B-15. Refraction Microtremor Line 6 (Reinterpreted).

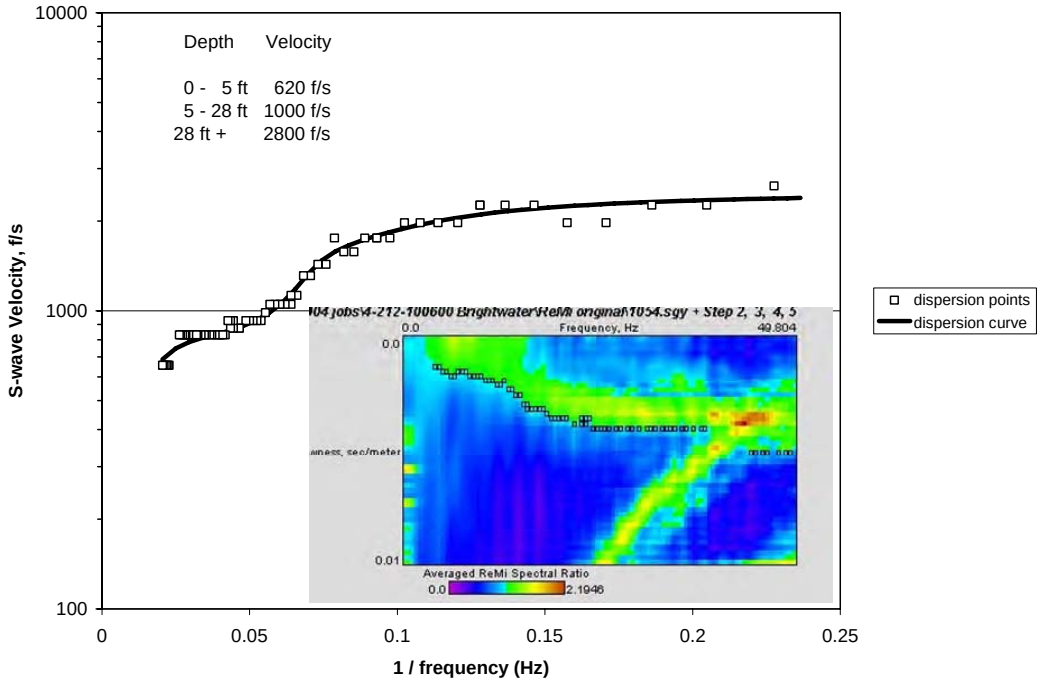

Figure B-16. Refraction Microtremor Line 7 (Reinterpreted).

TRENCH EXCAVATION LOG OF TRENCH 2a
BRIGHTWATER SITE, SNOHOMISH COUNTY, WASHINGTON

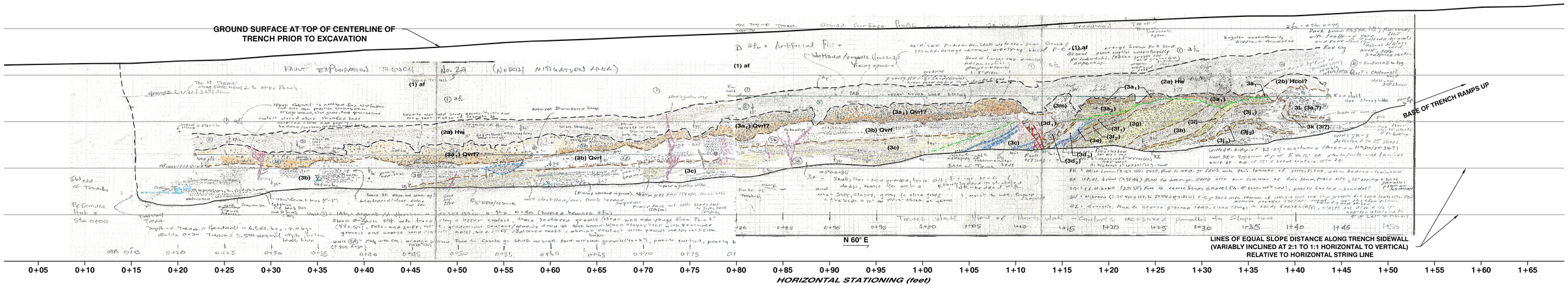

FIELD LOG OF TRENCH No. 2a
SCANNED IMAGE WITH GEOLOGIC CONTACTS HIGHLIGHTED

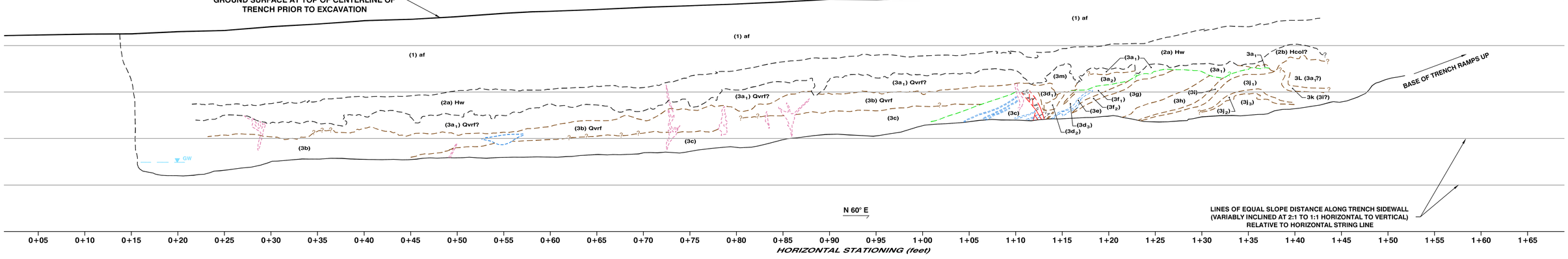

STRATIGRAPHIC LOG OF TRENCH No. 2a
SHOWING GEOLOGIC CONTACTS AND LITHOLOGIC UNITS

TRENCH No. 2a

View of Northeast Sidewall
Inclined Slope Angle View

10 5 0 5 10 20
HORIZONTAL SCALE IN FEET

GEOLOGIC UNITS

- (1) af — ARTIFICIAL FILL (UNDOCUMENTED)
- (2a) Hw — WETLAND - ALLUVIAL DEPOSITS
- (2b) Qcol — COLLUVIAL DEPOSIT
- ($3a_1$) Qvrf — VASHON FLUVIAL OUTWASH DEPOSITS OR POSSIBLE YOUNGER ALLUVIUM
- (3b) to (3L) — VASHON FLUVIAL OUTWASH DEPOSITS

- SEE ATACHED SHEET FOR LITHOLOGIC DESCRIPTION OF UNITS

GEOLOGIC CONTACTS

- CONTACT BETWEEN GEOLOGIC UNITS
- CONTACT BETWEEN FLUVIAL OUTWASH SUBUNITS
- STRATIGRAPHIC LAYER/MARKER BEDS
- ANGULAR UNCONFORMITY
- FAULT (WITH MEASURABLE DISPLACEMENT OF STRATA)
- SAND INTRUSION/INJECTION DIKE
- GW — GROUNDWATER LEVEL IN TRENCH WHILE MAPPING

NOTES:

1) Trench excavated by Komatsu PC 150 excavator on September 29, 2004.
2) Geologic contacts were measured as distances from level string line along variably inclined sidewall slope.
3) Groundwater level near base of trench fluctuated due to operation of sump pump and precipitation while trench was open.
4) Trench sidewall mapped by D.L. Perry, CEG on October 5, 2004 to October 11, 2004.
5) Detail of station 1+07 to 1+17 mapped on seperate log at scale of 1 inch = 2 feet.

Prepared By AMEC Earth & Environmental, Inc.

PLATE I

TRENCH EXCAVATION LOG OF A PORTION OF TRENCH 2a
BRIGHTWATER SITE, SNOHOMISH COUNTY, WASHINGTON

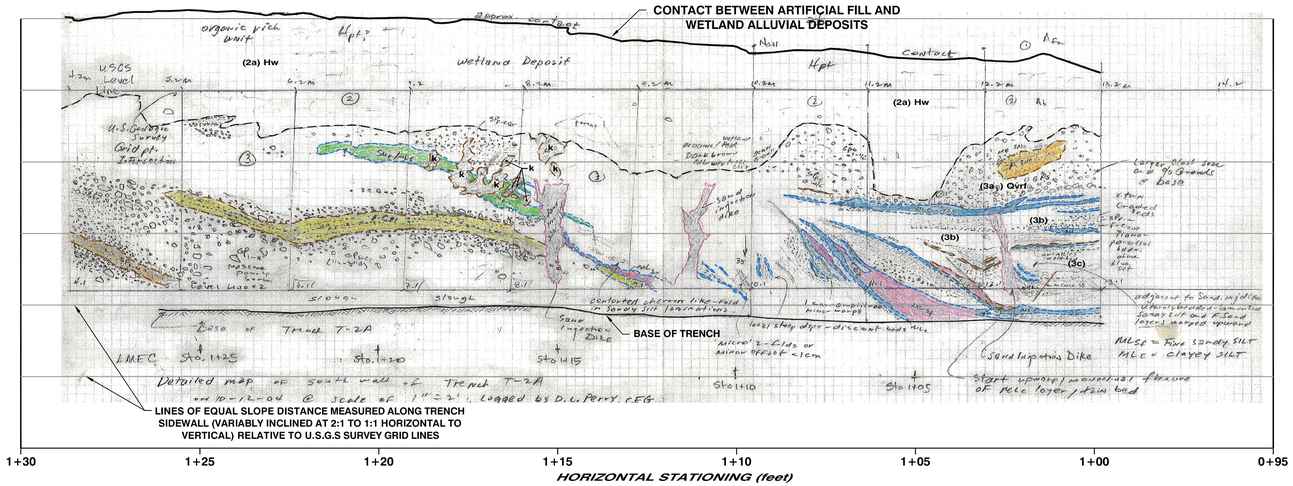

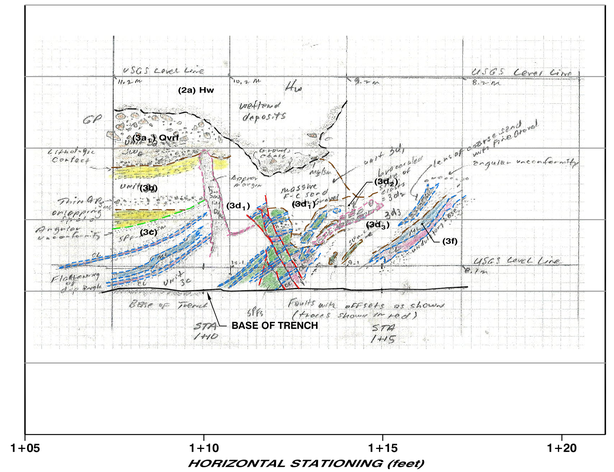

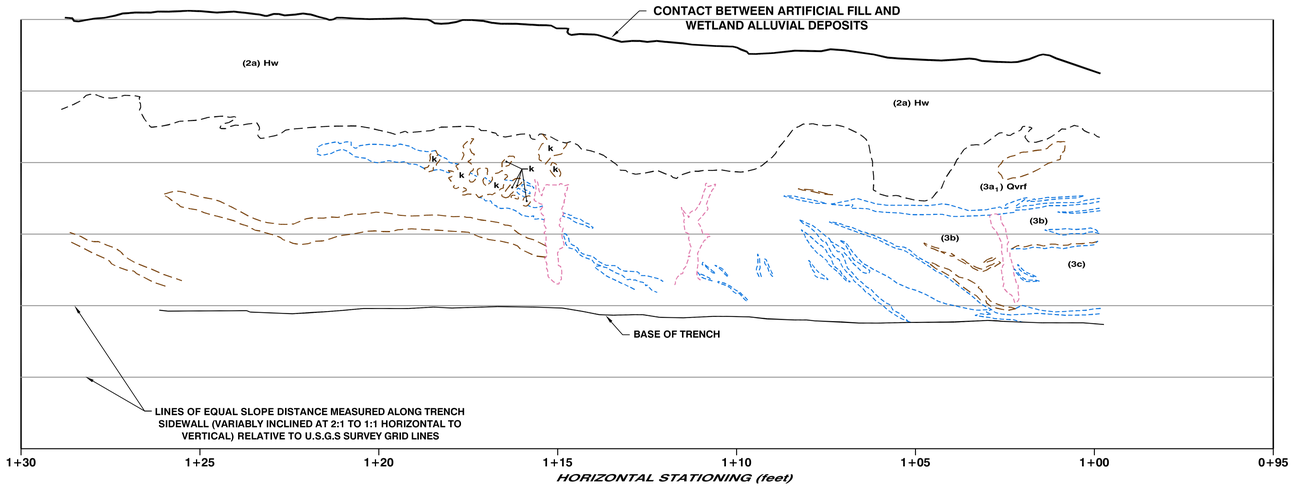

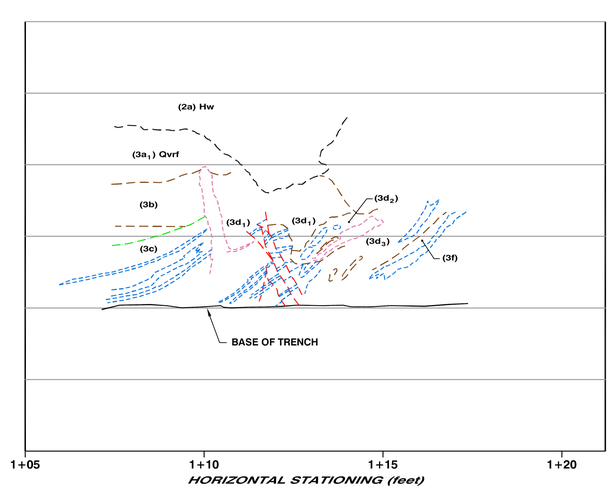

N 54° E

TRENCH No. 2a

Detail of South Sidewall of Trench

0 1 2 3 5
HORIZONTAL SCALE IN FEET

N 58° E

TRENCH No. 2a

Detail of North Sidewall of Trench

0 1 2 3 5
HORIZONTAL SCALE IN FEET

GEOLOGIC UNITS

(1) af	ARTIFICIAL FILL (UNDOCUMENTED)
(2a) Hw	WETLAND - ALLUVIAL DEPOSITS
(2b) Qcol	COLLUVIAL DEPOSIT
(3a$_1$) Qvrf	VASHON FLUVIAL OUTWASH DEPOSITS OR POSSIBLE YOUNGER ALLUVIUM
(3b) to (3f)	VASHON FLUVIAL OUTWASH DEPOSITS

- SEE ATACHED SHEET FOR LITHOLOGIC DESCRIPTION OF UNITS

GEOLOGIC CONTACTS

- CONTACT BETWEEN GEOLOGIC UNITS
- CONTACT BETWEEN FLUVIAL OUTWASH SUBUNITS
- STRATIGRAPHIC LAYER/MARKER BEDS
- ANGULAR UNCONFORMITY
- FAULT (WITH MEASURABLE DISPLACEMENT OF STRATA)
- SAND INTRUSION/INJECTION DIKE
- ANIMAL BURROWS

NOTES:

1) Trench excavated by Komatsu PC-140 excavator on September 29, 2004.
2) Geologic contacts shown on trench logs were measured as slope distances from level string line along variably inclined sidewall slope.
3) Groundwater level near base of trench fluctuated due to operation of sump pump and precipitation while trench was open.
4) Details of trench sidewall mapped by D.L. Perry, CEG on October 12, 2004 (south wall) and October 20, 2004 (north wall).

PLATE II

Prepared By AMEC Earth & Environmental, Inc.

TRENCH EXCAVATION LOG OF A PORTION OF TRENCH 2b
BRIGHTWATER SITE, SNOHOMISH COUNTY, WASHINGTON

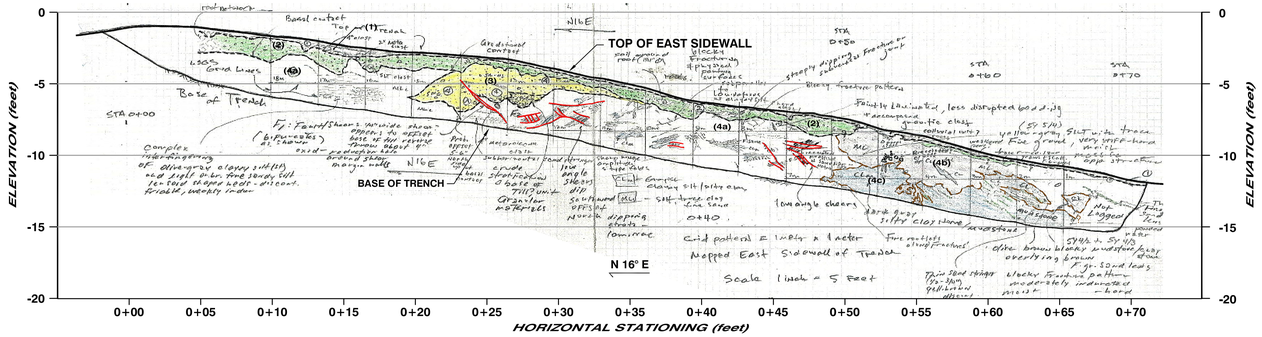

FIELD LOG OF TRENCH No. 2b
SCANNED IMAGE WITH GEOLOGIC CONTACTS HIGHLIGHTED

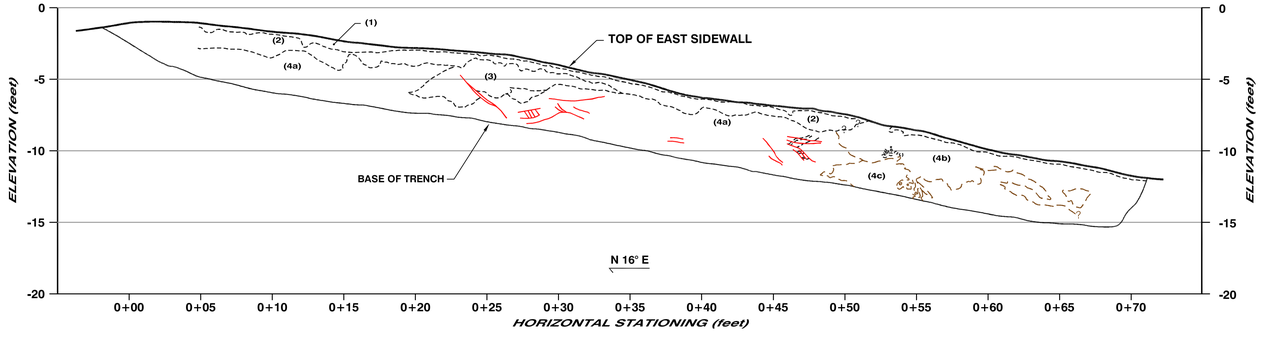

STRATIGRAPHIC LOG OF TRENCH No. 2b
SHOWING GEOLOGIC CONTACTS AND LITHOLOGIC UNITS

TRENCH No. 2b

HORIZONTAL=VERTICAL

Located Along Ridge Spur

5 0 5 10

SCALE IN FEET

EXPLANATION:

TRENCH No. 2b LITHOLOGIC UNITS:

HOLOCENE

(1) Ha **ORGANIC SOIL-A HORIZON**

Fine sandy SILT (MLs) with abundant root and bark fragments, dark brown; appeared loose and moist; undulatory basal contact

(2) Hcol/Qpogt? **COLLUVIUM /HIGHLY WEATHERED TILL (?)**

Gravelly to sandy SILT (GM/MLs) with scattered roots, light yellow-brown (2.5Y 5/5.5); appeared relatively loose to medium dense; well-rounded gravels comprised about 35 to 50 % of unit, gravels ranged typically from ¼- to ¾-inch diameter to maximum of 2-inch diameter; basal contact appeared sharp to gradational and undulatory.

PLEISTOCENE

(3) Qpogt **PRE-VASHON(?) TILL**

Silty to very silty, fine-grained SAND, with some scattered medium to coarse grains and fine gravels from ¼ to 1-inch diameter, mottled orange-brown and olive-gray (5Y 6/4); appeared dense and moist; poorly sorted and crudely stratified; lens shaped unit exposed between station 0+20 and 0+35; northern end of the lens interfingered with glaciolacustrine deposits; irregular to undulatory basal contact.

(4) Qpogl **GLACIOLACUSTRINE DEPOSITS: PRE-VASHON(?)**

Subdivided into three subunits as follows:

(4a) Clayey SILT, olive-gray with thin lenses of light orange-brown, sandy SILT; appeared stiff to hard; exposed from northern end of the trench to station 0+50; layers in this subunit difficult to trace laterally due to complex interfingering and pervasive shearing.

(4b) SILT with trace fine gravel, yellow-gray (5Y 5/4), stiff, massive appearance; locally contained clasts (rip-ups) of the underlying subunit; exposed between station 0+50 and the southern end of the trench; basal contact appeared highly irregular.

(4c) MUDSTONE (i.e., silty Clay with a hard consistency) containing thin, fine-grained sand stringers, dark-gray to brown (5Y 4/2 to 5Y 4/3); appeared hard, moderately indurated, and exhibited a blocky fracture pattern.

GEOLOGIC CONTACTS:

CONTACT BETWEEN GEOLOGIC UNITS

CONTACT BETWEEN SUBUNITS

SHEAR OR FAULT

NOTES:

1) Trench excavated by Komatsu PC 150 excavator on September 30, 2004.
2) Ground surface topography, and location of geologic contacts along east sidewall based on measurements made relative to U.S.G.S. grid lines.
3) Trench mapped by D.L. Perry, CEG on October 11, 2004 with some details added on October 20, 2004.
4) Geologic contacts shown on log are based on pronounced differences in lithology. The glaciolacustrine units exhibit shearing, brecciation, and lenticular bedding. These contacts are complex, interfinger and locally offset by shearing. thus, location of contacts should be considered approximate.
5) Location of shears that appeared conspicuous are shown. However, other minor shears are not shown.